Masthead Logo

University of Iowa
Iowa Research Online

Theses and Dissertations

Summer 2015

Generation and function of glucose-responsive insulin producing cells derived from human induced pluripotent stem cells

Gohar Shahwar Manzar
University of Iowa

Copyright © 2015 Gohar Shahwar Manzar

This dissertation is available at Iowa Research Online: https://ir.uiowa.edu/etd/5808

Recommended Citation

Manzar, Gohar Shahwar. "Generation and function of glucose-responsive insulin producing cells derived from human induced pluripotent stem cells." PhD (Doctor of Philosophy) thesis, University of Iowa, 2015.
https://doi.org/10.17077/etd.62pbfb1o

Follow this and additional works at: https://ir.uiowa.edu/etd

Part of the Biomedical Engineering and Bioengineering Commons

المنارة للاستشارات

GENERATION AND FUNCTION OF GLUCOSE-RESPONSIVE INSULIN PRODUCING CELLS DERIVED FROM HUMAN INDUCED PLURIPOTENT STEM CELLS

by

Gohar Shahwar Manzar

A thesis submitted in partial fulfillment of the
requirements for the Doctor of Philosophy
degree in Biomedical Engineering
in the Graduate College of
The University of Iowa

August 2015

Thesis Supervisor: Professor Nicholas Zavazava

Copyright by

GOHAR SHAHWAR MANZAR

2015

All Rights Reserved

Graduate College
The University of Iowa
Iowa City, Iowa

CERTIFICATE OF APPROVAL

PH.D. THESIS

This is to certify that the Ph.D. thesis of

Gohar Shahwar Manzar

has been approved by the Examining Committee
for the thesis requirement for the Doctor of Philosophy
degree in Biomedical Engineering at the August 2015 graduation.

Thesis Committee:

Nicholas Zavazava, Thesis Supervisor

Jose Assouline

Michael Mackey

Anne Kwitek

Fayyaz Sutterwala

To my parents and first teachers, Khalid and Surayya...

ACKNOWLEDGMENTS

My training as a scientist could not have been possible without the contributions of several outstanding people. First, I must thank Dr. Zavazava for his incredible guidance and support in mentoring me. He has been an ideal mentor because of his extensive expertise, constant availability, and for always challenging me with fantastic opportunities. What inspired me the most about Dr. Zavazava is how much he invests in my training as a graduate student. Dr. Zavazava's guidance has been nothing short of outstanding, and I am extremely privileged to have been under his tutelage. I could not have learnt a fourth of the things I know now as a young scientist without having trained under him, and it is truly an honor to be able to call him my mentor.

I must thank my other mentors in this process as well, beginning with the incredible scholars that preside over my thesis committee. Their constructive comments and insightful questions have challenged me and allowed me to explore facets of my project that I did not initially consider. Dr. Assouline has given me a strong background in tissue engineering with the four spectacular courses I took with him, and I appreciate his advice and support in my graduate career. Dr. Mackey and Dr. Reinhardt have been excellent advisors in the academic realm and I am grateful for their guidance and for their support of my fellowship applications. Dr. Norian and Dr. Lubaroff have also been very generous with their support of my fellowship applications throughout my graduate career, and I greatly appreciate their feedback on my first dissertation project. I thank my colleagues in the Department of Biomedical Engineering for moral support and for their company. Sharing our positive experiences and the challenges we encountered in our graduate training have helped me not lose sight of the bigger picture.

Dr. Chantal Allamargot from the Central Microscopy Research Facility was instrumental in training and assisting me in microscopy experiments, and I am indebted to her for that. I must also thank members of the Zavazava laboratory, past and present, for making this experience enjoyable and for teaching me various techniques. Probably the most significant of these figures is the exceptional and dedicated Dr. Eunmi "언니" Kim, who was my rotation supervisor and taught me many techniques that were vital for the success of this project, such as iPS cell culture and their differentiation into hematopoietic progenitor cells, flow cytometry and ^{51}Cr release assays. I must thank Pavana Rotti for her early collaboration with me in this project, and for establishing the matrigel 3D culture system in our lab. I would also like to thank all of the undergraduate and rotation students that I have supervised, because they taught me how to teach and because they helped with some aspects of my dissertation. The most notable of these students is Jhanelle Markes. I appreciate her deeply for her dedication and excellent help in the last stages of this project. These individuals listed above are like sisters to me, and it is testament to how much I've gained from them over the course of my graduate training. Other family I've made in the lab includes Diann McCoy, my lab "Mom". Thank you, Di, for letting your neighbor borrow sugar (lab reagents), for offering excellent technical advice and for always lending me spiritual and moral support.

Finally, I must acknowledge my family and closest loved ones for keeping me grounded and providing moral support in this journey. My parents, Khalid and Surayya, have always provided excellent advice and warm encouragement, as have my wonderful sisters, Johar and Bushra. My aunts and uncles have been nothing but supportive to me in this endeavor. Lastly, my four younger brothers have brightened my trips back home with their silliness and ability to make others see the beauty in the simplest things in life.

ABSTRACT

Type I diabetes (T1D) is caused by autoimmune destruction of pancreatic β-cells. Immediate consequences of T1D are severe weight loss, ketoacidosis and death unless insulin is administered. The long-term consequences of T1D are dysregulation of metabolism leading to cardiovascular complications, neuropathy and kidney insufficiency. It is estimated that 3 million Americans have T1D, and its prevalence among young individuals is progressively rising. Islet transplantation is the most effective way to treat T1D. Unfortunately, there is a chronic shortage of cadaveric organ donors to treat all of the patients on the waiting list. Thus, an alternative source of insulin producing cells (IPCs) could significantly improve patient treatment. Our lab seeks to establish human induced pluripotent stem (iPS) cells as a novel source of IPCs that are patient tailored. The aim of this thesis was to 1) compare the differentiation of T1D and nondiabetic (ND) patient-derived iPS cells into IPCs, and 2) devise an effective protocol for differentiating skin fibroblast-derived T1D iPS cells into functional, glucose-responsive IPCs. Initially, T1D iPS cells were differentiated into IPCs. However, the yield was very poor. We hypothesized that epigenetic barriers were prevalent in T1D iPS cells, limiting their differentiation into IPCs. To address this problem, we utilized 5-aza-2’-deoxycytidine (5-aza-DC), a potent demethylating agent that inhibits the DNA methyltransferase (Dnmt). We reasoned that the use of a demethylation agent might induce a more labile, permissive state, allowing for greater cell responses to differentiation stimuli. Typically, after the differentiation of T1D iPS cells, several cell cluster types are obtained, namely compact cell clusters and hollow cysts. 5-aza-DC treatment appeared to convert all of the cell clusters into characteristic islet-like compact structures. In contrast, in untreated T1D IPC cultures, we observed the dominant presence of many hollow cysts with only a few tight spheroids. The hollow cysts stained negative for insulin whereas the rare solid spheroids highly expressed insulin. Flow cytometry analysis indicated a much greater percentage of Pdx1$^+$ and insulin$^+$ cells in 5-Aza-DC-treated cultures. These cells express markers typical of pancreatic β-cells, possessed insulin granules in similar quantities as islets, and were glucose-responsive. When transplanted in immunodeficient mice that had developed streptozotozin-induced diabetes, there was a dramatic decrease of hyperglycemia within 28 days. These mice effectively managed glucose challenge by recovering to normoglycemia, whereas nontransplanted mice did not. Altogether, our data for the first time reveal a very high yield of functional IPCs derived from human iPS cells derived from a patient with T1D, which presents a novel alternative source of IPCs that could be used to treat T1D.

PUBLIC ABSTRACT

Type I Diabetes (T1D), also known as juvenile diabetes, is a chronic autoimmune disease that destroys pancreatic β-cells, and is fatal if left unmanaged. The decreased β-cell mass leads to insufficient insulin secretion, dysregulated metabolism and many secondary complications, such as neuropathy and kidney failure. Management of T1D is cumbersome and generally involves daily monitoring of blood glucose levels and insulin injections to accommodate glucose spikes. Long-term insulin independence requires islet transplantation, which is complicated by the severe shortage of available islets.

Thus, significant effort has been devoted to identify alternative sources of insulin producing cells (IPCs) for cell replacement therapy of T1D. Here, we seek to establish human induced pluripotent stem (iPS) cells as a novel and potentially unlimited source of IPCs that are derived from the patient themselves, thus eliminating the requirement for immunosuppression. iPS cells are generated by reprogramming adult cells (such as skin fibroblasts) into cells that resemble embryonic stem cells. Thus, iPS cells can be transformed into virtually any cell type if they are subjected to “recipes” in which they are exposed to biologically active chemical cocktails in a time-sensitive fashion. Current “recipes” to generate IPCs from iPS cells are inefficient, since only 10-15% of the cells express insulin, and they fail to generate functional, mature IPCs that respond to glucose with insulin secretion. By utilizing a novel 3D differentiation platform, modulators of DNA expression, and a highly optimized 5-step differentiation program, we have established a highly effective recipe to generate functional IPCs from a T1D patient’s human iPS cells with unparalleled efficiency, and we show that these cells rapidly cure T1D in mice.

TABLE OF CONTENTS

LIST OF TABLES xi

LIST OF FIGURES xii

CHAPTER I. INTRODUCTION 1

- An Introduction to Type 1 Diabetes 1
- The Potential of Pluripotent Stem Cells 2
- An Induced Pluripotent Stem (iPS)-Cell Based Strategy for the Cure of T1D 4
- Modulation of Signaling Pathways to Differentiate iPS Cells into IPCs Recapitulate Embryonic Development of the Pancreas 5
    - Stages 1 and 2 7
    - Stage 3 8
    - Stage 4 9
    - Stage 5 11
- Shortcomings of Prior Attempts to Generate Insulin Producing Cells 12
- A Five-Stage 3D Differentiation Protocol for the Differentiation of iPS Cells Into IPCs 13

CHAPTER II. MATERIALS AND METHODS 30

- Human iPS Cell Lines and Culture Conditions 30
- Differentiation of Human iPS Cells into Insulin Producing Cells *in vitro* 30
- Demethylation of iPS Cells 32
- Human Islets 33
- Flow Cytometry and Antibodies 34
- Immunofluorescence and Confocal Microscopy 36
- Quantitative-Real Time PCR (qRT-PCR) 37
- Dot Blot for 5-methylcytosine 37
- Dithizone Staining 39
- Quantitation of Cluster Size 39
- Transmission Electron Microscopy 40
- Glucose Stimulated Insulin Secretion (GSIS) 41
- Mice and Transplantation Experiments 44
- ^{51}Cr Release Assay 45
- Statistical Analysis 46

CHAPTER III. THE DIFFERENTIATION OF iPS CELLS FROM TYPE 1 DIABETIC PATIENTS INTO IPCS IS IMPAIRED IN COMPARISON TO THAT OF iPS CELLS FROM HEALTHY PATIENTS 52

- Introduction 52

Results 53
Optimization of the Generation of DE cells 53
The Early Differentiation of T1D and ND iPS Cells into DE cells is Comparable 55
T1D iPS cells Predominantly Derive Hollow Cysts that Do Not Express Insulin 55
T1D iPS Cells Give Rise to Significantly Fewer Insulin$^+$ Cells 57
T1D iPS Cell-Derived Differentiating Cells Poorly Express *Pdx1* 58
Summary 59

CHAPTER IV. DEMETHYLATION OF T1D iPS CELLS YIELDS GLUCOSE-RESPONSIVE IPC CLUSTERS CONSISTING OF MONOHORMONAL INSULIN-EXPRESSING CELLS 79

Introduction 79
Results 85
Effective Differentiation Outcomes Requires Precise Temporal Modulation of Demethylation Treatment 85
Demethylation of T1D DE Cells Leads to the Generation of Compact, Islet-Like Clusters that Strongly Resemble Islets 87
Demethylation of T1D DE Cells Yields >90% Pdx1$^+$ Cells and >50% Insulin$^+$ Cells while Averting the Generation of Glucagon$^+$ Cells 88
Demethylation of ND iPS Cells Does Not Enhance the Production of Pdx1$^+$ Cells or Insulin$^+$ IPCs 91
T1D IPCs Derived from Demethylated DE Cells Express Pancreatic β Cell-Specific Markers 92
T1D IPCs Possess Insulin Granules in Similar Quantities to Islets 92
T1D IPCs Are Functional and Respond to High Glucose with Insulin Secretion 93
Rapid Correction of Hyperglycemia in Diabetic Mice by T1D IPCs 95
iPS Cell-Derived IPCs are Poorly Antigenic and Do Not Stimulate NK Cell Killing Despite Poor MHC class I Expression 96
Summary 98

CHAPTER V. DISCUSSION 132

The Differentiation of T1D iPS Cells into IPCs is Impaired 132
An Epigenetic Modifier Enhances the Generation of Functional, Glucose-Responsive IPCs from T1D iPS Cells 134
Current Shortcomings of the Differentiation Procedure 135
Selection of an Optimal and Scalable Differentiation Platform to Improve the Functionality and Yield of IPCs from iPS Cells 138
The Role of Epigenetics in the Differentiation of T1D vs. ND iPS Cells 141
Identifying a Suitable and Minimally Disruptive Epigenetic Modifier to Safely Derive IPCs from T1D iPS cells 143

The Natural Islet Endocrine-Endothelial Cell Axis May Be Exploited to Enhance Differentiation and Maturity of iPS Cell-Derived IPCs...146
From Bench to the Bedside: Challenges and Concerns that Need to Be Addressed Before Translating this Technology into the Clinic..150
Consideration of the Immunological Interplay of iPS Cell-Derived IPCs in the Context of Autoimmune Disease 153
Summary and Future Directions 156

REFERENCES.. 163

LIST OF TABLES

Table

1. Differentiation timeline and media constituent information..47

2. Ordering information for differentiation supplements..48

3. Detailed information on the antibodies used for flow cytometric analysis of differentiating cells..49

4. Detailed information on the antibodies used for immunofluorescence staining 50

5. List of primers used for quantitative RT-PCR...51

LIST OF FIGURES

Figure

1. The etiology of T1D and the potential of iPS cells in therapy of T1D 19

2. Lineage bifurcations in the road to IPCs 21

3. Modulation of signaling pathways to impact lineage choices in the differentiation of iPS cells into IPCs 23

4. 3D differentiation involves seeding cell clusters in a matrigel scaffold 26

5. The differentiation of iPS cells into Insulin Producing Cells (IPCs) involves five stages of differentiation 28

6. Selection of the optimal culture conditions for Stage 1 differentiation into definitive endoderm (DE) cells 62

7. The differentiation of T1D and ND iPS cells into DE cells is equivalent 65

8. T1D iPS cells give rise to mostly hollow cyst-like clusters whereas ND iPS cells give rise to a mixture of hollow cysts and compact spheroids 67

9. Insulin expression appears in solid spheroids but not in the hollow cysts that comprise most of the T1D IPC cultures 69

10. Rare large organoids in T1D IPC cultures express insulin 71

11. T1D iPS cells give rise to significantly less IPCs compared to ND iPS cells 73

12. The insulin$^+$ peak in T1D IPCs is significantly smaller compared to ND IPCs 75

13. T1D IPCs express lower mRNA transcript levels of *Insulin*, *Glucagon* and the pancreatic master regulator *Pdx1* relative to ND IPCs 77

14. The mechanism of action for the transient demethylating agent 5-aza-2'-deoxycytidine (5-aza-DC) 83

15. Selection of a dose of 5-aza-DC to demethylate iPS cells while ensuring maximal cell viability 101

16. Demethylation on D0 of differentiation arrests cells in a CXCR4+ PDGFRα+ Sox17- mesendodermal state 103

17. Demethylation of T1D DE cells uniformly gives rise to compact clusters that resemble islets 105

18. T1D IPC clusters derived from demethylated DE cells stain strongly in dithizone solution in a manner similar to primary human islets....107

19. Demethylation of T1D DE cells significantly improves the yield of Pdx1$^+$ cells....109

20. Range of Pdx1$^+$ Nkx6.1$^+$ cells derived from T1D iPS cells after transient demethylation treatment 111

21. Demethylation of iPS cells significantly improves the yield of insulin$^+$ cells at the expense of glucagon$^+$ cells in a concentration-dependent manner 113

22. Demethylation consistently yields a significantly higher yield of IPCs from T1D iPS cells 115

23. 5-aza-DC converts T1D iPS cells into compact, islet-like clusters that consist almost entirely of insulin-expressing cells 117

24. Demethylation of ND iPS cells does not significantly enhance the yield of insulin$^+$ cells and Pdx1$^+$ cells 119

25. T1D IPCs express C-peptide in addition to the pancreatic β-cell specific transcription factor Nkx6.1....121

26. T1D IPCs resemble islets in their ultrastructure and possess insulin granules of various maturities....123

27. The average number of cells per IPC cluster resembles published findings on the number of cells per islet 125

28. T1D IPCs are functional and glucose-responsive....127

29. Rapid correction of hyperglycemia in diabetic mice by T1D IPCs....129

30. T1D DE cells and IPCs are poorly antigenic and are not susceptible to NK cell-mediated killing *in vitro* 131

31. Novel culture platforms for differentiating iPSCs into IPCs....158

32. Cooperative signaling along the endothelial-endocrine axis may enhance survival, maturation and function of iPS cell-derived IPCs....160

33. A humanized mouse model to investigate the autoimmune susceptibility of iPS cell-derived IPCs *in vivo* 162

CHAPTER I
INTRODUCTION

An Introduction to Type 1 Diabetes

The pancreas is a highly organized and complex organ that serves many vital functions in the human body. According to these functions, it can be divided into two major components: the exocrine pancreas and the endocrine pancreas[1,2]. The exocrine portion is responsible for neutralizing the acidic chyme that comes out of the stomach after preliminary digestion, and also produces many important enzymes that break down proteins[2]. The hormone-producing endocrine pancreas is organized into discrete round clusters called the Islets of Langerhans, which are dispersed among the exocrine acini[1]. The Islets of Langerhans contains five cell types[1]. The principal constituents of the islets are pancreatic β-cells, which secrete insulin[1]. Additionally, the islets consist of α-cells that secrete glucagon, δ-cells that produce somatostatin, ε-cells that secrete ghrelin, and PP (also known as γ-cells) that generate Pancreatic Polypeptide[1].

Type I Diabetes (T1D), also known as juvenile diabetes, is a condition in which the body is unable to produce insulin due to autoimmune destruction of pancreatic β-cells (Figure 1A)[3]. The exact basis of T1D remains vague, and it has been shown through studies involving monozygotic twins that there is clearly a non-immunological environmental component that drives the pathogenesis of T1D[4]. However, it is generally believed that autoreactive CD4$^+$ T cells license Dendritic Cells (DCs) to cross-present exogenous islet antigens, such as insulin, via MHC I to CD8$^+$ T cells, which eventually attack and destroy the pancreatic β-cells[4]. If not immediately managed with insulin replacement therapy, immediate consequences are severe weight loss, keotacidosis and death. The long-term consequences of T1D impact nearly every organ system. Some notable complications include hypertension, blindness, neuropathy and kidney insufficiency[3]. The significance of these secondary pathologies lends reason for why curing T1D has been devoted significant efforts by the scientific community. Unfortunately, current therapies merely serve to manage the condition in order to prevent advancement of the disease as opposed to curing it, and such management requires daily injections of insulin and close monitoring of blood glucose levels[3]. Even with treatment, these patients may succumb to the complications of T1D and thus face major health burdens.

Because of their high pancreatic β-cell content, islet transplantation is recognized as the most effective treatment for T1D[1,4,5]. Unfortunately, the source of cadaveric islets is extremely scarce and the possibility of immunological rejection precludes widespread matching of donors and recipients[5-7]. Mechanical insulin secreting technologies are being developed for automatic control of blood glucose levels and have met some success[8]. However, it can be argued that the inherent biosensor intrinsic to biological sources is superior in ensuring accurate and homeostatic regulation of blood glucose levels, which may be otherwise difficult to achieve with an artificial mechanical system. As a result, alternative cell sources have been sought towards pancreatic β-cell replacement.

The Potential of Pluripotent Stem Cells

Scientists have recognized that stem cells represent an alternative and potentially unlimited source of pancreatic β-cells[9]. There are several types of naturally found stem cells; namely, umbilical cord stem cells, mesenchymal stem cells, amniotic stem cells, hematopoietic stem cells found in the bone marrow, and embryonic stem cells isolated from the blastocyst, which is an early stage embryo[10,11]. Embryonic stem (ES) cells are the most pluripotent and versatile of these cell types, and thus have been pursued extensively as the stem cell of choice in the generation of pancreatic β-cells[12-16]. However, the generation of

ES cells requires the destruction of an embryo, which has made their use in research unpopular and extremely controversial[11]. Indeed, ethical baggage and government-imposed restrictions have limited progress in research utilizing ES cells for the derivation of IPCs.

Thus, when Shinya Yamanaka and colleagues from Japan announced the development of induced pluripotent stem cells (iPSCs) from mouse skin fibroblasts, it came as a groundbreaking discovery to scientists from all corners of the globe[17]. The retroviral transduction of four transcription factors critical for maintaining pluripotency (Oct4, Sox2, Klf4, and c-Myc) caused reprogramming of the cells into an ES cell-like state[17]. iPS cells generated this way were found to express characteristic pluripotent cell markers and shared similar growth properties, morphology, epigenetic profiles, and gene expression patterns as ES cells[17]. Remarkably, the cells were pluripotent and yielded teratomas containing all three germ layers upon their subcutaneous transplantation into nude mice[17]. Adult mice have been generated solely from iPS cells, which is a finding that validates their pluripotency to the most stringent standard[18]. The very next year after the first description of the generation of mouse iPS cells, the same team reported the generation of human iPS cells from adult human dermal fibroblasts through the overexpression of these same factors[19].

Moreover, methods employing other cocktails were published for the generation of iPS cells[20]. Largely motivated by safety concerns surrounding the use of viral integrative reprogramming approaches[21], several other reprogramming strategies have been devised since the generation of the first iPS cells, such as transfection-based reprogramming utilizing plasmids, non-integrative episomal-based reprogramming, microRNA or protein-based reprogramming, and arguably, the safest of all, small molecule based-reprogramming[22-26]. Furthermore, these cells can been generated from a variety of cell types, including those from the blood[27], liver[28], stomach[28], and more surprisingly, from keratinocytes attached to human hair[29], and even the cells that are found in the urine (UiPSCs)[30,31]. These last two cell sources demonstrate the outstanding potential for completely noninvasive patient-specific therapy utilizing iPS cells.

An Induced Pluripotent Stem (iPS)-Cell Based Strategy for the Cure of T1D

The recent advent of induced pluripotent stem (iPS) cells has met widespread enthusiasm in the field of regenerative medicine[9]. iPS cells, which are stem cells derived from reprogramming somatic cell types to a stem cell fate, hold tremendous promise as they are capable of forming any cell type if driven through appropriate cues, similar to ES cells. iPS cells have been successfully differentiated into hepatocyte-like cells[32,33], cardiomyocytes[34-36], neurons[35,37,38], kidney tubular cells[39,40], airway epithelial cells[41], hematopoietic progenitor cells[42], pancreatic endocrine precursor cells[14], and many other cell types[9]. Recently, a clinical trial was initiated using iPS cell-derived retinal pigment epithelial cells for the treatment of a debilitating eye disease known as macular degeneration[43]. Moreover, unlike ES cells that are fraught with controversy regarding their derivation from embryos, iPS cells are derived from pre-existing somatic cells and enable the possibility of developing patient-tailored therapies[6,9]. These characteristics of iPS cells allow a unique opportunity to engineer autologous Insulin Producing Cells (IPCs) that can be used to replace pancreatic β-cells destroyed in T1D[6,9,44,45].

For therapy of T1D patients, relatively noninvasive procedures can be used to obtain somatic cells that can be reprogrammed into iPS cells, which upon conversion into IPCs would be transplanted back into the patient for effective and long-term maintenance of homeostatic blood glucose levels (Figure 1B). Our rationale for differentiating IPCs from iPS cells is that these cells will be a superior source of therapeutic cells compared to cadaveric pancreatic islets in their 1) unlimited availability, 2) patient-tailored derivation, and most significantly, 3) poor expression of MHC complexes by these cells may allow for evasion of autoimmune detection, giving rise to cells that are permanently functional without the requirement for immunosuppression, encapsulation procedures or recurrent transplantation[6].

Because iPS cells resemble ES cells, which are derived from the early embryo, their differentiation into mature cell types often requires mimicking of signals delivered to embryonic stem cells during organogenesis. The development of pancreatic β-cells in the embryo is a highly controlled and multi-stage process involving sequential activation and suppression of multiple signaling pathways[46,47]. The natural organogenesis of pancreatic β-cells thus provides extensive insight into the basis for differentiation protocols aimed at converting pluripotent stem cells into IPCs[12-16,48]. Below, we discuss the temporal role of the various signaling pathways and the signaling crosstalk that promotes pancreatic endocrine cell generation from PSCs.

Modulation of Signaling Pathways to Differentiate iPS Cells into IPCs Recapitulate Embryonic Development of the Pancreas

The process of differentiating ES or iPS cells into pancreatic endocrine cells traces the developmental stages observed during the formation of the pancreas during embryogenesis (Figure 2)[47]. Embryonic development frequently serves as a perfect model for constructing schemes for the differentiation of pluripotent stem cells into mature, functional derivatives. The insight obtained from studying pathways along which cells are driven to adopt their final fates, and capturing the identities of chief transcription factors activated in each of these intermediary states, is invaluable in helping us replicate appropriate signaling cues *in vitro* to achieve desired differentiation outcomes. As such, the basis underlying the structure of previously described IPC differentiation protocols is the recapitulation of decisive signals that govern embryonic development of the endocrine pancreas[47].

During embryogenesis, the pancreas arises from the foregut endoderm, which is originally derived from definitive endoderm that is specified by the synergistic activity of the Nodal and Wnt signaling pathways[47,49]. Wnt signaling functions to posteriorize the endoderm during gastrulation and provides instructive signals for patterning of the foregut endoderm for eventual regional allocation[49]. Further downstream specification of the foregut into the pancreatic fate is directed by Retinoic Acid (RA) signaling and inhibition of the Sonic Hedgehog (Shh) pathway[47]. Reprieve from Shh signaling permits the upregulation of Pdx1, which is the first sign of pancreatic specification[47]. Pdx1 is a transcription factor that is critical for organizing downstream transcription events that activate the pancreatic differentiation program[7]. Its deletion results in pancreatic agenesis[50]. However, the expression of Pdx1 is not restricted to pancreatic cells, and it is actually the coexpresison of Ptf1a and Pdx1 that defines the pancreatic progenitor population[51]. Proliferation of the pancreatic precursor pool is thought to be due to FGF10, which is produced by the contiguous pancreatic mesenchyme[52,53]. FGF10 signaling promotes activation of the Notch pathway, which enhances expansion of the pancreatic precursor pool but inhibits their further differentiation by antagonizing expression of Neurogenin3 (Ngn3)[52,53]. However, repression of Notch signaling in some pancreatic epithelial cells permits the expression of Ngn3, which gives rise to pre-endocrine multipotent progenitor cells that eventually give rise to all of the pancreatic endocrine cell lineages by initiating the activation of a cascade of transcription factors that manifest various pancreatic endocrine cell fates[52,53]. Pancreatic β-cell development is mostly orchestrated by the actions of the transcription factors Nkx2.2, Nkx6.1, Neurod1, MafA, Pax4 and Pax6[46,48].

Mirroring the organogenesis of the pancreas, the differentiation of iPSCs into IPCs involves several major lineage choices that must be managed correctly in order to efficiency give rise to IPCs. Modulation of the cell fate decisions involves reinforcement of positive signals toward particular cell types while inhibiting alternative lineage choices in tandem[6,47]. These lineage bifurcations are summarized in a simplified cartoon (Figure 2).

Stages 1 and 2

In order to become IPCs, the iPSCs must first be instructed to differentiate into DE cells[6,12-16,47,48]. The endoderm constitutes the innermost layer of cells of the three germ layers that form during gastrulation[49,54]. The process of differentiating iPSCs into endodermal cells involves multiple pathways. The key players in this process are the FGF pathway, BMP pathway, Nodal/Activin pathway and the Wnt pathway[55] (Figure 3A). The differentiation of iPSCs into definitive endodermal cells not only requires the upregulation of Nodal signaling but also transient activation of the Wnt pathway. Repression of the Wnt pathway following its transient activation is necessary to prevent mesodermal commitment[56]. Importantly, the differentiation of pluripotent stem cells into endoderm or mesoderm cells passes through a bipotent mesendodermal cell fate[57], which is an intermediate cell fate from which the cells can differentiate to both endoderm precursors and mesoderm precursors (Figure 2). Mesendodermal cells are not mature enough to efficiently form progenitors of the primitive gut tube[57]. A study of bipotent mesendodermal population of mice indicated that the mesendodermal cells are characterized by the presence of GSC, E-cadherin, and the mesodermal marker PDGFR-α[57]. Our own studies have suggested that these bipotent mesendodermal cells express the endodermal marker CXCR4 as well, which demonstrates that these cells represent a sort of hybrid state between the endoderm and mesoderm cell fates. Upon differentiation of mesendodermal cells into definitive endoderm or mature endoderm, the cells only express CXCR4 and lose the expression of PDGFR-α (Figure 2). Unpublished observations in our own laboratory have shown that the use of immature mesendodermal cells ultimately yields low percentages of insulin$^+$ positive cells, which indicates the critical requirement to generate true endoderm cells that express only the endodermal marker CXCR4 and not the mesodermal marker PDGFR-α.

Provision of FGF-7 after generating true DE cells primes the cells to becoming posterior foregut progenitors (Figure 2) as opposed to midgut progenitors (which generate the intestines), or anterior foregut progenitors (which derive the thymus, thyroid, lung and trachea)[58]. Posterior foregut progenitors give rise to tissues such as the liver and pancreas[58]. Controlling the precise specification of the posterior foregut progenitors into pancreatic precursor cells is accomplished in Stage 3.

Stage 3

After the generation of posterior foregut progenitors, the next major lineage bifurcation in the road to IPCs involves enforcing pancreatic specification while suppressing hepatic commitment of the cells in tandem[47] (Figure 2). The key developmental signaling pathways that play important roles in deriving the pancreatic endoderm from DE cells are the retinoic acid signaling pathway, FGF signaling pathway, BMP signaling pathway, Wnt signaling pathway and the Sonic hedgehog (Shh) signaling pathway[59] (Figure 3B). The cells from the endoderm are able to differentiate into various organs such as the heart, gut tube, pancreas, thyroid glands, lungs, upper respiratory structures and the liver. If DE cells are given appropriate the cues, they will differentiate into pancreatic cells, which are characterized by the presence of Pt1fa and Pdx1[51] (Figure 2).

Critically, the suppression of the Shh and BMP pathways alongside provision of retinoic acid signaling is essential for pancreatic endocrine development as opposed to hepatic precursor commitment[59] (Figures 2 and 3B). Repression of Shh signaling is accomplished by the use of SANT-1, a small molecule inhibitor[16] (Figure 3B). Furthermore, in addition to inhibition of Shh signaling, repression of Bone Morphogenic Protein (BMP) signaling is required for specifying DE cells to become pancreatic progenitors as opposed to hepatic progenitors[59] (Figure 3B). The BMPs, like the FGFs, are cues from the mesoderm during embryogenesis[47,59]. Noggin is a known antagonist of the BMP pathway[60] and is used in many protocols that attempt to form pancreatic progenitor cells from PSCs[12-16,48,59]. During embryogenesis, Noggin is endogenously produced in the mesoderm and diffuses to form a morphogen gradient that inhibits the BMP pathway, resulting in pancreatic specification in the gut tube[60].

The focus of Stage 3 is thus to generate pancreatic progenitor cells and block hepatic commitment. Stage 4 will instruct the differentiation of these pancreatic progenitor cells into endocrine precursor cells.

Stage 4

Once Pdx1$^+$ pancreatic precursor cells are generated, they can give rise to acinar, endocrine and exocrine cells of the pancreas[51] (Figures 2 and 3C). Provision of key molecular signals *in vitro* coaxes the specific differentiation of these precursor cells into endocrine progenitors that have the potential to ultimately differentiate into IPCs.

Ptf1a, Pdx1, and Sox-9 are the transcription factors that are expressed initially to define the pancreatic progenitor region in the endoderm[51]. In order to channel the differentiation of pancreatic cells into endocrine β-cells, suppression of the pathways that induce exocrine, ductal and acinar cell fate is necessary[61] (Figure 2). Genetic lineage tracing of the developing pancreas in several model organisms have revealed the genes that define pancreatic lineage bifurcations[61]. While Pdx1 is expressed by all pancreatic cell types, upregulation of neurogenin3 (Ngn3), Nkx6.1 and Nkx2.2 indicates the presence of endocrine precursor cells[62-64].

Notch signaling has been identified as one of the pathways to influence the differentiation towards the endocrine cell fate[52,53,65,66]. Notch signaling is known to require direct cell-cell interaction, and it manipulates cell behavior through the mechanism of lateral inhibition[65,67]. This feature denotes the ability for a cell to inhibit the differentiation of adjacent cells. More specifically in the case of Notch signaling, a cell with active Notch signaling can inhibit Notch signaling in neighboring cells and thus prevent them from assuming the same cell fate[67]. Ngn3, Dll1 and Hes1-mediated lateral inhibition plays a critical role in pancreatic endocrine vs. exocrine cell specification and maintenance of both the endocrine and exocrine progenitor cell pools[65,66,68,69]. The lateral inhibition of cell fate induced by Notch signaling could explain the disproportionately low percentage of endocrine cells present in the natural pancreas[69]. Hence, protocols aiming to produce pancreatic β-cells aim to downregulate Notch signaling in the multipotent pancreatic progenitor cell pool produced after the initial upregulation of Notch[12-16,48] (Figures 2 and Figure 3C). In our protocol, Notch signaling inhibition is indirectly manifested using DAPT, a competitive inhibitor of γ-secretase, of which Notch is a substrate[41,65] (Figure 3C).

Additionally, the role of TGF-β in pancreatic endocrine cell specification has also been studied[70,71]. GDF11 is a ligand for TGF-β and it has been shown to negatively regulate the number of endocrine precursor cells in mice[71]. Additionally, TGF-β signaling has been demonstrated to promote hepatic commitment as opposed to pancreatic specification in differentiating PSC cultures *in vitro*, confirming a negative impact of TGF-β signaling on the differentiation of iPS cells into IPCs[58]. Thus, in our protocol, we utilize

Alk5 inhibitor II to block TGF-β signaling by inhibiting ALK5, a receptor for TGF-β[72] (Figure 3C).

By modulating these signals, the goal of Stage 4 is to generate endocrine precursor cells (Figure 3C). Stage 5 will differentiate these cells into specifically insulin-secreting pancreatic β-cells, as opposed to the other hormone-producing cell types in the endocrine pancreas.

Stage 5

The final stage of the differentiation into IPCs involves the differentiation of endocrine precursor cells into IPCs while blocking differentiation into multihormonal or glucagon-expressing lineages[6] (Figure 2). This process may be facilitated by exposure to hormones such as IGF-1 and GLP-1[73] as well as small molecules such as nicotinamide[74,75], which is a PARP inhibitor, and thyroid hormone (T3), which is thought to promote β-cell maturation[76,77]. Nicotinamide is widely known to promote the differentiation of progenitor cells into pancreatic β-cells[74]. It additionally acts to enhance islet cell regeneration and increase insulin biosynthesis[75]. It has been shown to be an inducer of endocrine differentiation in human pancreatic fetal cells[74]. Furthermore, its role in endocrine cell differentiation was found to be mediated by increased expression of *MafA*, a key transcription factor in the development and maturation of functional pancreatic β-cells[75,77]. T3 has also been shown to be a direct inducer of *MafA* by binding to its promoter, and was shown to promote pancreatic β-cell development in rats and enhance glucose-stimulated insulin secretion in a *MafA*-dependent manner *in vitro*[76]. GLP-1 has long been known to promote the survival, proliferation and function of pancreatic β-cells by activating the cAMP-protein kinase A (PKA) and cAMP-EPAC2 (a Guanine Exchange Factor) signaling pathways[78,79]. The inhibition of K^+ channels by GLP-1 depolarizes the membrane of the β-cell, which leads to the opening of voltage dependent Ca^{2+} channels, ultimately resulting in insulin secretion[80]. IGF-1 promotes the maturation of β-cells and signals through Insulin Receptor Substrate 2 (IRS-2), which is shared with insulin, to activate the Akt pathway[81-83]. The Akt pathway leads to cell proliferation and inhibition of apoptosis[81]. Combining all of these agents in the last stage of differentiation promotes the expression of insulin, insulin secretion and increase in cell proliferation.

Shortcomings of Prior Attempts to Generate Insulin Producing Cells

The generation of IPCs from human pluripotent stem cells is hardly unchartered territory, although ES cells have been predominantly used instead of iPS cells[12-16,48]. Several groups have successfully developed protocols for deriving pancreatic progenitor cells from human pluripotent stem cells through stepwise exposure to signaling factors designed to direct the cells through transitory progenitor stages toward the pancreatic β-cell fate[12-16,48]. These endocrine precursor cells appear to activate the expression of transcription factors normally expressed by pancreatic β-cells, such as Nkx6.1, Nkx2.2, and most notably, the pancreatic master regulator Pdx1[12-16,48]. Immunofluorescence analysis of the terminally differentiated cells confirms their expression of pancreatic endocrine hormones including insulin, glucagon, and more rarely, somatostatin[12-16,48]. Additionally, it has been shown independently by several groups with individual protocols that these cells acquire the capability to correct or prevent the onset of diabetes in streptozotocin (STZ)-treated mice after their transplantation by production of physiologically relevant levels of human insulin[13-16].

These reports, however salient, highlight the requirement for *in vivo* maturation of the endocrine precursor cells before they become competent insulin secreting cells. The cells derived *in vitro* are devoid of mature β-cell characteristics[12-16]. In fact, flow cytometry quantification of the percentage of cells that produce insulin in the *in vitro* cultures reveals that only 10-15% of the cells are actually insulin-expressing[12,16]. Additionally, when applied through glucose stimulated insulin secretion (GSIS) assays, which have often not been reported at all, glucose responsiveness is absent or at best, very poor[12-16,48]. Finally, it appears that the cultures mostly consist of "confused" cells that are in limbo between distinct pancreatic endocrine lineages, frequently co-expressing multiple pancreatic hormones[12-16,48]. Thus, it appears that although ES cell-derived pancreatic progenitor cells become functional IPCs when placed *in vivo* after a period of months, mature IPCs cannot currently be generated *in vitro*[12-16,48].

We envisioned that increasing the efficiency of IPC derivation *in vitro* would dramatically shorten the time required to make functional and robust insulin producing grafts *in vivo*, and also reduce the amount of biological material needed to exert the same glucose-correcting effects, which is significant especially considering the human size. Here, we reasoned that such substantial changes could be achieved by transforming the 2D culture systems used in the past into 3D differentiation platforms, which would greatly foster cell-cell contact and crosstalk through clustering[6]. For fabrication of 3D iPS cell clusters, we incorporated matrigel, a bioactive extracellular matrix concoction derived from mouse sarcoma cells, to exploit the scaffold-embedded signaling and for more effective capture of soluble growth factors supplemented into the differentiation media cocktail[84,85].

A Five-Stage 3D Differentiation Protocol for the Differentiation of iPS Cells Into IPCs

Recurrent issues inherent in many current protocols for the directed differentiation of ES and iPS cells into mature cell types *in vitro* is the poor efficiency of derivation and suboptimal functional capacity of these cells[12-16,48]. We attribute at least some of these shortcomings to the 2D cell culture systems commonly used by laboratories, which we believe limits cell-cell signaling by confining the communication across cells to only one plane[6]. The perfect example of efficient and complete differentiation lies in the Inner Cell Mass (ICM), the early embryonic structure that derives an entire organism. In fact, ES cells are isolated from the ICM, which is a cluster of pluripotent cells located within the cavity of the blastocyst, the wall of which forms the trophoblast[10] (Figure 4A). Given this knowledge, it is only logical that ES cells and iPS cells should be differentiated while assembled into similar 3D clusters, as this is much more physiologically relevant and often better organized than 2D platforms. The surface area allocated toward cell-cell contact and signaling crosstalk is much greater when cells are congregated into 3D clusters than if they were gathered into flat colonies, where communication across cells only occurs at one plane[6] (Figure 4B). Several tissues have successfully been derived from human pluripotent stem cells via a 3D platform[32,33,38]. Notably, a recent report on the derivation of cerebral organoids from human iPS cells established that 3D differentiation gave rise to larger organoids, with more physiologically relatable structure and much better organization of tissue, compared to what was achieved derived via 2D differentiation[38].

Ample evidence in the literature supports the use of 3D differentiation for the generation of IPCs from iPS cells[86]. In one report, a strategy was described for efficiently reprogramming pancreatic exocrine acinar cells, which produce digestive enzymes, into insulin-producing pancreatic β-cells[87]. The long-term persistence of these induced β-cells was shown to be strongly associated with the formation of 3D islet-like clusters[87]. This observation supports the longstanding notion that islets provide a niche that promotes survival of pancreatic β-cells. Pancreatic β-cells within natural islets lose functional glucose-stimulated insulin secretion once dissociated into single cells[88-91]. Additionally, crosstalk within the islet through Eph-ephrin signaling has been shown to be important for functionality of pancreatic β-cells[92], implicating a role for cell-cell contact and communication in promoting pancreatic β-cell function. Thus, 3D clustering is critical for the functionality of pancreatic β-cells and this feature must be incorporated into differentiation protocols aiming to convert iPS cells into IPCs.

To accomplish this, we decided to use a bioactive scaffold-based system to induce 3D clustering of the differentiating cells. The vast body of work demonstrating the regulation of dynamic behavior in cells by the ECM prompted us to utilize matrigel as a bioscaffold since it is uniquely endowed with both potent biological activity as well as physical features suitable for inducing 3D differentiation of iPS cells. Matrigel is prepared from the solubilized basement membranes of the Engelbreth-Holm-Swarm (EHS) mouse sarcoma, which results in a mixture that is rich in extracellular matrix (ECM) proteins[85]. The principal component of matrigel is laminin, a noncollagenous glycoprotein, followed by collagen IV, heparan sulfate proteoglycans (HSPGs) and entactin[84]. Matrigel also consists of ECM-bound growth factors, including bFGF, EGF, IGF-1, PDGF, NGF, TGF-β and tissue plasminogen activator[84]. Here, we utilized matrigel not only as a substrate for inducing 3D clustering, but also as a bioactive scaffold for enhancing the activity of stage-specific growth factors supplemented into differentiation media. By sequestering and tethering growth factors due to their negative charge, the ECM makes them more accessible to cells and in some cases may prolong their activity by increasing binding affinities or protecting them from degradation[93]. The ECM also acts as a storage site for growth factors, thereby modulating the local intensity of their activity upon cells in the immediate vicinity[94]. In fact, HSPGs have been shown to play critical roles during development in shaping morphogen gradients, and hence the ensuing signaling processes, of factors such as Wnt, Hedgehog, FGF, BMP, TGF-β and Dpp[95]. Additionally, ECM components have been described to play accessory roles in signaling transduction pathways as coreceptors or stabilizing components, which is the case for basic Fibroblast Growth Factor 2 (FGF-2)[96].

The interaction of the islet ECM with native pancreatic β-cells is predominantly via β1 integrins, which transmit signals that enhance β-cell survival and proliferation, as well as promote insulin expression[97]. Although pancreatic β-cells do not produce ECM directly, it is their effect on intra-islet endothelial cells that results in the production of a rich ECM that encases the islets[98]. This ECM consists of laminins, type IV collagen and perlecan. The laminins produced by intra-islet endothelial cells support islet function[99] and have been shown to transduce downstream signaling cascades involving survival and adhesion-related proteins, such as focal adhesion kinase (FAK), MAPK, Akt and Rho family small GTPases, among many others[100]. Altogether, these findings suggest an important role for the ECM in maintaining the survival and function of pancreatic β-cells. In turn, we have adapted the ECM as a physiological substrate in our differentiation scheme by utilizing matrigel, which is very rich in laminin.

In addition to employing a 3D platform for instructing pancreatic endocrine differentiation of human iPS cells, we have adapted the relevant key signaling pathways that play roles in the induction of the pancreatic β-cell fate. As described above, the process of differentiating ES or iPS cells into pancreatic endocrine cells traces the developmental stages observed during the formation of the pancreas during embryogenesis[47]. Figure 2 elucidates the developmental stages that the cells trace when differentiating to IPCs. These transitions in cell fate typically involve various signaling pathways that direct cells to assume temporary identities in the path to becoming the final cell type. We and others[12-16,48] have incorporated each of these critical signaling events into a comprehensive and dynamic stepwise differentiation scheme that drives the pluripotent stem cells through various progenitor cell populations before reaching the final pancreatic β-cell fate (Figure 5).

The process first begins with specifying the definitive endoderm germ layer[47], from which the pancreas is derived, through Activin A and Wnt3a signaling[16] (Stage 1). L-Ascorbic acid, also known as Vitamin C, is added to promote extracellular matrix production and enhance cell proliferation[77]. Incorporated next is FGF-7, which acts to regionalize the definitive endoderm into the posterior foregut[16] (Stage 2).

Following this, the cells are exposed to Retinoic Acid and SANT-1, an inhibitor of the Shh pathway[16], in order to posteriorize the gut tube and promote pancreatic differentiation as opposed to hepatic specification[59]. Reinforcing suppression of hepatic differentiation, Noggin is added to this media cocktail as well[16], and it functions to inhibit BMP signaling[60]. The cells are simultaneously treated with TPB[16], an activator of Protein Kinase C, which is involved in the proliferation and differentiation of pancreatic β-cells and also plays a role in the regulation of glucose-stimulated insulin secretion[101]. The aim of this stage is to generate Pdx1$^+$ pancreatic precursor cells (Stage 3).

The cells are then instructed to become pancreatic endocrine precursor cells by carrying over certain cues from Stage 3, such as Noggin and low-dose Retinoic Acid signaling, and supplementing them with inhibitors of TGF-β signaling[58] and suppression of Notch signaling[77,102], which actively inhibits endocrine differentiation by the process of lateral inhibition[65-69]. Suppression of TGF-β signaling comes in the form of treatment with the ALK5 inhibitor II, which is an ATP-competitive inhibitor of the TGF-β family receptor activin receptor-like kinase (ALK5)[72]. Repression of Notch signaling is indirectly accomplished by blockade of its ligand, γ-secretase, using DAPT[41]. In addition, this stage of differentiation introduces several drivers of pancreatic β-cell development, such as thyroid hormone (T3)[76,77] and the incretin GLP-1[73]. Heparin is added to the differentiation cocktail to promote cell survival[77] (Stage 4).

Finally, in the last stage of differentiation, the goal of which is to convert pancreatic endocrine precursor cells into insulin$^+$ IPCs, specific inducers of insulin are added in addition to agents that promote the maturation and development of pancreatic β-cells, such as nicotinamide[44,74,75], IGF-1[73,83], GLP-1 and T3. TGF-β blockade by ALK5i is sustained and heparin treatment is continued (Stage 5).

By combining a novel 3D bioscaffold-based culture platform with well-selected and optimized signaling cues inspired by embryogenesis of the pancreatic β-cell, we envisioned that we could drastically improve the efficiency of generation of IPCs that not only expressed insulin and resembled pancreatic β-cells, but were also functional and responded to high glucose stimulation with insulin secretion.

Figure 1. The etiology of T1D and the potential of iPS cells in therapy of T1D

(A) T1D is the result of autoimmune destruction of pancreatic β-cells located in the Islets of Langerhans. These cells produce insulin, which regulates blood glucose levels in the body by transporting glucose into cells. Ablation of pancreatic β-cells results in insufficient insulin production, leading to less glucose transport into cells and high blood glucose levels, which can cause many secondary pathologies. **(B)** In the case of cell replacement therapy for T1D using iPS cells, the diabetic patient would donate fibroblasts through a skin biopsy, which upon being reprogrammed into self-renewing iPS cells, would be converted into Insulin Producing Cells (IPCs) that can be transplanted back into the patient. This strategy allows for the provision of a potentially unlimited source of patient-specific IPCs, obviating the need for immunosuppression.

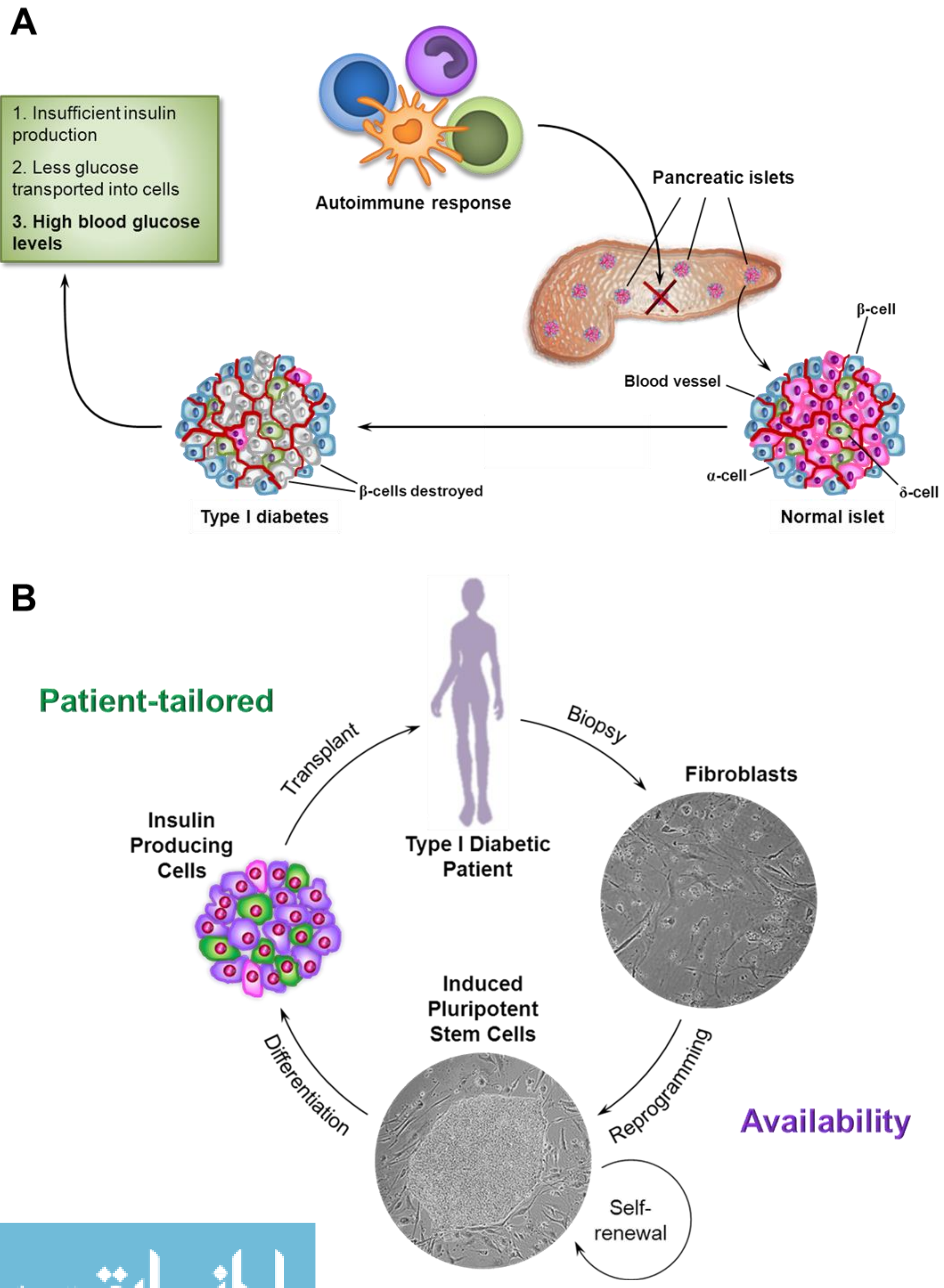
A
1. Insufficient insulin production
2. Less glucose transported into cells
3. High blood glucose levels
Autoimmune response
Pancreatic islets
β-cell
Blood vessel
α-cell
δ-cell
Normal islet
β-cells destroyed
Type I diabetes
B
Patient-tailored
Transplant
Biopsy
Type I Diabetic Patient
Fibroblasts
Insulin Producing Cells
Induced Pluripotent Stem Cells
Differentiation
Reprogramming
Availability
Self-renewal

Figure 2. Lineage bifurcations in the road to IPCs

Pluripotent stem cells (PSCs) encounter several major cell fate decisions in the process of differentiating into insulin producing cells (IPCs). Optimal transition of the cells through various progenitor stages requires the simultaneous provision of positive signals instructing differentiation as well as inhibitory cues to suppress alternative lineage commitment. To generate IPCs, the DE cell fate must first be specified, which is achieved with continuous Nodal signaling and Wnt signaling only in the early stage of the differentiation. DE cells express CXCR4, Sox17 and Foxa2. It is critical to ensure that the cells become true DE cells as opposed to maintaining the mesendodermal identity, which is meant to be a transitional state in the differentiation to DE cells. If the cells fail to transition into the DE cell fate, this may compromise the yield and maturity of resultant IPCs. After DE cells have been generated, they must be directed to become pancreatic endoderm (Ptf1a$^+$/Pdx1$^+$ cells) as opposed to hepatic endoderm. Here, retinoic acid signaling strongly promotes pancreatic differentiation and slightly promotes hepatic differentiation. To primarily differentiate the cells toward the pancreatic lineage, hepatic differentiation cues must be suppressed by inhibiting Shh and BMP signaling with SANT-1 and Noggin, respectively. After generating pancreatic precursor cells, Ngn3$^+$ endocrine progenitors are cultivated by suppressing the differentiation toward exocrine or ductal progenitors. Finally, Ngn3$^+$ endocrine progenitor cells must mature to become monohormonal insulin producing cells (IPCs), ideally with minimal generation of immature multihormonal cells or glucagon-expressing cells.

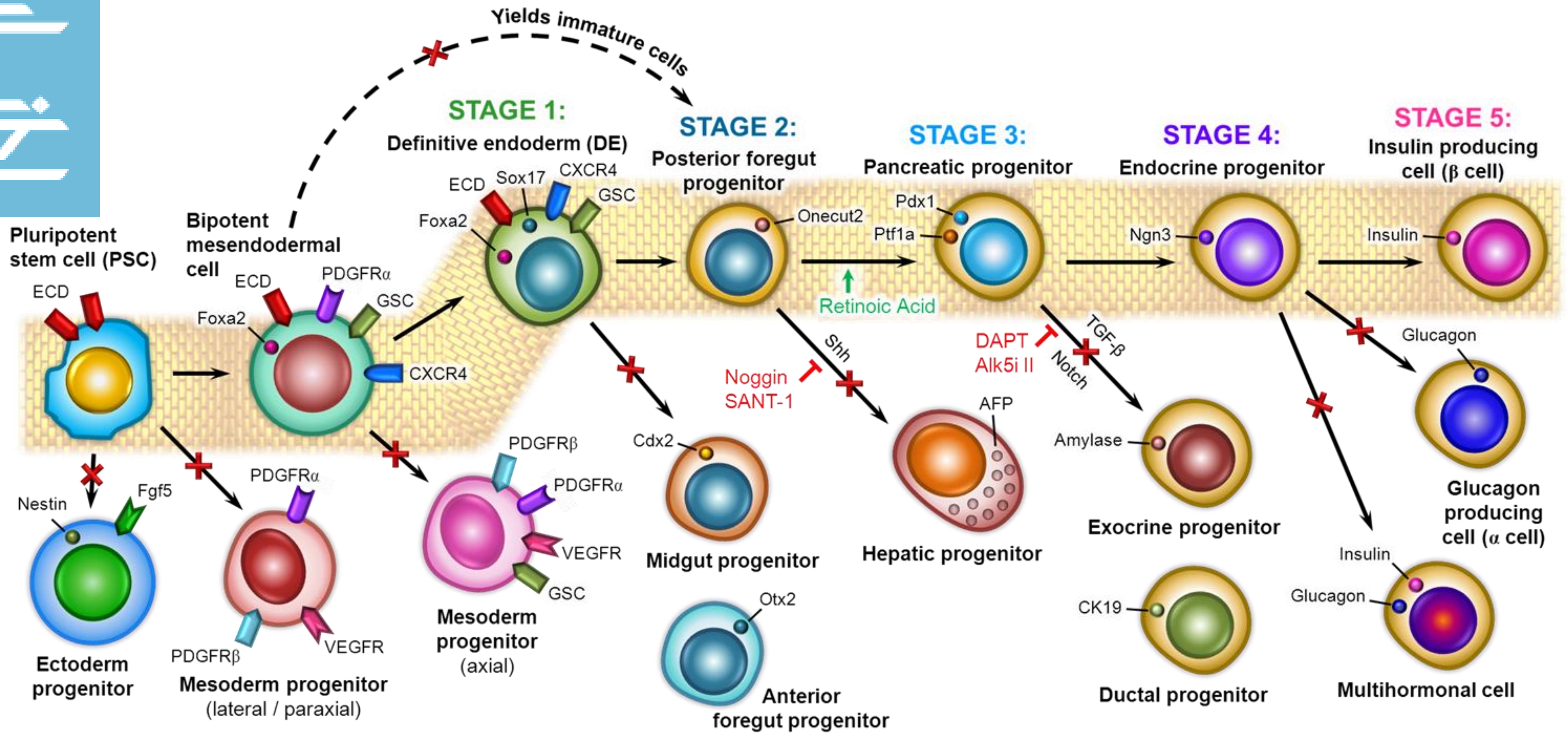
Yields immature cells
STAGE 1:
Definitive endoderm (DE)
STAGE 2:
Posterior foregut progenitor
STAGE 3:
Pancreatic progenitor
STAGE 4:
Endocrine progenitor
STAGE 5:
Insulin producing cell (β cell)
Pluripotent stem cell (PSC)
ECD
Bipotent mesendodermal cell
ECD
Foxa2
PDGFRα
GSC
CXCR4
ECD
Sox17
CXCR4
GSC
Foxa2
Onecut2
Pdx1
Ptf1a
Retinoic Acid
Ngn3
Insulin
Nestin
Fgf5
Ectoderm progenitor
PDGFRα
PDGFRβ
VEGFR
Mesoderm progenitor
(lateral / paraxial)
PDGFRβ
PDGFRα
VEGFR
GSC
Mesoderm progenitor
(axial)
Cdx2
Midgut progenitor
Otx2
Anterior foregut progenitor
Noggin
SANT-1
Shh
AFP
Hepatic progenitor
DAPT
Alk5i II
TGF-β
Notch
Amylase
Exocrine progenitor
CK19
Ductal progenitor
Glucagon
Glucagon producing cell (α cell)
Insulin
Glucagon
Multihormonal cell

Figure 3. Modulation of signaling pathways to impact lineage choices in the differentiation of iPS cells into IPCs

(A) The endoderm cell choice. iPSCs have the potential to develop into cells of all three germ layers, namely the endoderm, mesoderm and ectoderm. Cells from each of these germ layers have unique phenotypes and exclusive potential to derive particular tissues. Activin/Nodal signaling strongly promotes endoderm generation, whereas BMP signaling promotes mesodermal commitment while suppressing endoderm differentiation. On the other hand, Wnt signaling drives both the endodermal and mesodermal cell fates. In order to recapitulate the delivery of such signals for *in vitro* differentiation of iPSCs into DE cells, transient Wnt3a treatment and long-term Activin A treatment are utilized. Wnt3a has been replaced with a superior and specific GSK-β inhibitor, CHIR99021, which mimics the action of canonical Wnt signaling by promoting β-catenin accumulation and transcriptional activity.

(B) The hepatic vs. pancreatic cell choice. In addition to deriving the lung and thyroid, DE cells have the potential to generate both the pancreatic and hepatic tissues. Since these two lineages are closely related, it is paramount that the differentiation cues are optimized to promote selective differentiation of $Pdx1^+/Ptf1a^+$ pancreatic precursors as opposed to $AFP^+/Hnf\text{-}3\beta^+$ hepatic precursors. Retinoic acid and FGF signaling strongly endorse pancreatic specification but may also slightly promote hepatic differentiation. On the other hand, the Shh, Wnt and BMP signaling pathways strongly reinforce hepatic lineage commitment while actively suppressing pancreatic differentiation. As a result, in order to convert DE cells into the pancreatic endoderm, positive signals (such as retinoic acid and FGF-7) are provided in tandem with cues that actively suppress signaling pathways driving hepatic differentiation (SANT-1 and Noggin serve to inhibit Shh and BMP signaling, respectively).

(C) The endocrine cell choice. Pancreatic precursor cells have the potential to derive progenitor cells that eventually become the three major cell types in the pancreas: Ngn3$^+$ endocrine progenitors, p48$^+$ exocrine progenitors and Hnf-6$^+$ ductal progenitors. Notch-mediated lateral and TGF-β signaling inhibition typically inhibit endocrine specification in the embryonic pancreas, which likely explains the disproportionately small percentage of endocrine islets in the natural pancreas. To improve endocrine differentiation of Pdx1$^+$ pancreatic precursor cells *in vitro*, effective differentiation protocols implement suppression of Notch signaling by exploiting gamma secretase inhibitors such as DAPT, as well as repression of TGF-β signaling using Alk5 inhibitor II (Alk5i), which blocks Alk5, a receptor for TGF-β. In addition to suppressing alternative lineage commitment, effective differentiation protocols provide reinforcing signals that promote endocrine specification and maintenance. This is mediated by utilizing PKC agonists, such as TPB.

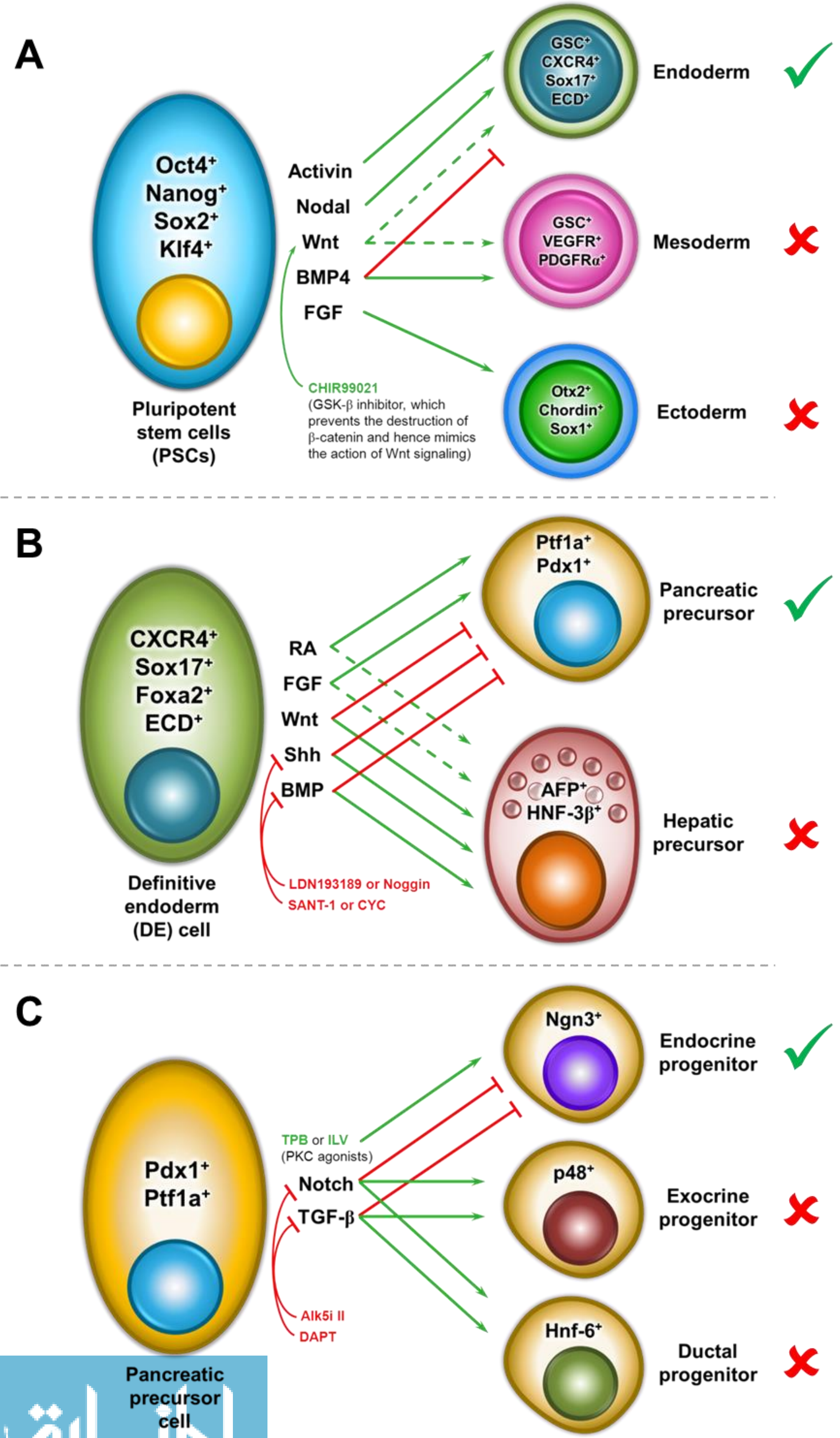
A
Oct4+
Nanog+
Sox2+
Klf4+
Pluripotent stem cells (PSCs)
Activin
Nodal
Wnt
BMP4
FGF
CHIR99021
(GSK-β inhibitor, which prevents the destruction of β-catenin and hence mimics the action of Wnt signaling)
GSC+
CXCR4+
Sox17+
ECD+
Endoderm
✓
GSC+
VEGFR+
PDGFRα+
Mesoderm
✗
Otx2+
Chordin+
Sox1+
Ectoderm
✗
B
CXCR4+
Sox17+
Foxa2+
ECD+
Definitive endoderm (DE) cell
RA
FGF
Wnt
Shh
BMP
LDN193189 or Noggin
SANT-1 or CYC
Ptf1a+
Pdx1+
Pancreatic precursor
✓
AFP+
HNF-3β+
Hepatic precursor
✗
C
Pdx1+
Ptf1a+
Pancreatic precursor cell
TPB or ILV
(PKC agonists)
Notch
TGF-β
Alk5i II
DAPT
Ngn3+
Endocrine progenitor
✓
p48+
Exocrine progenitor
✗
Hnf-6+
Ductal progenitor
✗

Figure 4. 3D differentiation involves seeding cell clusters in a matrigel scaffold

(A) The blastocyst, which is a cavity-filled ball of cells, contains a cluster of cells termed the inner cell mass (ICM) that gives rise to all of the tissues of the organism. The wall of cells surrounding the ICM and the blastocoel is the trophoblast that derives the placenta. 3D clustering of cells naturally occurs in embryonic development and affords greater cell-cell contact than flat 2D culture systems. **(B)** 3D differentiation of cells allows clustering and hence much greater surface area for cell-cell contact and communication to take place, enhancing transmission of molecular signals and hence differentiation. In contrast, 2D differentiation limits the contact among cells to only one plane.

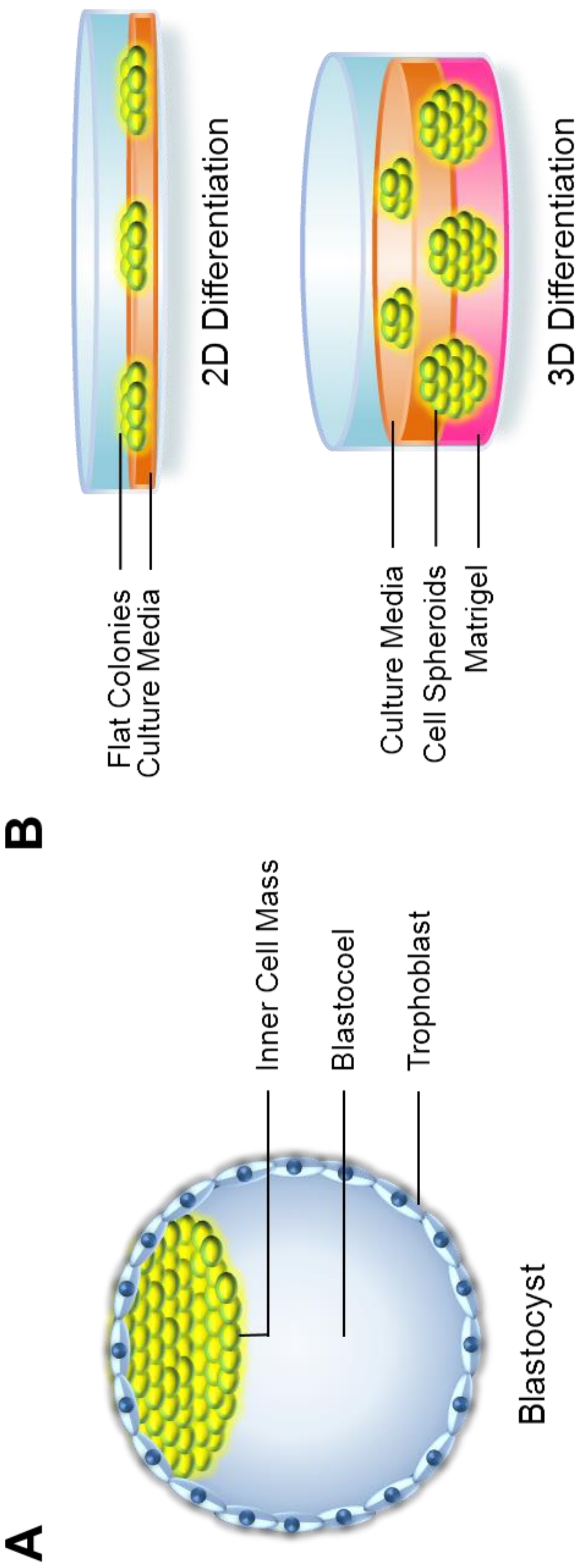
A
Blastocyst
Inner Cell Mass
Blastocoel
Trophoblast
B
Flat Colonies
Culture Media
2D Differentiation
Culture Media
Cell Spheroids
Matrigel
3D Differentiation

Figure 5. The differentiation of iPS cells into Insulin Producing Cells (IPCs) involves five stages of differentiation

This differentiation schema shows in a clockwise manner the five stages of differentiation that iPSCs undergo in order to become IPCs, and it summarizes the components and signaling molecules are supplemented into in each differentiation media cocktail.

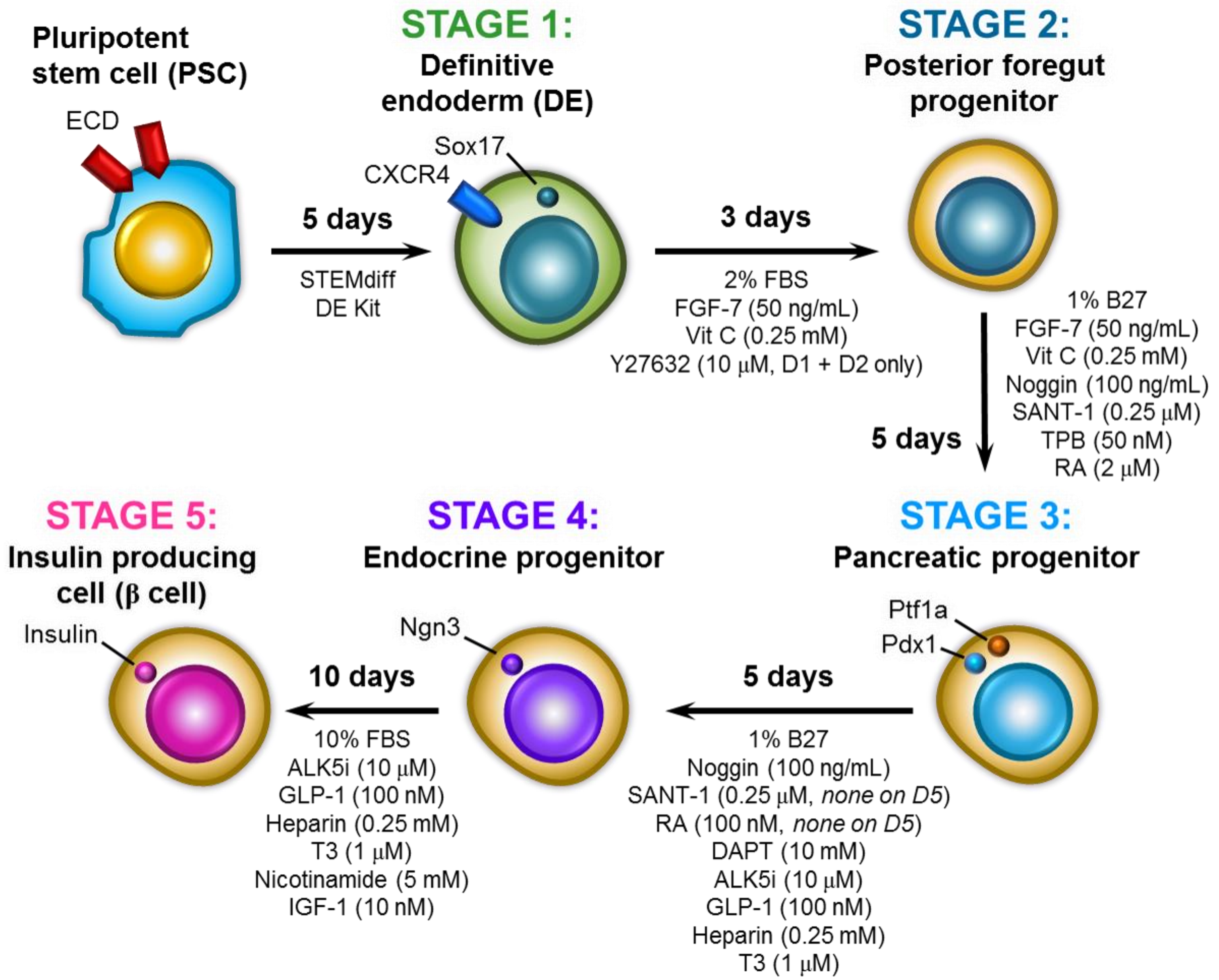
Pluripotent stem cell (PSC)
ECD
5 days
STEMdiff
DE Kit
STAGE 1:
Definitive endoderm (DE)
Sox17
CXCR4
3 days
2% FBS
FGF-7 (50 ng/mL)
Vit C (0.25 mM)
Y27632 (10 µM, D1 + D2 only)
STAGE 2:
Posterior foregut progenitor
5 days
1% B27
FGF-7 (50 ng/mL)
Vit C (0.25 mM)
Noggin (100 ng/mL)
SANT-1 (0.25 µM)
TPB (50 nM)
RA (2 µM)
STAGE 3:
Pancreatic progenitor
Ptf1a
Pdx1
5 days
1% B27
Noggin (100 ng/mL)
SANT-1 (0.25 µM, *none on D5*)
RA (100 nM, *none on D5*)
DAPT (10 mM)
ALK5i (10 µM)
GLP-1 (100 nM)
Heparin (0.25 mM)
T3 (1 µM)
STAGE 4:
Endocrine progenitor
Ngn3
10 days
10% FBS
ALK5i (10 µM)
GLP-1 (100 nM)
Heparin (0.25 mM)
T3 (1 µM)
Nicotinamide (5 mM)
IGF-1 (10 nM)
STAGE 5:
Insulin producing cell (β cell)
Insulin

CHAPTER II
MATERIALS AND METHODS

Human iPS cell lines and culture conditions

Two human iPS cell lines were utilized in this study. GM23226 (ND human iPS cells) and GM23262 (T1D human iPS cells) were purchased from the Coriell Institute for Medical Research (Camden, NJ). As described previously[42], these human iPS cells were grown on irradiated Mouse Embryonic Feeder (MEF)-coated (Catalog Number: GSC-6001G, Global Stem, Gaithersburg, MD) 6-well plates in culture medium containing Dulbecco's modified Eagle's medium/F-12 (DMEM/F-12) supplemented with 20% KnockOut Serum Replacement (Catalog Number: 10828-028, Invitrogen, Grand Island, NY), 50 µg/mL penicillin, 50 µg /mL streptomycin, 1mM GlutaMAX, 1X NEAA, 100 µM 2-mercaptoethanol (Sigma-Aldrich, St. Louis, MO), and 10ng/mL basic Fibroblast Growth Factor (bFGF, Catalog Number: PHG0261, Invitrogen, Grand Island, NY). Unless otherwise noted, all cell culture reagents were purchased from Invitrogen (Grand Island, NY). Cells were incubated at 37°C in a 5% CO_2 humid atmosphere. The cells were maintained in their undifferentiated state through daily media changes and were passaged every 5-7 days.

Differentiation of human iPS cells into Insulin Producing Cells *in vitro*

The differentiation of human iPS cells into IPCs lasted 27 days and was performed by driving cells through five stages of differentiation, each with its own set of media cocktails, listed in Table 1. The cell culture media was changed for the cells every day and the media prepared fresh every day. Small molecules and growth factors (ordering information for which is listed in Table 2) were supplemented into warm base media immediately prior to media changes in a dim-light hood.

To initiate the differentiation of iPS cells into definitive endoderm (DE) cells, they were first maintained in the STEMdiff™ Definitive Endoderm Kit (Catalog Number: 05110, Vancouver, BC) for 5 days, while cultured on feeder cells as colonies. On day 5, expression of DE cell markers, such as CXCR4 and Sox17, was assessed on these cells to ensure that differentiation was proceeding properly. After confirmation that the culture contained >90% CXCR4$^+$Sox17$^+$ cells, the rest of the DE cells were harvested and 3D differentiation was initiated with Media 2. On the day prior to initiating 3D differentiation, human ESC-qualified matrigel (Catalog Number: 354277, Corning Inc., Tewksbury MA) was thawed on ice overnight in a 4°C refrigerator. On the day of 3D differentiation (D5), a 1:1 (vol/vol) mixture of liquid matrigel was mixed with cold DMEM/F-12 in a chilled conical tube. Then, in a 24 well plate, 100 µL of the 1:1 mixture was deposited in the center of each well and the plate was incubated at 37°C for 5 minutes. When a rigid dome had formed in the center of each well, 400 µL of the 1:1 mixture was added on top of this dome and the plate was shaken to allow the matrigel mixture to spread evenly, resulting in a 500 µL layer of matrigel in each well. The plate was replaced at 37°C for 3 hours to allow the matrigel to solidify sufficiently.

2.5 hours into the incubation, the DE cells were harvested via cell scraping with a 1000 µL pipette tip and suspended in warm Media 2, which contains Y27632, a ROCK inhibitor intended to promote cell survival. This cell suspension was distributed on top of the matrigel, with each well thus containing 500 µL of the matrigel mixture and 500 µL of the cell suspension. Typically, we transferred two wells of DE cells cultured in a 6 well plate into one well of a 24 well plate containing matrigel. Generally, within the first 24 hours, most of the DE cell clusters embed into the matrigel scaffold, forming sphere-like clusters at varying depths in the matrigel layer. The plate was left undisturbed for 24 hours, at which point, the first media change in 3D culture was performed by tilting the plate, removing the media, centrifuging the media to pellet unembedded cell clusters, and resuspension of any leftover cells in fresh, warm Media 2 for replacement into the wells.

48 hours post-initiation of 3D culture, any unembedded cells were discarded and no longer replaced into the wells. After beginning to use Media 7, which contains 10% FBS and thus contains some enzymes that digest the matrigel, the matrigel layer becomes weaker and so some cell clusters are liberated from the gel layer. Thus, in the last ten days of differentiation during which Media 7 is utilized, the media is centrifuged to rescue unembedded cells and leftover cell clusters are replaced into the wells so that they are not lost.

Demethylation of iPS cells

5-aza-2’-deoxycytidine (5-aza-DC, Catalog Number: A3656-5MG, Sigma-Aldrich, St. Louis, MO) was used to transiently demethylate iPS cells at concentrations of 1 nM and 10 nM, the latter of which was most effective while enabling cell viability. These concentrations were selected after a thorough screen of concentrations that could be used to induce demethylation while maintaining cell viability (described in Chapter IV).

After completing 4 days of differentiation in DE differentiation media, the cells were treated with fresh media supplemented with 5-aza-DC. 5-aza-DC was treated for 18 hours, which spanned the last day of DE differentiation, before being washed with warm DMEM/F-12 three times and harvested as described in the next section for initiating 3D differentiation into pancreatic precursor cells.

Because of the highly unstable nature of 5-aza-DC[103], special measures were taken to efficiently and rapidly aliquot the compound while preserving its effectiveness. Prelabeled Eppendorf tubes were kept at -20°C to keep them cold, and any 15 mL conical tubes were kept on ice. To dissolve 5-aza-DC, first a 100mM "superstock" solution was prepared by adding 219 µL of DMSO to 5 mg (21.9 µmole) of 5-aza-DC. After vortexing the solution, a 1:10 dilution with a final concentration of 10 mM was prepared by adding 1970 µL of sterile ultrapure water. This mixture was filter-sterilized using a chilled 0.22 µM mesh attached to a cold 3 mL syringe. 250 µL aliquots of the 10 mM superstock were frozen in large Eppendorfs for later dilution. A separate fraction of the 10 mM superstock was diluted in 2250 µL of sterile ultrapure water to yield a 1 mM superstock, of which 25 µL were distributed to approximately 100 chilled small Eppendorf tubes and immediately frozen at -80°C. On the day of demethylation treatment, a vial of 1 mM 5-aza-DC was thawed on ice and diluted 1:100 in cold sterile ultrapure water to yield a 10 µM stock solution that was finally ready for treatment.

1 µL of the 10 µM stock per 1 mL of differentiation media was used to create a final concentration of 10 nM 5-aza-DC, whereas 0.1 µL of the 10 µM stock per 1 mL of differentiation media was used to create a final concentration of 1 nM 5-aza-DC.

Human islets

Human islets used in this study were provided by the Integrated Islet Distribution program (IIDP). All methods and practices regarding the culture of islets were followed based on IIDP standard operating procedures. Briefly, immediately upon their receipt, islets were removed from the original flask and deposited into low attachment T75 flasks in the media they were supplied in. The islets were cultured upright for 48-72 hours in a 5% CO_2 humid atmosphere at 37°C to allow for the restoration of homeostatic metabolism prior to using the islets for any experimental procedures.

Flow cytometry and antibodies

For all flow cytometry experiments, undifferentiated iPS cells were used as negative controls for staining, and human islets (supplied by the IIDP, rarely available in sufficient quantities) or βTC3 mouse insulinoma cells (supplied as a gift) were used as positive controls for staining. Cells were stained with the primary antibodies listed in Table S1. All antibodies except for the rabbit anti-glucagon were pre-conjugated to fluorochromes to minimize background staining. Isotype controls were produced for all cell types in all staining procedures. Data were acquired on a BD LSR II instrument and analyzed with FlowJo Software (Ashland, OR). The list of antibodies used for flow cytometric analysis is provided in Table 3.

Definitive Endoderm Marker Expression Analysis

For assessment of DE differentiation efficiency, cells from D5 of differentiation (end of Stage 1) were incubated at room temperature for 2-5 minutes with TrypLE Express (Invitrogen, Grand Island, NY), dissociated into a single cell suspension, filtered through a 70μm mesh and washed with 1X PBS (Invitrogen, Grand Island, NY) before being distributed into FACS tubes. After extracellular staining with antibodies against CXCR4 or PDGFR-α for 15 minutes in the dark at room temperature, the cells were washed and then permeabilized via saponin using the BD Cytofix/Cytoperm Kit (Catalog Number: 554714, BD Biosciences, San Jose, CA). The cells were incubated with anti-Sox17 for 30 minutes in the dark at room temperature before being washed and resuspended in 1X PBS for flow cytometric analysis.

Pancreatic Transcription Factor Expression Analysis

For assessment of expression of pancreatic transcription factors (Pdx1, Nkx6.1 and NeuroD1), matrigel-seeded differentiating cell clusters on differentiation D15 (end of Stage 4) were recovered by treatment with Dispase (Catalog Number: 354235, BD Biosciences, San Jose, CA) for 5 minutes at 37°C, followed by gentle suspension to further break down the matrigel. After washing with 1X PBS and centrifugation, the cell clusters were incubated with TrypLE Express for 5-10 minutes at room temperature. Following gentle resuspension and centrifugation, the cells were permeabilized using methanol as described below. The cells were fixed in 2% paraformaldehyde in PBS for 10 minutes at 37°C, followed by centrifugation, and resuspension of the vortexed cells in 1 mL of chilled Perm Buffer III (Catalog Number: 558050, BD Biosciences, San Jose, CA). The cells were incubated for 30 minutes on ice in sealed tubes. Subsequently, the cells were washed thrice in 3 mL Staining Buffer (1% FBS, 0.09% sodium azide in PBS) and finally resuspended in an appropriate volume of Staining Buffer that would allow for distribution of 100 μL of cell suspension to each FACS tube. The cells were incubated with fluorochrome-conjugated antibodies at the dilutions listed in Table S1 for 60 minutes at room temperature while protected from light. After one wash with 3 mL Staining Buffer, the cells were resuspended in 1X PBS for flow cytometric analysis.

Pancreatic Hormone Expression Analysis

For assessing the expression of the pancreatic hormones insulin and glucagon, matrigel-seeded differentiating cell clusters on differentiation D27 (end of Stage 5) were recovered by treatment with Dispase (Catalog Number: 354235, BD Biosciences, San Jose, CA) for 5 minutes at 37°C, followed by gentle suspension to further break down the matrigel. After washing with 1X PBS and centrifugation, the cell clusters were incubated with TrypLE

Express for 5-10 minutes at room temperature. Following gentle resuspension and centrifugation, the cells were permeabilized via saponin using the BD Cytofix/Cytoperm Kit (Catalog Number: 554714, BD Biosciences, San Jose, CA). For insulin staining, the cells were incubated with anti-inulin-PE for 30 minutes in the dark at room temperature before being washed and resuspended in 1X PBS for flow cytometric analysis. For glucagon staining, the cells were incubated with purified rabbit anti-human glucagon for 30 minutes in the dark at room temperature before being washed and incubated with anti-rabbit APC (1:100) for an additional 30 minutes in the dark at room temperature. Subsequently, the cells were washed and resuspended in 1X PBS for flow cytometric analysis.

Immunological Profile Analysis

Dissociated single cells were stained with the antibodies listed in the last 4 rows of Table 3 for 15 minutes at room temperature, while protected from light, before being washed twice in 1X PBS and fixed in 2% PFA. The cells were then subjected to analysis.

Immunofluorescence and confocal microscopy

IPC clusters were cytospun onto SuperFrost Plus charged slides, rehydrated with 1X PBS, permeabilized with 0.2% Triton-X-100 and simultaneously blocked with PBS containing 10% BSA and 5% serum from the same species as the secondary antibody. After washing with PBS, slides were incubated at 4°C overnight in primary antibody solutions or PBS (for the isotype control). The antibodies used for staining are detailed in Table S2. The slides were washed and then incubated with secondary antibodies for 1 hr at room temperature. Slides were mounted with VectaSheild Mounting Medium containing DAPI (Catalog Number: H-1200, Vector Laboratories, Burlingame, CA), covered with a coverslip, and sealed with nail polish. All experiments consisted of an appropriate negative control (undifferentiated iPS cells) and positive control (human islets). Each sample was stained in conjunction with an isotype control not exposed to the primary antibodies. Staining was documented by confocal microscopy using the Zeiss 710 Confocal Microscope at the Central Microscopy Research Facility at The University of Iowa. The list of antibodies used for immunofluorescence staining is provided in Table 4.

Quantitative-Real Time PCR (qRT-PCR)

The RNeasy Mini Kit (Qiagen, Valencia, CA) was used to extract total RNA and the SuperScript III First Strand Synthesis System for RT-PCR (Invitrogen, Grand Island, NY) was used for reverse-transcription (Applied Biosystems, Foster City, CA) of 1 μg total RNA according to the manufacturer’s instructions. cDNA (12.5 ng) was amplified by PCR using the SYBR Green PCR Master Mix (Applied Biosystems, Grand Island, NY) in a 7500 Real-Time PCR System (Applied Biosystems, Grand Island, NY). Data were normalized to undifferentiated human iPS cells using the ΔΔCt method, with TATA binding protein selected as the normalizer across samples. TBP was used after screening among three housekeeping genes, and it showed the most optimal amplification values relative to the other primers used in these experiments. Primers used for these experiments are listed in Table 5[12,13].

Dot blot for 5-methylcytosine

To detect the effectiveness of demethylation treatment, dot blots were performed on genomic DNA (gDNA) samples isolated from demethylated and nondemethylated control iPS cells to determine levels of 5-methylcytosine (5-MC). gDNA was isolated using the DNeasy Blood & Tissue Kit (Qiagen, Valencia, CA). First, Amersham Hybond-N+

(Catalog Number: RPN119B, GE Healthcare, Pittsburgh, PA), which is a positively charged nylon membrane, was placed on the surface of ultrapure water for at least 10 minutes to allow moistening of the membrane. In the meantime, 100 ng of DNA from each sample was distributed into separate Eppendorf tubes and the volume was equalized across all tubes by adding ultrapure water. Subsequently, 0.1 volume of 4 M NaOH (10X stock) and 0.1 volume of 100 mM EDTA at a pH of 8.2 (10X stock) were added to each sample to give a final concentration of 0.4 M NaOH and 10 mM EDTA. The mixture was vortexed and spun down. The DNA was then denatured at 99°C for 7 minutes, chilled on ice, spun down and neutralized with 0.1 volume of 6.6 M ammonium acetate (10X stock) to give a final concentration of 0.66 M ammonium acetate. In the meantime, the membrane was removed from the water and allowed to dry on a pipette reload rack (with holes facilitating uniform dotting of DNA samples) until barely moist. This is ideal for allowing absorption of the DNA mixture into the membrane without being too dry.

The DNA mixture was then spotted onto the membrane and air-dried for 30 minutes before being subjected to UV cross-linking (2x ‘auto cross-link’ on a Stratalinker). The antibody selected for our experiments was the monoclonal antibody of clone 33D3 (Catalog Number: A-1014-050, Epigentek, Farmingdale, NY). The membrane was incubated overnight at 4°C with the 5-mC antibody diluted at a concentration of 1:250 (4 µg/ml) in blocking solution (PBS containing 10% milk, 1% BSA, 0.1% Tween). After washing the blot 3 times with 0.1% Tween in PBS for 10 minutes each, the blot was subsequently incubated with HRP-conjugated anti-mouse antibody, diluted 1:2,000 in blocking solution for 1 hour at room temperature. The blot was then washed 3 times with 0.1% Tween in PBS at 10 minutes intervals. Finally, HRP signal was detected with a 5 minute incubation at room temperature in Amersham ECL Prime solution (Catalog Number: RPN2232, GE Healthcare, Pittsburgh, PA) and processed via X-ray films.

Dithizone staining

Freshly prepared dithizone solution was used for all experiments. First, 20 mg of dithizone (Catalog Number: D5130, Sigma-Aldrich, St. Louis, MO) was added to 0.6 mL of 95% ethanol in a 15 mL conical tube. Subsequently, 1-5 drops of ammonium hydroxide was added and the resulting orange stock mixture was vortexed thoroughly until completely dissolved. 0.3 mL of this stock solution was dispensed in 99.7 mL of 1X PBS and the pH was adjusted to 7.4 with 1N HCl. Islets (supplied by the IIDP) or picked IPC clusters were added to separate wells, each well containing 200 μL of the final dithizone solution in a 96 well plate. The cell clusters were incubated for 2-5 minutes before images were captured using a standard light microscope (Nikon Eclipse, TS100) attached to a color camera.

Quantitation of cluster size

Cluster sizes were measured manually from pictures taken of the differentiating cultures. Scale bars (representing 100 μm) annotating all of the pictures were measured using a ruler to millimeter precision. Subsequently, cultures were measured with a ruler and the size in μm calculated by first taking a ratio of the cluster size (mm) to scale bar size (mm) to identify the relative size of the cluster compared to the scale bar, and then multiplying this ratio value by 100 μm to identify the cluster size in μm. This is represented in the equation below:

$$Cluster\ size\ (\mu\mathrm{m}) = \frac{Cluster\ size\ (\mathrm{mm})}{Scale\ bar\ size\ (\mathrm{mm})} \times 100\ \mu\mathrm{m}$$

Transmission electron microscopy

IPC clusters were dissociated from matrigel via gentle suspension of the matrigel scaffold and washed with PBS. Dispase was not utilized due to the risk that the enzyme might compromise the integrity of cellular structures. Meanwhile, human islets (supplied by the IIDP) were isolated and pelleted after washing with PBS. Cell cluster pellets were resuspended in 2.5% gluteraldehyde in 0.1 M Sodium Cacodylate buffer at 4°C, typically overnight although samples are generally considered to be indefinitely stable in this buffer. After rinsing in 0.1 M phosphate buffer twice (4 minute incubations each), the clusters were fixed using the secondary-staining, lipid-fixing agents 1% OsO_4/1.5% Potassium Ferrocyanide in 0.1 M phosphate buffer for 30 minutes on a shaker platform. The clusters appeared black at this point and were rinsed twice in double distilled H_2O (ddH_2O). Subsequently, the clusters were incubated in ultrasaturated 2.5% Uranyl Acetate stock solution for 5 minutes. It was important to not disturb the artifact-inducing precipitate at the bottom of the bottle by minimizing shaking or movement of the solution.

The cell clusters were then successively washed in higher concentrations of ethanol in order to dehydrate the samples. First, the clusters were incubated in 25% ethanol for 5 minutes, followed by 4 minute incubations in 50% ethanol, 75% ethanol, 95% ethanol and two incubations in 100% ethanol. Finally, the clusters were incubated for 30 minutes in 1 part 100% ethanol and 1 part Spurr’s resin. Next, the clusters were incubated twice for 15 minutes in only Spurr’s resin and finally placed in Beem Capsules in a 70°C oven overnight. The embedded capsules were kept indefinitely until microtomy. After microtomy and depositing the embedded sections onto copper grids, the grids (always containing sections on the left side) were stained facedown in Uranyl Acetate droplets for 3 minutes. Subsequently the grids were rinsed in water by first plunging the grid into the surface of an H_2O beaker 30 times, and then by using a dropper to allow water to run down the tweezer over the sample. After drying completely, the grids were stained for 2 minutes in Lead Citrate droplets (only the non-surface fraction of the solution was used). NaOH pellets in the petri dishes with the Lead Citrate droplets were used to trap air and prevent oxidation of the Lead Citrate buffer. After washing in water as described above and drying the grids on a rack, the grids were replaced into grid holders and imaged using the JEOL JEM 1230 Transmission Electron Microscope. This microscope is located in the Central Microscopy Research Facility at the University of Iowa and was operated by Dr. Chantal Allamargot of the core facility.

Glucose stimulated insulin secretion (GSIS)

We performed static glucose stimulated insulin secretion (GSIS) assays in order to determine the glucose-responsiveness of the IPC clusters as compared to human islets (supplied by the IIDP).

Following IIDP standard operating procedures, Krebs buffer stock solution was prepared as follows by combining the following in a 500 mL flask: 2.98 g HEPES power (25mM), 3.36 g NaCl (115mM), 1.01 g $NaHCO_3$ (24 mM), 0.1864 g KCl (5 mM), 0.1017 g $MgCl_2 \bullet 6\ H_2O$ (1 mM), 0.5 g BSA (0.1%). These powders were stirred in deionized water so that the total volume was 500 mL and stirred until dissolved. Subsequently, 0.183 g $CaCl_2 \bullet 2\ H_2O$ (2.5 mM) was added and pH of the solution was adjusted to 7.4. After mixing thoroughly, the mixture was filter-sterilized through a 0.22 µm bottle top filter into a sterile bottle and stored at 4°C until expiration at 4 weeks post-preparation. 280 mM glucose solution was prepared by adding 2.5 g of D-(+)-Glucose (Catalog Number: G5767, Sigma-Aldrich, St. Louis, MO) to 50 mL of Krebs buffer stock solution. This mixture was filter sterilized and stored at 4°C until expiration at 4 weeks post-preparation. On the day of the GSIS assay, 30 mL of a 28 mM (“high glucose”) stock solution was prepared by making a 1:10 dilution of the 280 mM glucose stock solution using Krebs buffer stock solution. Additionally, 30 mL of a 2.8 mM (“low glucose”) stock solution was prepared by making a 1:10 dilution of the 28 mM glucose stock solution using Krebs buffer stock solution. Finally, for KCl polarization challenge assessment, 30 mL of a 30mM KCl solution was prepared by mixing 22.2 mg KCl in 10 mL of 2.8 mM (“low glucose”) stock solution. These sterile diluted solutions were stored at 4°C until expiration at 1 week post-preparation, or warmed and equilibrated to 37°C if used the same day.

Differentiated IPCs (Day 27-30 of culture) from 1 well (~300 clusters) or human islets (approximately 200 IEQ) were sampled. After washing the cell clusters twice in 1 mL 2.8 mM (“low glucose” or LG), the clusters were resuspended in LG solution and divided into duplicate wells of a 96-well plate. The cells were then preincubated at 37°C in 200 µL/well of LG solution for 2 hours to bring cells to remove residual insulin and bring cells to a common baseline. The plate was very gently centrifuged and the supernatant discarded. The pelleted cells on the plate were resuspended in 200 µL/well of fresh, equilibrated LG buffer. The plate was placed at 37°C and the cells were allowed to incubate in LG solution for 1 hour. The plate was very gently centrifuged and the supernatant collected into separate duplicate Eppendorf tubes for future analysis by ELISA (low glucose samples). The pelleted cell clusters were resuspended in 200 µL/well of fresh, equilibrated 28 mM (“high glucose” or HG) buffer. The plate was placed at 37°C and the cells were allowed to incubate in HG solution for 1 hour. The plate was very gently centrifuged and the supernatant collected into separate duplicate Eppendorf tubes for future analysis by ELISA (high glucose samples). Finally, the pelleted cells were resuspended in 200 µL/well of fresh, equilibrated 30mM KCl in LG buffer (polarization challenge) for 30 min to release all residual insulin in the cells. The plate was very gently centrifuged and the supernatant collected into separate duplicate Eppendorf tubes for future analysis by ELISA (KCL polarization challenge samples). If not analyzed by ELISA immediately, the supernatants were stored at -80°C.

The cell clusters were then resuspended in PBS, removed from the plate and pelleted in separate Eppendorf tubes in order to assess total protein content as a means of normalizing insulin production across samples. The cell cluster pellets were lysed by resuspension in RIPA lysis buffer (Catalog Number: 20-188, EMD Millipore, Billerica, MA) supplemented with a protease inhibitor cocktail (Catalog Number: 11836170001, Roche, Indianapolis, IN). The cells were also dissociated using a 30 G needle and syringe apparatus to break cell membranes. After incubating on ice for 30 minutes, the cell clusters were centrifuged at 14,000 rpm for 20 minutes at 4°C. The supernatant containing protein was collected and placed into separate Eppendorf tubes for immediate quantitation by Bradford Assay analysis, which was measured at an O.D. of 595 nm using a BioTek µQuant™ spectrophotometer.

On the day of ELISA, supernatant samples were thawed on ice while the ELISA kit components were brought to room temperature. The volume of each sample (generally about 200 µL) was recorded and the samples were processed using the Human Ultrasensitive Insulin ELISA (Catalog Number: 80-INSHUU-E01.1, ALPCO Diagnostics, Salem, NH) according to manufacturer's instructions. The samples were quantitated by a BioTek µQuant™ spectrophotometer at an O.D. of 450 nm. Based on a standard curve, a quadratic equation was derived correlating the amount of insulin in a standard sample to the O.D. Using this equation, the amount of insulin in a test sample (µIU/mL) was calculated and tabulated. The amount of insulin produced was normalized by the total protein in each sample, which was calculated as described above via the Bradford Assay of the lysate generated from the cell clusters.

Mice and transplantation experiments.

Immunodeficient male Rag2$^{-/-}\gamma_c^{-/-}$ mice (B6 background) of 6-10 weeks of age were purchased from Taconic Farms and used for all animal experiments. All animal procedures were approved by the Institutional Animal Care and Use Committee (IACUC) at the University of Iowa and the Iowa City VA Medical Center, and procedures were conducted in accordance with NIH guidelines.

For induction of diabetes in mice, we followed the NIH Diabetic Complications Consortium recommendations, which suggest using a multiple low dose regimen of Streptozotocin, which is a toxin that selectively kills mouse pancreatic β-cells[104]. Pre-weighed mice were placed on a 4 hour fast by placing the mice in a fresh cage with a new food rack that does not have food. 3.5 hours into the fast, fresh Sodium Citrate buffer was prepared by weighing out 0.735g of enzyme grade Sodium Citrate (Catalog Number: S279-500, Fisher Scientific, Waltham, MA) and dissolving it in 25 mL of ddH$_2$O. The pH was adjusted to 4.5 using HCl and the buffer placed on ice. Subsequently, a sufficient amount of powdered Streptozotocin (STZ, Catalog Number: 572201, Millipore, Billerica, MA) was placed into a 1.5ml Eppendorf tube protected from light with aluminum foil so that each mouse would receive 100 mg STZ/kg mouse body weight. At 4 hours post-fast, STZ was resuspended in fresh Sodium Citrate buffer and injected i.p. within 5 minutes of dissolution so that each mouse received 100 µL of STZ solution to achieve the dose of 100 mg/kg. After commencing with the injections, food and water were supplied to all of the mice. This procedure was repeated for each mouse on D2 and D3 after the first injection of STZ at a dose of 50 mg/kg. If the blood glucose levels were still not ≥300 mg/dL at D4, a fourth injection of 50 mg/kg STZ was performed on that day. At 5 days after the first STZ injection, blood glucose levels and weights of the STZ-injected mice were measured, and only mice showing evidence of hyperglycemia (≥300 mg/dL blood glucose[104]) were used for transplantation experiments.

Hyperglycemic mice were anesthetized and injected with IPCs s,c. into the right shoulder flank, which was shaved and marked to indicate transplant site. Mice received 900 IPC clusters (~1.25 million IPCs). After transplantation, mice were weighted and their blood glucose levels measured every 7 days.

For the glucose tolerance test, pre-fasting blood glucose levels were recorded and the mice were then fasted for 16 hours in new cages with only water to prevent access to food remnants. Weights of the mice were determined to ensure accurate dosage of glucose. Following the fast, blood glucose levels were again determined (0 min), and the mice were injected i.p. with 2 mg/kg of (D)-+-Glucose solution suspended in water. Blood glucose levels were assessed at 15, 30, 60, 90, 120, and 240 min after glucose challenge.

^{51}Cr Release Assay

Specific cell lysis of target cells by NK cells was determined using the 4 hour ^{51}Cr release assay, as described previously[42]. The effector cells used in this assay were human peripheral blood mononuclear cells (PBMCs), of which typically 10-15% of the cells are $CD56^{+}$ $CD3^{-}$ NK cells[105], activated for 48 hours with the lymphokine IL-2 (200 U/mL). Target cells were labeled for 1 hour in radioactive ^{51}Cr, and washed three times before incubation with effector cells for 4 hours at various effector : target cell ratios. Target cells incubated on their own were the source of spontaneous “minimum” release of the radioactive ^{51}Cr, whereas 2% Triton-X-treated target cells served as a measure of complete cell death, or “maximum” release. The target cells used in this assay were IPCs, undifferentiated iPS cells (negative control), or human K562 leukemia cells (highly sensitive to NK cell killing[42] and thus a positive control in this assay). After coculture for 4 hours, the radioactive ^{51}Cr release in the supernatant was measured using a Beckman LS 6500 Scintillation Counter (Beckman Coulter, Brea, CA). Specific lysis was calculated using the following formula[42]:

$$\%\, Specific\ Lysis = \frac{(Experimental\ Count - Minimum\ Release)}{(Maximum\ Release - Minimum\ Release)}$$

Statistical analysis

Evaluation of experimental data for significant differences was performed through the Students *t* test, which was conducted using the Prism software package (GraphPad Software). $p < 0.05$ was considered significant for these studies. Unless noted otherwise, all experiments were repeated at least 3 times.

Table 1. Differentiation timeline and media constituent information

STAGE 1: Definitive Endoderm D0 → D5	**Media 0:** (D0 → D1) DE Base Media + Supplement A + Supplement B
	Media 1: (D1 → D2, D2 → D3, D3 → D4, D4 → D5) DE Base Media + Supplement B
STAGE 2: Posterior Foregut D5 → D8	**Media 2:** (D5 → D6, D6 → D7) DMEM/F-12 + 2% **Hyclone FBS** + **KGF** (50 ng/ml) **+ L-Ascorbic Acid** (0.25 mM) + **Y27632** (10 µM)
	Media 3: (D7 → D8) DMEM/F-12 + 2% **Hyclone FBS** + **KGF** (50 ng/ml) **+ L-Ascorbic Acid** (0.25 mM)
STAGE 3: Pancreatic Endoderm / Progenitors D8 → D12	**Media 4:** (D8 → D9, D9 → D10, D10 → D11, D11 → D12) DMEM-HG + **SANT-1** (0.25 µM) + **Retinoic acid** (2 µM) + **Noggin** (100 ng/mL) + 1% (vol/vol) **B27** + **TPB** (50 nM) **+ L-Ascorbic Acid** (0.25 mM) + **KGF** (50 ng/ml)
STAGE 4: Endocrine Precursors D12 → D17	**Media 5:** (D12 → D13, D13 → D14, D14 → D15, D15 → D16) DMEM-HG + **ALK5i** (10 µM) + **Noggin** (100 ng/ml) + 1% (vol/vol) **B27** Supplement + **GLP-1** (100 nM) + **SANT-1** (0.25 µM) + **Retinoic acid** (100 nM) + **DAPT** (10 µM) **+ Heparin** (0.25 mM) **+ T3** (1 µM)
	Media 6: (D16 → D17) DMEM-HG + **ALK5i** (10 µM) + **Noggin** (100 ng/mL) + 1% (vol/vol) **B27** Supplement + **GLP-1** (100 nM) + **DAPT** (10 µM) **+ Heparin** (10 µg/ml) **+ T3** (1 µM)
STAGE 5: Insulin Producing Cells D17 → D27	**Media 7:** (D17 → D27) DMEM-HG + 10% **HyClone FBS** + **Nicotinamide** (5 mM) + **IGF-1** (10 nM) + **GLP-1** (100 nM) + **ALK5i** (10 µM) **+ T3** (1 µM) + **Heparin** (10 µg/ml)

Table 2. Ordering information for differentiation supplements

Compound	*Type*	*Company*	*Catalog #*	*Size*
5-aza-2'-deoxycytidine	97% HPLC	Sigma-Aldrich	A3656-5MG	5mg
Nodal	Recombinant Human	R&D Systems	3218-ND-025	25µg
Wnt3A	Recombinant Human	R&D Systems	5036-WN-010	10µg
KGF (FGF-7)	Recombinant Human	Peprotech	100-19	10µg
SANT-1	98% HPLC	Sigma-Aldrich	S4572-5MG	5mg
Retinoic acid	98% HPLC	Sigma-Aldrich	R2625-100MG	100mg
Noggin	Recombinant Human	Peprotech	120-10C	100µg
GLP-1	Recombinant Human	Sigma-Aldrich	G3265-.1MG	1mg
ALK5 inhibitor II	N/A	Enzo	ALX-270-445-M005	5mg
TPB	α-Amyloid Precursor Protein Modulator	EMD Chemicals	565740-1MG	1mg
IGF-1	Recombinant Human	Promega	G5111	25µg
Nicotinamide	Cell culture tested	Sigma-Aldrich	N0636-100G	100g
B27	Without Vitamin A	Invitrogen	12587-010	10mL
L-Ascorbic Acid (25°C)	Dry powder	Fisher Scientific	A61-25	25g
DAPT (4°C)	N/A	Tocris Biosciences	2634	10mg
Heparin	Cell culture tested	Sigma-Aldrich	H3149-25KU	25KU
T3 (3,3′,5-Triiodo-L-thyronine sodium salt)	Cell culture tested	Sigma-Aldrich	T6397-100MG	100mg

Table 3. Detailed information on the antibodies used for flow cytometric analysis of differentiating cells

PRIMARY ANTIBODY						
Antigen	**Host**	**Dilution**	**Manufacturer**	**Cat. #**	**Fluorochrome**	**Permeabilization Method**
CXCR4	Rat	1:20	BD Biosciences	551510	PE	N/A
PDGFRα	Rabbit	1:10	Santa Cruz Biotechnology	sc-338	PE	N/A
Sox17	Goat	1:10	R&D Systems	IC1924A	APC	Saponin
Pdx1	Mouse	1:20	BD Biosciences	562161	PE	Methanol
Nkx6.1	Mouse	1:20	BD Biosciences	563338	Alexa Flour 647	Methanol
NeuroD1	Mouse	1:20	BD Biosciences	563566	Alexa Flour 647	Methanol
Insulin	Rabbit	1:50	Cell Signaling Technology	8508S	PE	Saponin
Glucagon	Rabbit	1:200	LS Biosciences	LS-C166525	unconjugated	Saponin
MHC class I	Mouse	1:20	Biolegend	311405	PE	N/A
MHC class II	Mouse	1:20	BD Biosciences	556644	PE	N/A
CD80	Mouse	1:20	Biolegend	305219	PE	N/A
CD86	Mouse	1:20	Biolegend	305405	PE	N/A

Table 4. Detailed information on the antibodies used for immunofluorescence staining

PRIMARY ANTIBODY					SECONDARY ANTIBODY				
Antigen	**Host**	**Dilution**	**Manufacturer**	**Cat. #**	**2° Antibody**		**Dilution**	**Manufacturer**	**Cat. #**
Insulin	Mouse	1:100	abcam	ab9569	Goat α-Mouse	AF-568	1:200	Life Technologies	A11019
					Donkey α-Goat	AF-568	1:200	Life Technologies	A11057
Glucagon	Rabbit	1:10	LS Biosciences	LS-C166525	Goat α-Rabbit	AF-488	1:200	Life Technologies	A11070
C-peptide	Rabbit	1:100	Cell Signaling Technology	4593S	Goat α-Rabbit	AF-488	1:200	Life Technologies	A11070
Nkx6.1	Mouse	1:50	DSHB	F55A10 concentrate	Goat α-Mouse	AF-568	1:200	Life Technologies	A11019
Nkx2.2	Mouse	1:10	DSHB	74.5A5 concentrate	Goat α-Mouse	AF-568	1:200	Life Technologies	A11019
Glut4	Rabbit	1:300	abcam	ab654	Goat α-Rabbit	AF-488	1:200	Life Technologies	A11070
MafA	Rabbit	1:100	abcam	ab26405	Goat α-Rabbit	AF-568	1:200	Life Technologies	A21069
Pdx1	Goat	1:50	Santa Cruz Biotechnology	SC14664	Donkey α-Goat	AF-488	1:200	Life Technologies	A11055

*DSHB = Developmental Studies Hybridoma Bank

Table 5. List of primers used for quantitative RT-PCR

mRNA	**Forward** (5'-->3')	**Reverse** (5'-->3')	**T_m Forward**	**T_m Reverse**
TBP	TGTGCACAGGAGCCAAGAGT	ATTTTCTTGCTGCCAGTCTGG	59.1	55.9
IPF-1/PDX-1	CCTTTCCCATGGATGAAG	CGTCCGCTTGTTCTCCTC	53.1	55.7
Glucagon	AAGCATTTACTTTGTGGCTGGATT	TGATCTGGATTTCTCCTCTGTGTCT	55.6	57.2
Glucokinase	TGCAGATGCTGGACGACAG	GAACTCTGCCAGGATCTGCTCTA	57.6	58.1
Ghrelin	TGAACACCAGAGAGTCCAGCA	GCTTGGCTGGTGGCTTCTT	58.1	58.6
Somatostatin	CCCCAGACTCCGTCAGTTTC	TCCGTCTGGTTGGGTTCAG	57.5	57.1
Insulin	AAGAGGCCATCAAGCAGATCA	CAGGAGGCGCATCCACA	56.4	58.1

CHAPTER III

THE DIFFERENTIATION OF iPS CELLS FROM TYPE 1 DIABETIC PATIENTS INTO IPCS IS IMPAIRED IN COMPARISON TO THAT OF iPS CELLS FROM HEALTHY PATIENTS

Introduction

Our goal is to establish human iPS cells as an innovative source of individualized IPCs, thereby obviating the need for immunosuppression[6]. If successful, such a novel alternative could provide for an unlimited source of IPCs. Ideally, the diabetic patient would donate a skin biopsy from which fibroblasts can be outgrown. After reprogramming of the fibroblasts into iPS cells, pancreatic β-cells can be derived and made available for use in therapies[6].

However, we perceived an issue in this approach when we considered a report published by a Harvard group, which briefly introduced (but did not elaborate on) the finding that iPS cells isolated from a T1D patient fail to differentiate into Pdx1$^+$ pancreatic progenitor cells[106]. They utilized T1D patient iPS cells as a negative control for their differentiation experiments, without addressing the basis for this impairment or attempting to correct it[106]. The reasons for this impairment remain elusive. If this is common to all T1D cell lines, autologous iPS cell therapy for T1D will be a challenge to overcome.

All of the mainstream publications on the differentiation of pluripotent stem cells into IPCs use human ES cells with no apparent link to T1D[12,13,15,16,77,102], or, more rarely, iPS cells that are derived from healthy, normal individuals[14,102]. Here, we focused on iPS cells derived from T1D patients (T1D iPS cells) because these cells are most relevant to the treatment of diabetic patients[6]. We were the first to successfully pursue the goal of generating functional, glucose-responsive IPCs with high efficiency from iPS cells derived from T1D patients, focusing on these patients since they represent the target clientele for this therapy.

As such, we sought to identify differences in the differentiation of T1D and nondiabetic patient-derived iPS cells (ND iPS cells), and we aimed to correct any defects, if present, in the differentiation of T1D iPS cells into IPCs. Our rationale in pursuing this question was that recognizing an intrinsic defect in the differentiation of T1D iPS cells is critical before advancing clinical application of such therapy for T1D. Our *hypothesis* is that the differentiation potential of T1D iPS cells is similar to that of ND iPS cells, and T1D iPS cells can give rise to functional, glucose-responsive IPCs which can be used to treat Type 1 Diabetes.

Results

Optimization of the Generation of DE cells

Our first step in creating this protocol was to optimize the generation of DE cells in a manner that would yield the highest frequency of $CXCR4^+Sox17^+PDGFR\text{-}\alpha^-$ true definitive endodermal cells. For this, we performed a pilot experiment where we tested six different culture conditions outlined in Figure 6A for the differentiation of T1D iPS cells into IPCs. We compared the following culture conditions for DE differentiation in various combinations: 1) 2D vs. 3D matrigel culture; 2) utilizing feeder cells in 2D differentiation vs. a thin layer of diluted matrigel in 2D differentiation to allow cell attachment to the plate; and 3) maintaining the iPS cells as colonies vs. dismantling them into single cells and replating them on the day that the differentiation was initiated.

At the conclusion of the differentiation (day 5), the cells were harvested into a single cell suspension and analyzed by flow cytometry for the expression of the DE cell markers CXCR4 and Sox17. Additionally, we assessed the expression of the mesodermal marker PDGFR-α. An effective differentiation of iPS cells into DE cells should yield a high percentage of CXCR4$^+$ and Sox17$^+$ cells while containing as few as possible PDGFR-α$^+$ cells[58] (Figure 6B). CXCR4$^+$ PDGFR-α$^+$ cells represent the immature, bipotent mesendodermal cells[57] and indicate the differentiation has not proceeded optimally.

As evidenced in Figure 6C, the greatest yield of CXCR4$^+$ Sox17$^+$ cells (black bar) was found in Culture Condition 1, which involved using 2D differentiation using feeders while the iPS cells were assembled as colonies. Additionally, this culture consisted of mostly PDGFR-α$^-$ Sox17$^+$ cells (gray bar), demonstrating their true endodermal identity. Culture Condition 4 also yielded a relatively high percentage of CXCR4$^+$ Sox17$^+$ PDGFR-α$^-$ cells (Figure 6C).

The other four culture conditions yielded largely mesendodermal cells expressing both CXCR4 and PDGFR-α, but no Sox17 (Figure 6C). These cells are not true DE cells and instead represent an immature hybrid cell fate that eventually severely compromises the outcome of the differentiation (Figure 2). The worst culture conditions in this regard were 5 and 6, which involved 3D differentiation. At first, we were perplexed by these results, but eventually we realized that the block of matrigel in these cultures would sequester growth factors[96] and create a morphogen gradient that that may impede rapid transitions between differentiation media. The generation of DE cells critically requires Wnt signaling only in the first day[56]. Precise temporal control of this signal is key, otherwise sustained Wnt signaling has been shown to induce mesendodermal differentiation if coupled with Nodal signaling[56] (Figure 3A). In the case of 3D differentiation of iPS cells into DE cells, we reasoned that the transition between media of day 1 and 2 would be blurred due to the matrigel sequestering the growth factors that ideally should be eliminated in day 2 media. The result of this would be imprecise differentiation control and sustained Wnt signaling that would ultimately yield “bad” CXCR4$^+$ PDGFR-α$^+$ Sox17$^-$ mesendodermal cells.

Through this pilot experiment, we were able to select the optimal culture conditions for the generation of DE cells. In future experiments, described next, we were able to raise the percentage of CXCR4$^+$ Sox17$^+$ PDGFR-α$^-$ cells from ~55% to >90% by optimizing cell numbers and refining certain details of the differentiation protocol.

The Early Differentiation of T1D and ND iPS Cells into DE cells is Comparable

After making optimizations to maximize the yield of DE cells, ND and T1D iPS cells were subjected to the differentiation towards DE cells and the efficacy of differentiation was assessed on day 5 by determining the expression of CXCR4, Sox17 and PDGFR-α. Undifferentiated iPS cells were utilized as negative controls and did not express any of the aforementioned markers (Figure 7). Both T1D and ND differentiated cultures contained >90% CXCR4$^+$ Sox17$^+$ endodermal cells (Figure 7). Additionally, these cells were mostly PDGFR-α$^-$ (Figure 7), which suggests that they are true endodermal cells and not arrested in the transitory, immature mesendodermal state.

Thus, we concluded that we were able to achieve a virtually pure population of DE cells from both ND and T1D iPS cells at comparable yields. For further differentiation into IPCs, we dissociated the 2D differentiating DE cells by scraping the monolayer into chunks, and then deposited these cell clusters into matrigel blocks (1:1 diluted with DMEM/F-12). The cells coalesced into discrete spheroids that embedded into the matrigel within 24 hours. All further differentiation of the cells occurred in a 3D fashion.

T1D iPS cells Predominantly Derive Hollow Cysts that Do Not Express Insulin

T1D and ND iPS cells were differentiated in parallel through five stages of differentiation into IPCs (Figure 8B), following the simplified schema outlined in Figure 8A. After 2D differentiation in Stage 1, the cells were differentiated in a 3D format using matrigel.

Early in the 3D differentiation procedure, we recognized that the DE cells from both T1D and ND cultures coalesced into compact cell clusters. However, in the final stage of the differentiation, which lasts 10 days, we observed the formation of clusters with two distinct morphological phenotypes: hollow cysts that appeared to be like bubbles, and compact spheroids that resembled islets (Figure 8B). Strikingly, we observed that the T1D culture consisted almost entirely of hollow cysts, whereas the ND iPS cells gave rise to a nearly 50:50 mixture of hollow cysts and compact spheroids (Figure 8C). Notably, these hollow cysts have been observed by another group that differentiated human ES cells into islet-like clusters using low attachment culture dishes[107]. To determine the significance of these structures, we stained them for insulin. The hollow cysts collapse upon fixation in paraformaldehyde (Figure 9), which is an observation that is consistent with what has been described in the literature[108]. When we stained these structures for insulin, the hollow cysts were negative, whereas the compact spheroids stained positive for insulin (Figure 9).

This is consistent with data that was elaborated in a recent manuscript by Greggio *et al.*, which reported the use of growth-factor depleted matrigel to expand mouse embryonic pancreatic progenitor cells[108]. Depending on their medium composition, they were able to derive two discrete sets of cell clusters. In one form of media, pancreatic progenitors underwent further differentiation *in vitro* into complex organoids with evidence of pancreatic morphogenesis and branching into mature endocrine, acinar and ductal lineages[108]. However, a different set of media sustained pancreatic progenitors that assembled into hollow spheres, which consisted of cells that retained expression of Pdx1 but had not differentiated into end-stage, mature cells[108]. This alludes to a possible bivalent state for the clusters in our differentiating cultures, which consist of compact spheroids that contain mature IPCs and express insulin, as well as hollow, vacuolar cysts that contain immature pancreatic progenitor cells that do not yet express insulin or other terminal stage pancreatic markers. Significantly, the dominant presence of hollow cysts in the T1D culture suggests that most of the cells are immature.

Remarkably, the morphology of the compact spheroids resembled that of islets (Figure 9), and the insulin expression by these spheroids but not the hollow cysts suggested to us that we needed to improve the yield of compact spheroids in our differentiating cultures. Supporting this notion, we found that the very rare and compact large organoid-like structures found in the T1D differentiating cultures (Figure 10A) strongly expressed insulin (Figure 10B).

T1D iPS Cells Give Rise to Significantly Fewer Insulin$^+$ Cells

Similarly, we observed that T1D iPS cells poorly differentiated into IPCs when the cells were analyzed by flow cytometry. The yield of IPCs derived from ND iPS cells was approximately 50% (Figure 11), which is comparable to the percentage of insulin$^+$ cells found in primary human islets in our experiments and in the literature[1]. Moreover, the yield of ~50% insulin$^+$ IPCs is consistent with the 50:50 ratio of hollow cysts (which are insulin$^-$) and compact spheroids (which are insulin$^+$). This yield of IPCs from ND iPS cells is exemplary when compared to previous reports of only 10-15%[12-16,48] and is evidence for the effectiveness imparted by 3D differentiation in the differentiation of IPCs. However, despite the effectiveness of our protocol with ND iPS cells, only 15.9% of the T1D culture expressed insulin (Figure 11). This too is remarkably consistent with the ~16% yield of compact insulin$^+$ spheroids in the T1D culture (Figure 8).

This disparity between the T1D and ND cultures is especially evident in histogram plots depicting the size of the insulin$^+$ peak in the differentiating cultures (Figure 12). Whereas the ND iPS cells contains a population of insulin$^+$ cells that aligns with and closely resembles that of human islets, the T1D culture gave rise to a much smaller population of cells that express insulin, evidenced by the much smaller peak (Figure 12).

T1D iPS Cell-Derived Differentiating Cells Poorly Express Pdx1

We corroborated these immunofluorescence and flow cytometry data by gene expression analysis in order to compare the expression of several pancreatic genes among Stage 4 or Stage 5 cells derived from ND and T1D iPS cells. As can be seen in the top panel of Figure 13, the expression of *Insulin* transcript in the ND cells increases from Stage 4 to Stage 5, and this is accompanied by a decline in the expression of *Glucagon*, suggesting commitment of the cells toward insulin$^+$ cells in the last stage of the differentiation. However, in the T1D differentiating cultures, we observed significantly lower expression of *Insulin* at both Stage 4 and Stage 5, confirming our previous results. We also observed significantly poorer expression of *Glucagon* in the T1D cultures compared to ND cultures. The expression of other genes, such as *Somatostatin* and *Glucokinase* was not significantly different between the T1D and ND cultures, and *Ghrelin* showed a very small but significant difference (Figure 13).

To determine if the inefficiency in differentiation manifests earlier than the last stage of differentiation, we determined the expression of *Pdx1* in T1D and ND differentiating cultures. Pdx1 is the pancreatic master regulator gene and its expression appears midway through the differentiation process[16]. In ND cultures, *Pdx1* is expressed at high levels at Stage 4 (Figure 13), which precedes the expression of *Insulin* in Stage 5, consistent with embryonic development of the pancreas[46]. *Pdx1* levels continue to increase in Stage 5 in the ND culture. However, at both Stage 4 and Stage 5, the T1D culture expressed significantly lower levels of *Pdx1* than the ND culture (Figure 13). This likely explains why the expression of downstream genes, such as *Insulin*, is also impaired in the T1D culture. Pdx1 is indispensable for the development of pancreatic β-cells[50]. Pdx1 knockout mice fail to form a pancreas[50], which is evidence for how critical this gene is in pancreatic development. Therefore, we believe that such a glaring deficiency in the T1D culture sets the rest of the differentiation up for failure.

Summary

These data demonstrate that we have established a robust protocol for the generation of human iPS cell-derived IPCs if the iPS cells are derived from healthy, nondiabetic individuals. These findings are an enormous advance from prior protocols that generally yielded 10-15% insulin$^+$ cells from healthy iPS cells or ES cells[12-16,48]. Here, we utilized a highly optimized system to generate a virtually pure population of CXCR4$^+$ Sox17$^+$ DE cells that did not express PDGFR-α, which marks mesodermal and mesendodermal cells. These cells were then driven through four more developmental stages in a 3D platform to yield >50% insulin$^+$ IPCs. These cells were organized in compact cell clusters that resemble islets and expressed insulin as determined by flow cytometry, quantitative RT-PCR and immunofluorescence.

However, the success of this protocol in yielding IPCs from ND iPS cells was clearly not recapitulated in T1D iPS cells. Although the early differentiation of T1D and ND iPS cells into DE cells (Stage 1) was equivalent, downstream 3D differentiation of the iPS cells showed striking disparities between the two cell types. Indeed, in the differentiating T1D cultures, we observed the dominant presence of hollow cyst-like structures. These cysts did not express insulin, and their presence overwhelmingly outweighed that of the compact, islet-like clusters that expressed insulin. Only approximately a tenth of the end-stage cells expressed insulin, and the transcript levels of *Insulin* were significantly lower in the T1D cultures compared to the ND cultures. Tracing the disparity in the differentiations backward to earlier in the pancreatic differentiation program[46] revealed that the expression of *Pdx1* transcript was extremely poor in T1D differentiating cultures, suggesting that the differentiation of T1D DE cells into Pdx1$^+$ pancreatic progenitor cells was impaired. Naturally, this would translate into significantly impaired yield of insulin-expressing IPCs at the end of the differentiation.

Thus, we conclude from these data that the differentiation of T1D iPS cells into IPCs is impaired compared to that of ND iPS cells. Interestingly, our findings are consistent with those of a Harvard group that used different T1D iPS cells as a negative control in their differentiation experiments[106], which suggested that T1D iPS cells poorly differentiate into Pdx1$^+$ pancreatic cells. However, the context of our findings is completely different because we are surpassing the use of T1D iPS cells as a negative control, and we have additionally established that T1D iPS cells go on to poorly differentiate into IPCs rather than simply concluding that T1D iPS cells fail to efficiently differentiate into Pdx1$^+$ cells and stopping there. Whereas that prior report briefly introduced their finding and did not elaborate on it whatsoever[106], here we have reproduced it with another cell line, examined the downstream implications of the impaired expression of Pdx1, and last but not least, we identified a new goal for this project: to correct this impaired differentiation of T1D iPS cells into IPCs.

The use of iPS cells in cell replacement therapy for T1D will, in all likelihood, involve the diabetic patient themselves, since the aim of this therapy is to enable autologous, patient-tailored engineering of IPCs[6,9]. As such, recognizing and correcting the intrinsically impaired differentiation of T1D iPS cells into IPCs is critical before advancing such therapy into the clinic. Having completed our first goal, which was to identify differences in the differentiation of T1D and ND iPS cells into IPCs, we next sought to correct the impaired differentiation of T1D iPS cells into IPCs in order to facilitate autologous iPS cell therapy for T1D.

Figure 6. Selection of the optimal culture conditions for Stage 1 differentiation into definitive endoderm (DE) cells

(A) T1D iPS cells were subjected to six different differentiation conditions for the generation of DE cells. The following combinations of culture systems were used: 1) 2D vs 3D, 2) using feeders vs matrigel (either a thin layer for 2D or a block for 3D) as a support layer, and 3) maintaining the iPS cells as colonies vs. generating single cells for the generation of DE cells.

(B) These flow plots depict what parameters were used to assess efficacy of differentiation into DE cells in order to compare the six different culture conditions. We determined the expression of CXCR4, Sox17 and PDFGR-α. DE cells are CXCR4$^+$ Sox17$^+$ and PDGFR-α$^-$ Sox17$^+$. This translates into a high frequency of cells in the quadrants marked with black (CXCR4$^+$ Sox17$^+$) or gray (PDGFR-α$^-$ Sox17$^+$) squares, and a low frequency of cells in the white (CXCR4$^+$ Sox17$^-$) or dashed (PDGFR-α$^+$ Sox17$^-$) quadrants. On the other hand, “bad” differentiations yield bipotent, immature mesendodermal cells that express PDGFR-α as well as CXCR4, but not Sox17. Thus, these cells are CXCR4$^+$ PDGFR-α$^+$ Sox17$^-$. This translates into a high frequency of cells in the quadrants marked with white (CXCR4$^+$ Sox17$^-$) or dashed (PDGFR-α$^+$ Sox17$^-$) squares, and a low frequency of cells in the black (CXCR4$^+$ Sox17$^+$) or gray (PDGFR-α$^-$ Sox17$^+$) quadrants.

(C) Depiction of the frequency of cells obtained in each population from the six culture conditions investigated. The black (CXCR4$^+$ Sox17$^+$) or gray (PDGFR-α$^-$ Sox17$^+$) bars should contain a similar frequency of cells since they both represent the same population of true DE cells (CXCR4$^+$ Sox17$^+$ PDGFR-α$^-$). A high percentage of cells in these columns represents a good differentiation outcome. The highest values are found in the first condition (2D, feeders, colonies) and the second highest yield comes from the fourth condition investigated (2D, matrigel, colonies). In contrast, the other conditions poorly yielded true DE cells (black and grey bars) and instead mostly yielded cells that were arrested in the transitory, immature mesendodermal state, represented by the white and dashed bars (CXCR4^{+} PDGFR-α^{+} Sox17^{-}).

A

Condition	Culture Platform	Culture Support	Cell Format
1	2D	Feeders	Colonies
2	2D	Feeders	Single cells
3	2D	Matrigel	Colonies
4	2D	Matrigel	Single cells
5	3D	Matrigel	Colonies
6	3D	Matrigel	Single cells

B

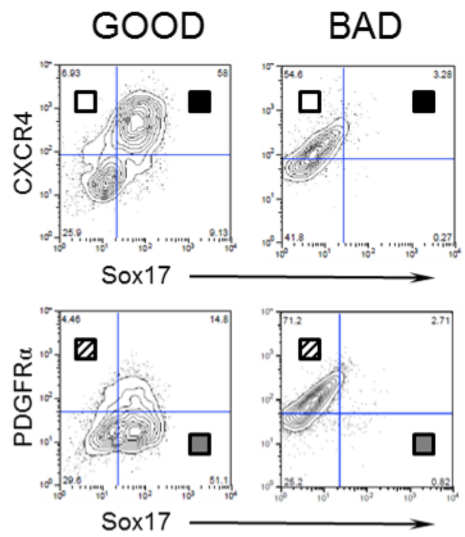

C

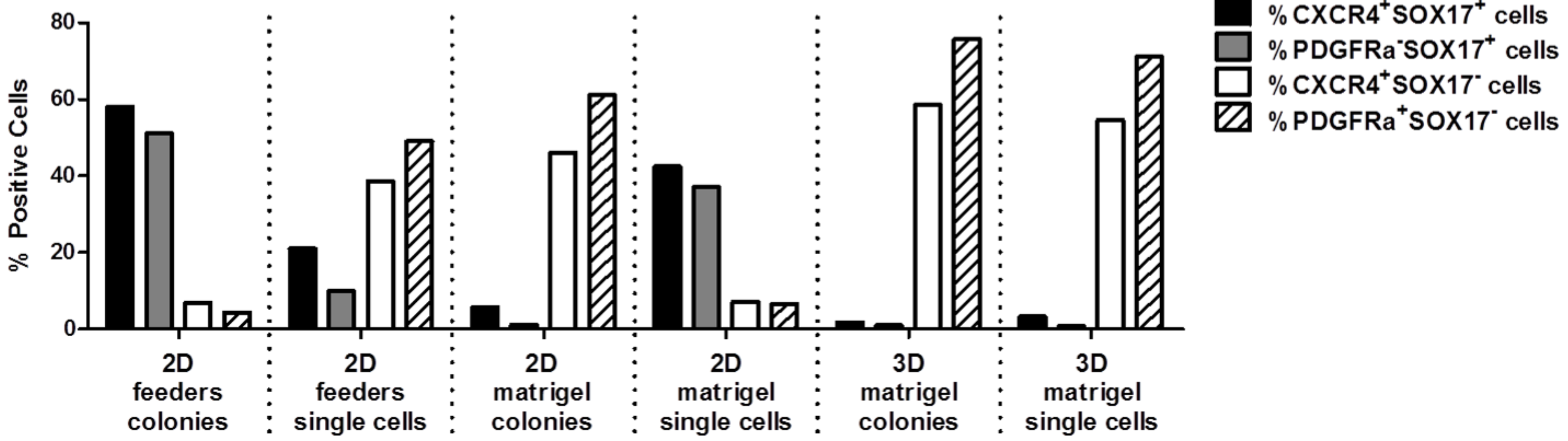

Figure 7. The differentiation of T1D and ND iPS cells into DE cells is equivalent

T1D and ND iPS cells were differentiated in parallel under Stage 1 to generate CXCR4$^+$ Sox17$^+$ PDGFR-α^- DE cells. Over 90% of the resultant cells derived from both T1D and ND iPS cells co-expressed CXCR4 and Sox17, and almost all of these cells were PDGFR-α^-. This demonstrates that the early differentiation into true DE cells is equally effective from both T1D and ND iPS cells. Undifferentiated iPS cells are negative for all three of these cell markers and were used as a negative control cell line for these stains.

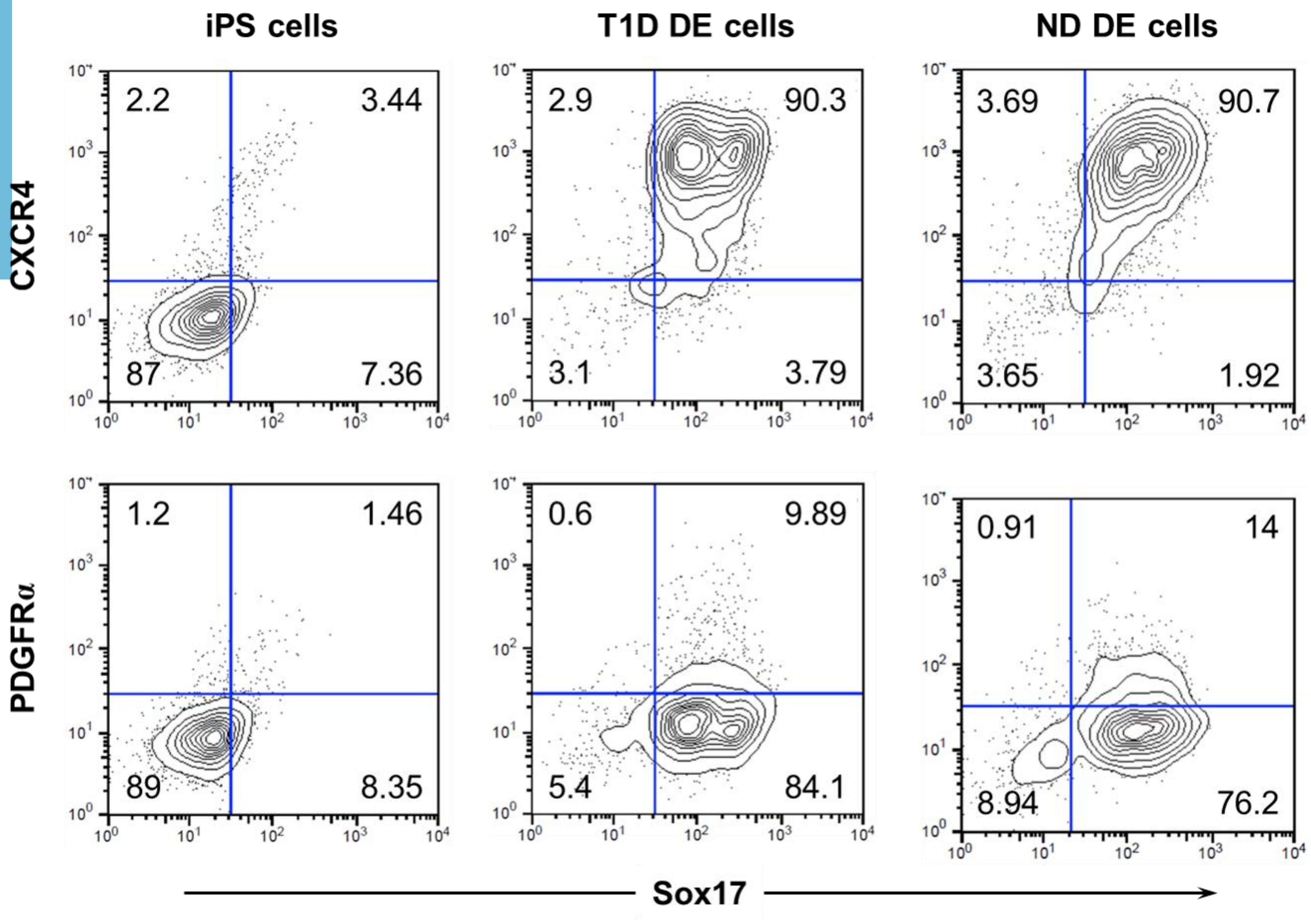
iPS cells
T1D DE cells
ND DE cells
CXCR4
PDGFRα
Sox17
2.2
3.44
87
7.36
2.9
90.3
3.1
3.79
3.69
90.7
3.65
1.92
1.2
1.46
89
8.35
0.6
9.89
5.4
84.1
0.91
14
8.94
76.2
10^0
10^1
10^2
10^3
10^4

Figure 8. T1D iPS cells give rise to mostly hollow cyst-like clusters whereas ND iPS cells give rise to a mixture of hollow cysts and compact spheroids

(A) Summary of the five stages iPS cells undergo in the process of differentiating into IPCs. **(B)** The parallel differentiation of T1D and ND iPS cells in 3D culture after Stage 1 results in distinct morphologies of hollow cyst-like (asterisk) and compact (arrowheads) IPC clusters. The appearance of hollow cysts and tight spheroids was slightly evident on D8 (middle panel) but became markedly prominent by D20 (rightmost column), which is in the middle of the final stage of the differentiation. Based on reports in the literature, we suspected that the hollow cysts consist of immature pancreatic progenitor cells whereas the compact clusters contain mature insulin$^+$ cells. **(C)** Comparison of the ND and T1D cultures revealed significant disparities in the yield of these two cluster morphologies. Similar to fetal development of the pancreas, we observed in both cases the presence of hollow vacuoles and tight spheroids. However, cells from the T1D patient consisted of significantly more hollow vacuoles than the cells from the ND patient, which had a nearly 50:50 mix of hollow cysts and compact spheroids (*n* = 2 differentiations for ND cells and 8 for T1D cells). Data are represented as mean ± SEM, $^{**}p < 0.01$.

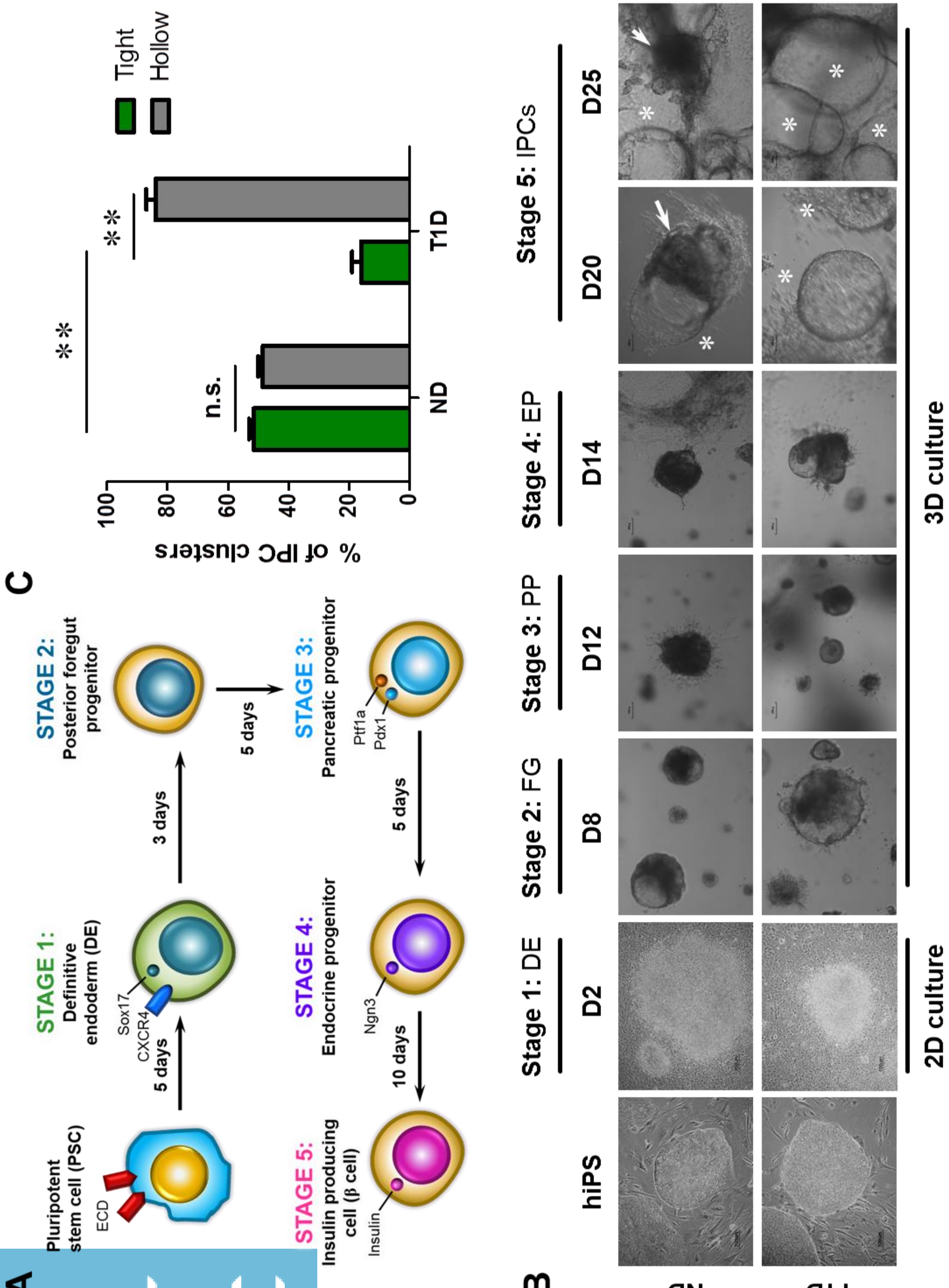
A
Pluripotent stem cell (PSC)
ECD
5 days
STAGE 1: Definitive endoderm (DE)
Sox17
CXCR4
3 days
STAGE 2: Posterior foregut progenitor
5 days
STAGE 3: Pancreatic progenitor
Ptf1a
Pdx1
5 days
STAGE 4: Endocrine progenitor
Ngn3
10 days
STAGE 5: Insulin producing cell (β cell)
Insulin
B
ND
T1D
hiPS
Stage 1: DE
D2
Stage 2: FG
D8
Stage 3: PP
D12
Stage 4: EP
D14
Stage 5: IPCs
D20
D25
2D culture
3D culture
C
% of IPC clusters
100
80
60
40
20
0
ND
T1D
n.s.
**
**
Tight
Hollow

Figure 9. Insulin expression appears in solid spheroids but not in the hollow cysts that comprise most of the T1D IPC cultures

The hollow cysts prevalent in T1D IPC cultures, which collapse upon fixation, are insulin negative (column 1). Insulin appears in tight clusters found rarely in T1D cultures (column 2) and more predominantly in the ND cultures (column 3). Controls for staining were iPS cells (not shown) and islets (column 4). Scale bar = 50 μm.

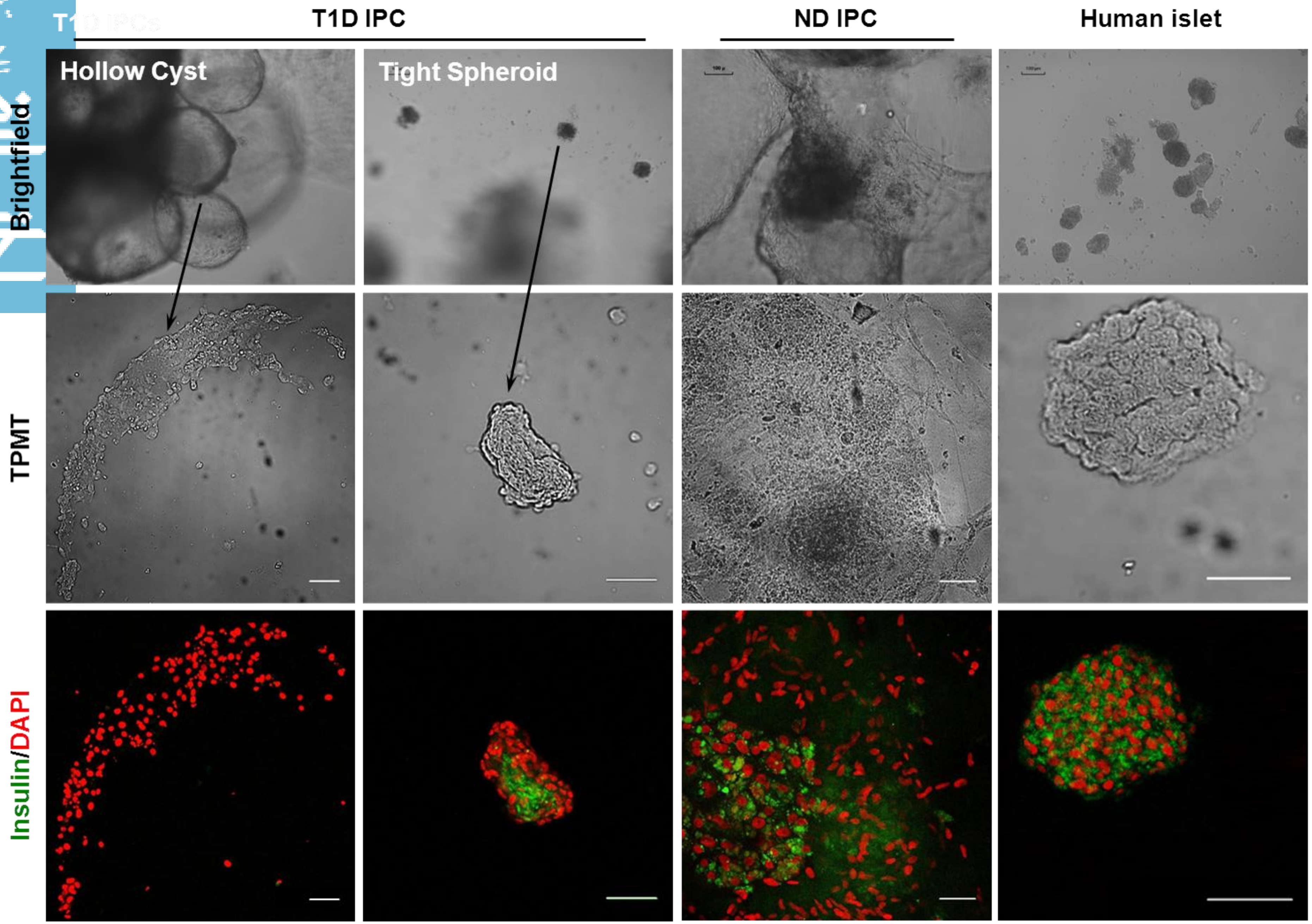
T1D IPC
ND IPC
Human islet
Hollow Cyst
Tight Spheroid
Brightfield
TPMT
Insulin/DAPI

Scale bar represents 50µm

Figure 10. Rare large organoids in T1D IPC cultures express insulin

(A) T1D iPS cells rarely yielded large, compact organoid-like structures measuring several millimeters in length. Immunostaining of these structures reveals strong expression of insulin. Scale bar = 500 µm. **(B)** A higher magnification of the staining reveals cytoplasmic staining of insulin in these rare structures. Scale bar = 50 µm.

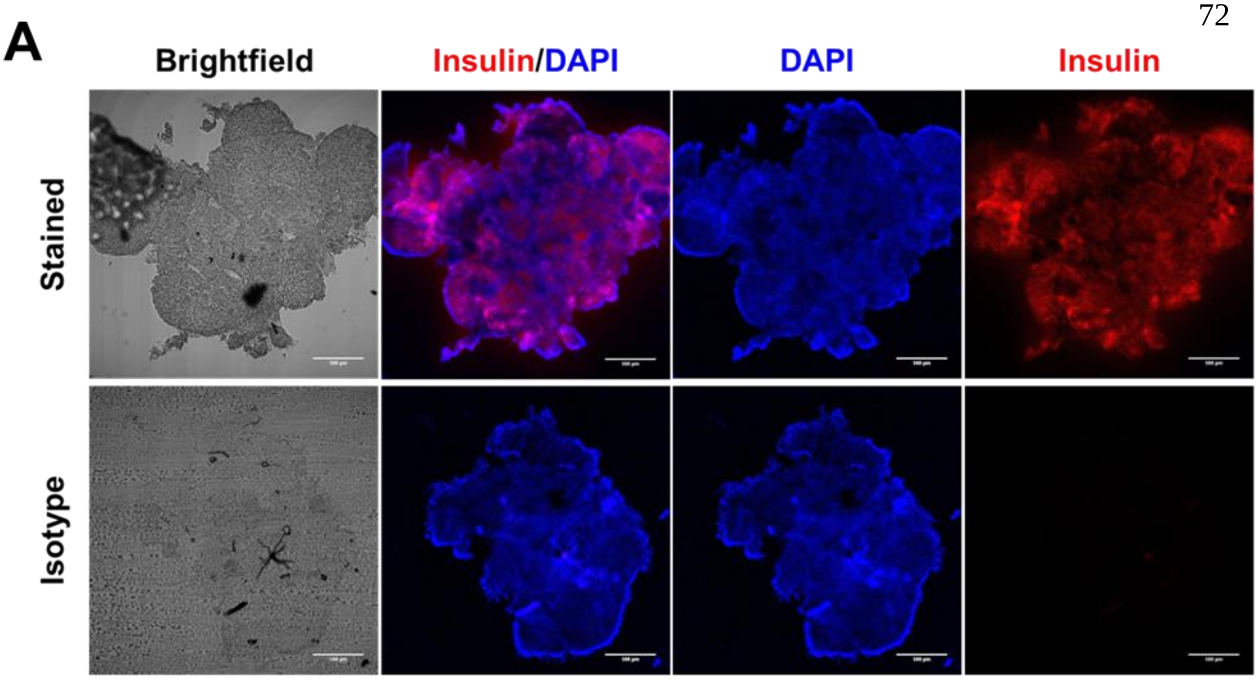
A
Brightfield
Insulin/DAPI
DAPI
Insulin
Stained
Isotype

Scale bar represents 500µm (0.5mm)

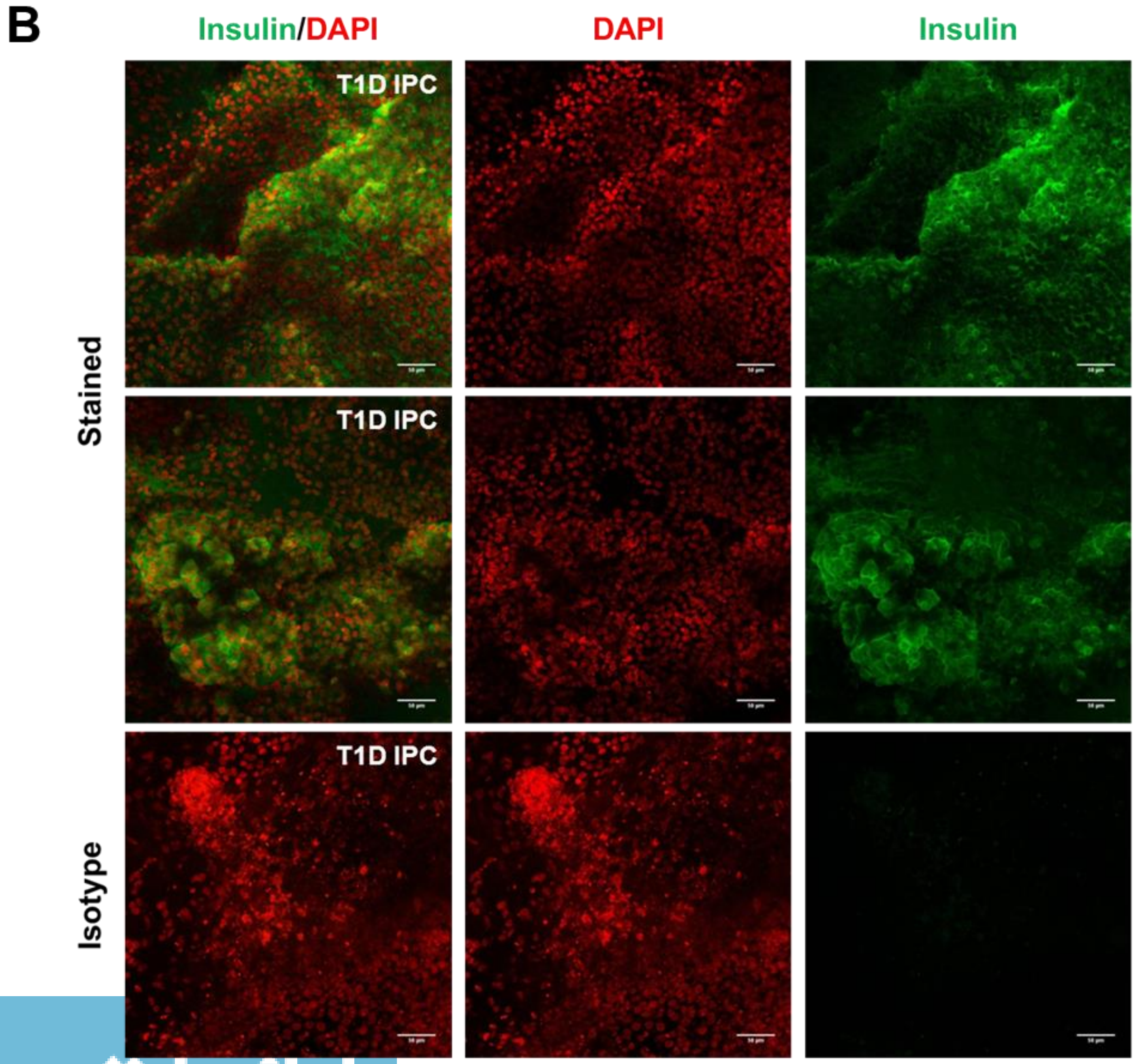
B
Insulin/DAPI
DAPI
Insulin
T1D IPC
T1D IPC
T1D IPC
Stained
Isotype

Scale bar represents 50µm

Figure 11. T1D iPS cells give rise to significantly less IPCs compared to ND iPS cells

Whereas up to 50% of the ND iPS cell-derived IPCs are insulin-expressing (consistent with the 50:50 mixture of insulin$^-$ hollow cysts and insulin$^+$ compact spheroids, Figure 8), only 15% of the T1D IPCs express insulin (consistent with the finding that 16% of the clusters are compact spheroids that express insulin, Figure 8). Controls for insulin staining were undifferentiated iPS cells (negative) and primary human islets (positive), which consist of both insulin$^+$ and insulin$^-$ cells, as expected. Remarkably, ND iPS cells yielded a population of insulin$^+$ cells that was a comparable percentage to what was observed in human islets (*n* = 3).

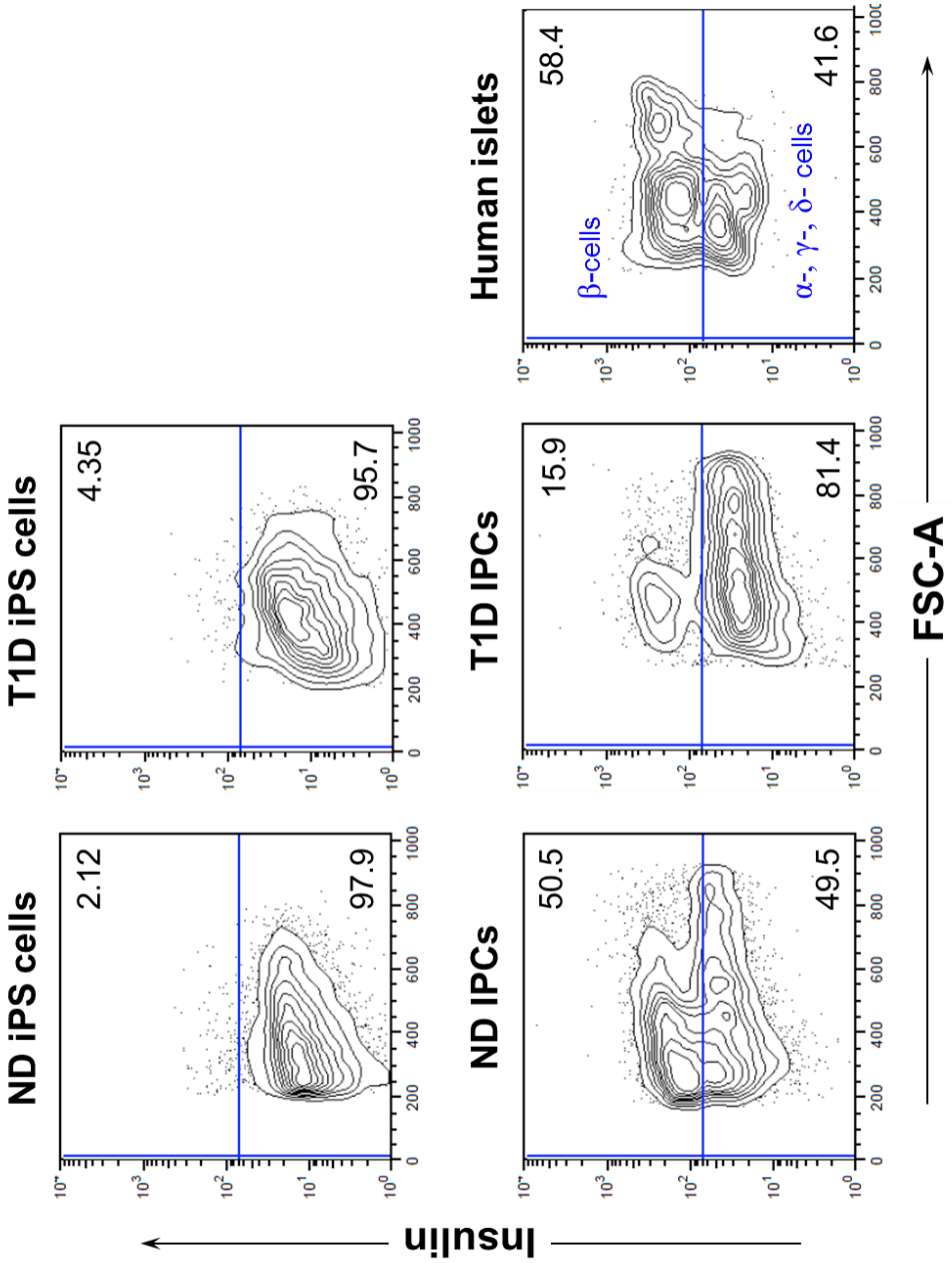
ND iPS cells
2.12
97.9
T1D iPS cells
4.35
95.7
ND IPCs
50.5
49.5
T1D IPCs
15.9
81.4
Human islets
58.4
41.6
β-cells
α-, γ-, δ- cells
Insulin
FSC-A
10^0
10^1
10^2
10^3
10^4
0
200
400
600
800
1000

Figure 12. The insulin$^+$ peak in T1D IPCs is significantly smaller compared to ND IPCs

All cell types consisted of insulin$^+$ and insulin$^-$ cells, separated in peaks demarcated by the dashed line. Remarkably, the insulin$^+$ peak in ND IPCs almost completely aligned with that of primary human islets. However, a significantly diminished insulin$^+$ peak was observed in the T1D IPCs (*n* = 3).

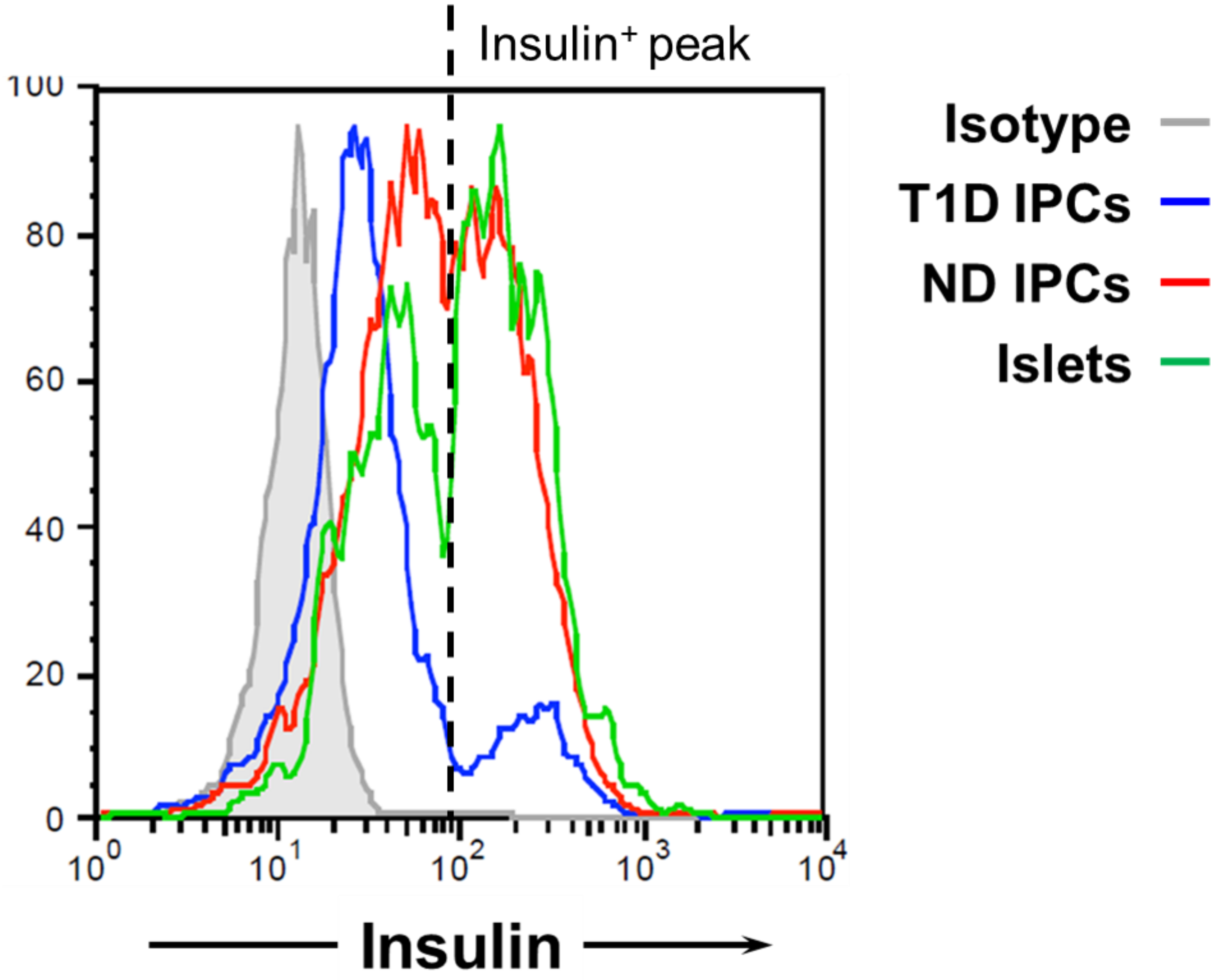
Insulin⁺ peak
100
80
60
40
20
0
10^0
10^1
10^2
10^3
10^4
Insulin
Isotype
T1D IPCs
ND IPCs
Islets

Figure 13. T1D IPCs express lower mRNA transcript levels of *Insulin*, *Glucagon* and the pancreatic master regulator *Pdx1* relative to ND IPCs

Using qRT-PCR, mRNA levels of various pancreatic genes were quantified in ND IPCs and T1D IPCs. Notably, the increase in *Insulin* expression in Stage 5 was accompanied by a striking decrease in *Glucagon* expression in the ND differentiating cultures, confirming the influence of the last stage of differentiation in directing the cells toward the insulin-expressing lineage. However, the T1D culture expressed significantly lower levels of *Insulin* and *Glucagon* compared to ND IPCs. This is likely due to significantly poorer expression of the pancreatic master regulator gene *Pdx1* in T1D differentiating cultures compared to in ND cultures ($n = 5$).

These data were generated by normalizing Ct values to an iPS cell line. The internal control used in this experiment was the TATA Binding Protein (TBP) housekeeping gene, which was selected after a screen of three potential housekeeping genes (GAPDH and β-actin were the other two genes). TBP was selected because its amplification pattern best resembled the ones observed for the test genes. Data are represented as mean ± SEM, $*p < 0.05$, $**p < 0.01$, $***p < 0.001$.

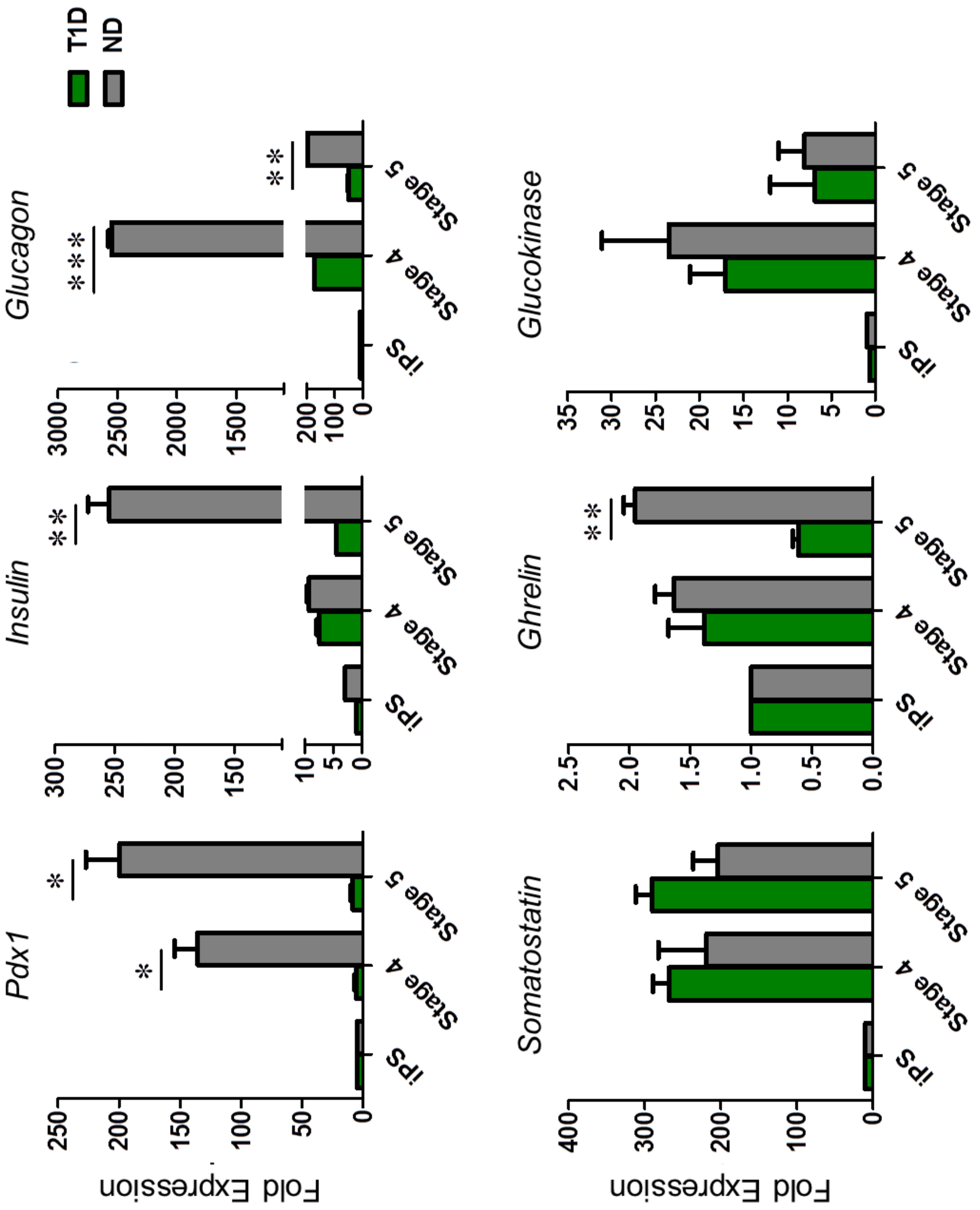
T1D
ND
Pdx1
Insulin
Glucagon
Somatostatin
Ghrelin
Glucokinase
Fold Expression
Fold Expression
0
50
100
150
200
250
0
5
10
150
200
250
300
0
100
200
1500
2000
2500
3000
0
100
200
300
400
0.0
0.5
1.0
1.5
2.0
2.5
0
5
10
15
20
25
30
35
iPS
Stage 4
Stage 5
*
*
**
***
**
**

CHAPTER IV

DEMETHYLATION OF T1D iPS CELLS YIELDS GLUCOSE-RESPONSIVE IPC CLUSTERS CONSISTING OF MONOHORMONAL INSULIN-EXPRESSING CELLS

Introduction

The process undertaken by a stem cell in assuming the distinct identity of a somatic cell is reliant on signals received by neighboring cells as well as on various physical and chemical environmental cues. The objective of these signals is to shape the genome common to all cells in such a way that a tissue-specific proteome is manifested to define the cells' ultimate identity, and to enable unique functions of the cell as a unit of that tissue[109]. Alteration of genome expression is accomplished through epigenetic silencing or activation of genes, which occurs following modulation of the activity of specific enzyme complexes, each of which may perform one of a variety of epigenetic modifications, such as methylation or demethylation of DNA nucleotides, or acetylation and deacetylation of histone complexes around which DNA is wound[15,109].

Recent evidence suggests that pancreatic endocrine cells generated from human ES cells *in vitro* possess inappropriate repressive epigenetic marks on critical genes that manifest mature pancreatic β-cell features, and that such epigenetic defects are primarily rectified in ES cell-derived pancreatic endocrine organoids that have matured *in vivo*[15]. In undifferentiated ES cells, activating H3K4me3 and repressive H3K27me3 histone marks coexist on the same locus of tissue-specific genes, thereby inducing a state of bivalency—that is, a sort of developmental limbo—where the doubly marked genes are destined for expression in the future but remain silenced until elimination of the repressive H3K27me3 histone mark[15]. During lineage progression into pancreatic endocrine cells *in vitro*, bivalent marks are retained on many genes that are essential for mature β-cell function, suggesting incomplete chromatin remodeling due to the inability to reverse Polycomb complex-mediated accumulation of repressive H3K27me3 marks[15]. This defect likely confers a high degree of plasticity to the *in vitro* differentiated cells, which manifests in the low frequency of insulin$^+$ cells and overwhelming number of "confused" polyhormonal cells reported in previous differentiation protocols *in vitro*[12-16,48]. In contrast, pancreatic endocrine cells matured *in vivo* exhibit marked resolution of bivalency at most of the critical β-cell genes, thereby cementing their lineage choice as pancreatic β-cells, which is evident by the functional competence of these cells *in vivo*[15]. Altogether, these data suggest that the aberrant chromatin remodeling of β-cell genes during *in vitro* differentiation may underlie the immature properties and suboptimal function of IPCs generated *in vitro* so far[15].

For such a dramatic disparity between *in vitro*-derived and *in vivo*-matured pancreatic endocrine cells to be rooted in epigenetic inconsistencies should come as no surprise since epigenetics represents the very basic level of transcriptional control in the cell[109]. Rewiring of the epigenetic circuitry is thus fundamental to the molecular basis of processes that alter cell fate, such as differentiation, dedifferentiation and transdifferentiation[109]. In theory, it should follow that tools which enhance epigenetic restructuring of the genome by creating a more malleable genome, somewhat like an epigenetic "blank slate", would promote the impact of stimuli utilized to direct the differentiation of stem cells into desired somatic cell lineages. Unraveling of epigenetic marks by treatment with the DNA methyltransferase (Dnmt) inhibitor 5-azacytidine has been exploited for inducing the transdifferentiation of fibroblasts into IPCs that produced insulin *in vivo* and protected mice from developing hyperglycemia after STZ challenge[110]. Additionally, 5-aza-2'-deoxycytidine, a more effective variant of 5-azacytidine that is incorporated into only DNA[111], was utilized for the transdifferentiation of human nonendocrine pancreatic progenitor cells[112] and rat liver epithelial stem-like WB-F344 cells[113] into functional insulin secreting cells. Collectively, these studies implicate a striking application for epigenetic modifiers such as 5-azacytidine in fashioning a more plastic state of the stem cell, allowing for potentially greater efficiencies of IPC derivation.

The vast evidence documenting the importance of epigenetics in controlling cell differentiation may explain why the differentiation of T1D iPS cells into IPCs is impaired. Interestingly, although iPS cells and ES cells have been shown to possess similar levels of the Dnmts[114], the phenomenon of epigenetic memory may impact the differentiation potential of iPS cells. This denotes the persistence of residual DNA methylation footprints from the somatic cell of origin in the pluripotent stem cell, impacting their differentiation into downstream cell types[115].

In Chapter III, we demonstrated that the differentiation of T1D iPS into IPCs was impaired for reasons that were unclear. Considering the importance of epigenetics in cell differentiation and the lack of expression of *Pdx1* in T1D differentiating cultures, we *hypothesized* that epigenetic barriers were prevalent in T1D iPS cells, preventing the expression of critical genes such as Pdx1 and ultimately limiting their differentiation into IPCs. To address this problem, we utilized 5-aza-2'-deoxycytidine (5-aza-DC), a potent demethylating agent that inhibits the DNA methyltransferase (Dnmt), thereby inhibiting methyl group deposition on cytosine residues of DNA, including on gene promoters[111] (Figure 14). This allows for the binding of transcriptional machinery and promotes gene expression. We reasoned that the use of a demethylation agent might induce a more labile, permissive state of the stem cell, allowing for greater cell responses to differentiation stimuli, and ultimately enhance the yield of IPCs from T1D iPS cells.

Our first goal was to compare the IPC differentiation potential of T1D and ND iPS cells, which was the subject of Chapter III. Now that we had indeed identified a difference, our new goal was to correct the impaired differentiation of T1D iPS cells into IPCs. Our *rationale* in pursuing this question was that recognizing and correcting an intrinsic defect in the differentiation of T1D iPS cells is critical before advancing clinical application of this therapy for T1D.

Figure 14. The mechanism of action for the transient demethylating agent 5-aza-2'-deoxycytidine (5-aza-DC)

5-aza-DC is a potent inhibitor of the DNA methyltransferase (Dnmt), which deposits gene-silencing methyl groups on cytosine residues of nascent DNA strands during semi-conservative replication. By utilizing a transient inhibitor of Dnmts, nascent DNA strands arising from DNA replication are not methylated. This allows silenced genes to become transiently re-expressed. This demethylation of genes is temporary, and the re-expressed genes become re-methylated (and hence re-silenced) eventually. Our hope in using this agent in our differentiation process is that critical genes such as *Pdx1* would be spared from the remethylation process due to signals from the differentiation-inducing media, which would allow for continual expression and rescue of the poor differentiation outcomes in T1D cultures. In summary, we aimed to make the T1D differentiating cells more receptive to differentiation cues. This would manifest in expression of *Pdx1* by T1D differentiating cells, as well as expression of its downstream targets, such as *Insulin* and *Nkx6.1*, which is a pancreatic β-cell-associated transcription factor.

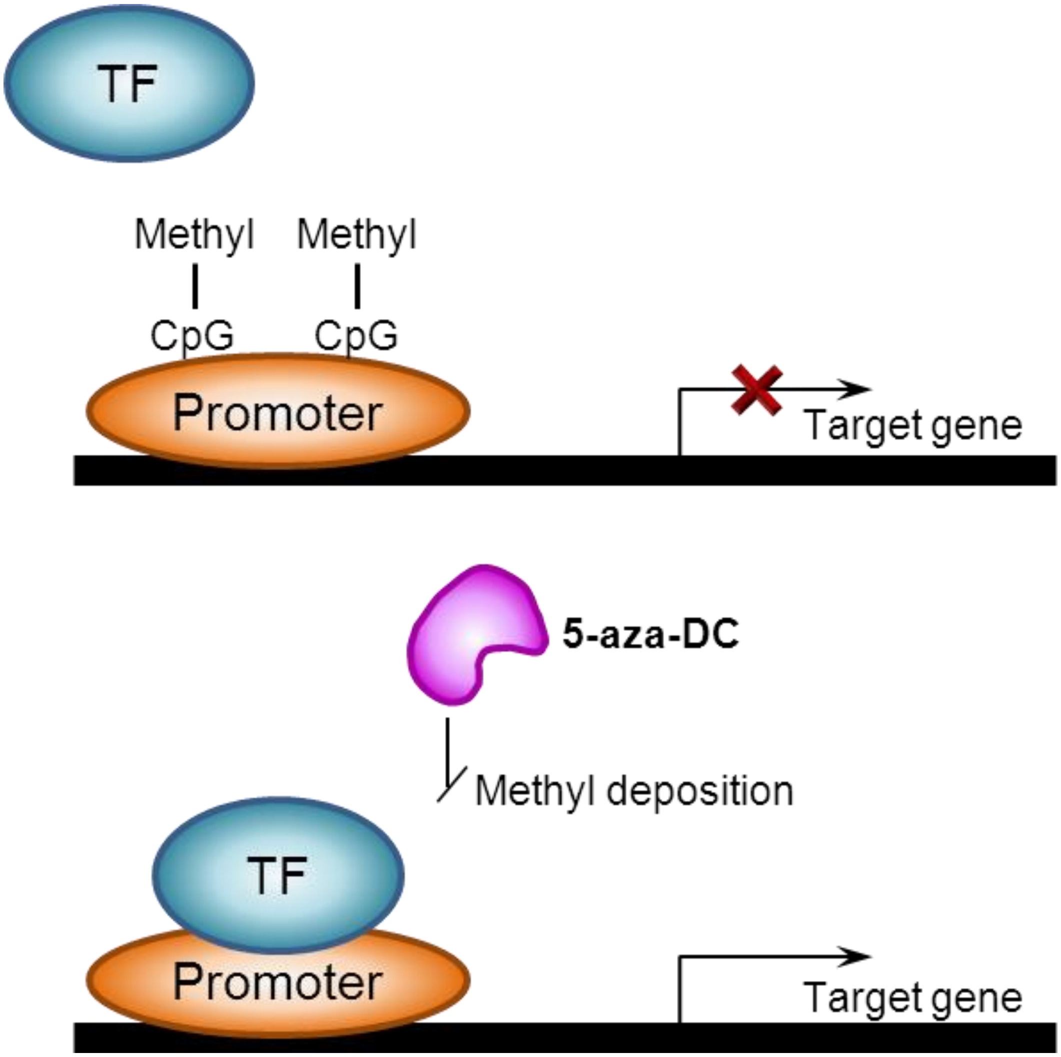
TF
Methyl
Methyl
CpG
CpG
Promoter
Target gene
5-aza-DC
Methyl deposition
TF
Promoter
Target gene

Results

Effective Differentiation Outcomes Requires Precise Temporal Modulation of Demethylation Treatment

Our first step in utilizing 5-aza-DC in these differentiation experiments was identifying an optimal dose for treatment that would preserve cell viability while effectively demethylating cells. 5-aza-DC is toxic to cells if the dose is too high or if the time of treatment is too long[116]. This toxicity is high individual to particular cell lines, and so we performed a screen to identify the dose range at which toxicity would be observed in T1D iPS cells.

Most reports use 100 nM, 1 μM or 10 μM for demethylation experiments in cancer cells[103,110,111,116]. Because iPS cells are fragile and much more refractory to toxic effects, we used 90 nM as a maximum dose, 30 nM as a minimum dose, and 50 nM and 70 nM as intermediary doses. iPS cells were treated at these various doses for 18 hours[110] before 5-aza-DC was washed away. The quality of the culture checked daily for 4 days. As evidenced in Figure 15A, one day after the demethylation treatment (top row), slight toxicity was observed only in the 90 nM dose, where we observed single cells floating in the cell culture.

On day 2 (second row), we could see the completely intact colony architecture that is characteristic of iPS cells in the 30 nM dose. At 50 nM, we could observe some disintegration of the colony edge, which was more pronounced at 70 nM with some thinning of the colony bed. The 90 nM treatment resulted in drastically compromised colony structure (Figure 15A). On day 3, the 30 nM and 50 nM doses showed much better colony structure than the 70 nM and 90 nM doses. These observations were exaggerated on day 4, where we observed slight thinning of the colonies at 50 nM and extensive loss of the colony bed in the 70 nM and 90 nM doses. Almost all of the colonies at 30 nM appeared completely unscathed. However, there were still very few colonies at this minimal dose that showed signs of thinning and loss of integrity. In order to ensure that the integrity of the differentiating cells would be preserved, we decided to utilize smaller doses than what showed minimal toxicity (30 nM) in our dose screen experiments (Figure 15A). We utilized 1 nM and 10 nM 5-aza-DC for our pilot differentiation.

Before we progressed, we used the proposed doses above to assess their effectiveness in demethylating iPS cells. As cells become demethylated, their 5-methylcytosine content decreases, since the replicating DNA is now no longer being modified by the Dnmts due to the inhibitor[110]. As a result, methyl groups are not being added to the nascent DNA strands. One can thus quantify the degree of demethylation by determining the levels of 5-methylcytosine in genomic DNA (gDNA)[110]. To determine the effectiveness of the proposed doses in demethylating iPS cells, we thus performed a dot blot assay[110] for 5-methylcytosine on gDNA isolated from iPS cells that were treated with 1 nM or 10 nM 5-aza-DC for 18 hours. Untreated iPS cells were used as a negative control. At the 1 nM and 10 nM 5-aza-DC treatments, we observed loss of methylation in iPS cells as evidenced by the lighter spots on the film corresponding to lower levels of 5-methylcytosine in these cells (Figure 15B).

Having confirmed that the doses above resulted in decreased 5-methylcytosine content in the iPS cells, we next sought to assess what time point in the differentiation the demethylation treatment should be implemented. We considered two possible time points for the demethylation treatment: 1) at the start of the differentiation into DE cells, or 2) after the generation of DE cells, before the cells progress into the stage in which Pdx1$^+$ cells are generated. We reasoned that because the generation of DE cells was optimal in T1D cells, and since it was only the stage after that in which the differentiation was impaired (evidenced by the poor yield of Pdx1$^+$ cells), the impact of demethylation would be most needed after the generation of DE cells, while the cells are making the choice between hepatic vs. pancreatic commitment.

Before we compared the two time points in the full differentiation procedure, we addressed the impact of demethylation on only DE cell differentiation if the demethylation was initiated in the very beginning or during the last day of DE differentiation before the cells received signals to become Pdx1$^+$ progenitor cells. Interestingly, we observed that the treatment of iPS cells with 10 nM 5-aza-DC on day 0 of differentiation (before initiating the generation of DE cells) resulted in cells on day 5 that were arrested in the immature CXCR4$^+$ PDGFRα$^+$ Sox17$^-$ mesendodermal state (Figure 16). In contrast, demethylation of the cells on day 4 of differentiation, which is the last day of DE culture, generated a pure population of CXCR4$^+$ Sox17$^+$ PDGFRα$^-$ DE cells, similar to what we were able to generate without any demethylation whatsoever. This pilot experiment allowed us to conclude that the demethylation treatment needed to be implemented after the generation of DE cells, immediately before the cells received signals instructing them to differentiate into Pdx1$^+$ pancreatic progenitor cells.

Demethylation of T1D DE Cells Leads to the Generation of Compact, Islet-Like Clusters that Strongly Resemble Islets

After identifying the doses and time point at which demethylation would be performed, we initiated a full differentiation of T1D iPS cells into IPCs, demethylating the DE cells on day 4 for 18 hours with two doses of 5-aza-DC: 1 nM and 10 nM. Untreated cells were used as a control. After this, the cells were transferred into matrigel and the differentiation proceeded for 22 more days. Morphologically, we noticed a striking impact of the demethylation treatments in the T1D differentiating cultures. Typically, T1D iPS cells gave rise to a disorganized mix of cysts and spheroids, with a dominant presence of hollow cysts. At a dose of 10 nM, 5-aza-DC treatment instead promoted the formation of compact clusters (Figure 17). Juxtaposition of the clusters derived from the three treatment conditions showed that regardless of the dose, demethylation generated cell clusters that uniquely resembled human islets (Figure 18). Next, we stained these cell clusters with dithizone, which is an organic compound that complexes with Zn^{2+} ions found in insulin hexamers of β-cell insulin granules[117], and thus suggests the presence of insulin. Dithizone staining revealed the strong red color of the compact clusters found in the 1 nM and 10 nM 5-aza-DC treated cultures, which was reminiscent of islets (Figure 18). This was in contrast to what was observed in the IPCs derived from untreated iPS cells, which stained brown in a manner similar to undifferentiated iPS cells (Figure 18).

Demethylation of T1D DE Cells Yields >90% Pdx1$^+$ Cells and >50% Insulin$^+$ Cells while Averting the Generation of Glucagon$^+$ Cells

Next, we assessed whether the demethylation rescued the expression of Pdx1 in the differentiating T1D cultures. We chose to address this question by determining the expression of Pdx1 in the differentiating cells using flow cytometry. Undifferentiated iPS cells were exploited as negative controls in these experiments, and the mouse insulinoma βTC3 served as a positive control[118] for all of these stains.

As described above, the yield of insulin$^+$ cells from T1D iPS cells was approximately 15% at the end of Stage 5 (Figure 11), which is consistent with the 12% yield of Pdx1$^+$ pancreatic progenitor cells observed in regular differentiations at the end of Stage 4 (Figure 19). However, after treatment with 10 nM 5-aza-DC, we observed robust expression of Pdx1 (~95%) at the end of Stage 4 (Figure 19). Additionally, a significant proportion of cells co-expressed Pdx1 and the pancreatic β-cell specific transcription factor

Nkx6.1, which is critical for maintaining the identity and function of pancreatic β-cells[63,64] (Figure 20A), although there was some variability in this yield at the end of Stage 4 (Figure 20B). Altogether, this data suggested that the transient demethylation treatment allowed the expression of Pdx1 in differentiating T1D cultures.

This then led us to wonder if the demethylation treatment enhanced the expression of downstream targets of Pdx1[46], such as insulin, and made the cells more receptive to small molecule signals promoting IPC differentiation while averting commitment towards alternative lineages. Specifically, we sought to determine the proportion of insulin producing cells relative to those that stain for glucagon, which is another pancreatic hormone that counteracts the impact of insulin[119]. Most reports published so far generate multihormonal cultures that express both insulin and glucagon[12-16,48], which is obviously counterproductive and inefficient.

Thus, we wondered what impact demethylation had on the percentage of insulin- versus glucagon-expressing cells. That percentage would indicate how efficient our differentiation protocol was for the selective generation of IPCs. For this question, we chose to use flow cytometry to analyze the expression of both of these hormones.

As can be seen in Figure 21, the proportion of glucagon-expressing cells was quite high when the iPS cells were not demethylated, whereas very few of the cells were insulin expressing (second column in Figures 21A and 21B). Indeed, the untreated cells only yielded up to 13% insulin-expressing cells and 50% glucagon-producing cells. However, that proportion was reversed when the iPS cells were treated with 5-aza-DC at doses of 1 nM and 10 nM. In these cultures, up to 56% of the demethylated iPS cell-derived IPCs expressed insulin, with a much smaller portion of the remaining cells expressing glucagon (Figures 21A and 21B, third and fourth columns). Additionally, this yield proportionally improved in a concentration-dependent manner (Figure 21C). Because the highest yield resulted from treatment of the cells with 10 nM 5-aza-DC, we chose to use this dose for all subsequent experiments.

This experiment has been repeated multiple times and we have obtained as many as 65% insulin$^+$ cells from demethylated T1D iPS cells (Figure 22A). Histogram depiction of these data demonstrates that the insulin$^+$ peak found in the T1D IPCs aligns with the peak found in the βTC3 mouse insulinoma cells (positive control[118]). The much smaller insulin$^-$ peak aligns with that of the undifferentiated iPS cells and the isotype control (Figure 22B). When these data are compared with the histogram depicted in Figure 12, there is an obvious improvement in the yield of insulin$^+$ cells after demethylation of T1D iPS cells. Collective pooling of data from several differentiations reveals that 5-aza-DC treatment consistently enhances the yield of IPCs by more than 4-fold (Figure 22C).

Mainstream published protocols for the generation of IPCs from iPS or ES cells generally give rise to a multihormonal pool of cells, of which very few cells only express insulin[12-16,48]. The data in Figure 21 suggested that our advances to this protocol allowed for the selective generation of insulin-expressing cells from T1D iPS cells while generating very few glucagon-expressing cells. Immunofluorescence analysis of the differentiated cell clusters corroborated these findings, whereby we learned that the demethylated iPS cells gave rise to islet-like clusters that consisted almost entirely of unihormonal insulin-expressing cells and very few glucagon-producing cells (Figure 23). Thus, 5-aza-DC appears to promote the generation of unihormonal insulin-expressing cells while averting the formation of glucagon-producing cells.

Demethylation of ND iPS Cells Does Not Enhance the Production of Pdx1$^+$ Cells or Insulin$^+$ IPCs

Following the provocative finding that 5-aza-DC significantly enhanced the yield of IPCs from T1D iPS cells, we wondered whether the demethylation treatment would improve the already high yield of IPCs from ND iPS cells. Our *hypothesis* prior to initiating this experiment was that the poor differentiation yield from T1D iPS cells was the result of hypermethylation (and hence silencing) of specific loci, such as Pdx1, in the genome of T1D differentiating cells. We reasoned that since ND iPS cells yielded IPCs efficiently, these loci must not be aberrantly methylated in ND cells. Thus, we *hypothesized* that demethylation should not significantly improve the yield of IPCs from ND iPS cells, since their differentiation was not impaired in the first place.

To test this hypothesis, we initiated parallel differentiations of ND iPS cells into IPCs, with one control group of wells and another set of wells undergoing demethylation with 10 nM 5-aza-DC. At the end of the differentiation (Stage 5), we analyzed the expression of Pdx1 and insulin by flow cytometry. Undifferentiated iPS cells served as negative controls in these experiments, whereas βTC3 mouse insulinoma cells were our positive control cell line[118]. Confirming what we demonstrated in Chapter III, the yield of Pdx1$^+$ cells (~70%, Figure 24A) and insulin$^+$ cells (~45% in Figure 24B and ~50% in Figure 11) at the end of Stage 5 is already very high in regular ND differentiating cultures. Demethylation of the cells at the end of Stage 1 did not significantly improve the yield of Pdx1$^+$ cells (~76%, Figure 24A) or insulin$^+$ cells (~50%, Figure 24B). This finding is consistent with our expectations, which we reasoned based on our hypothesis that specific gene loci are aberrantly methylated in specifically T1D iPS cells, which explains why demethylation selectively improves the differentiation of only T1D iPS cells.

T1D IPCs Derived from Demethylated DE Cells Express Pancreatic β-cell Specific Markers

To further characterize the authenticity of the IPCs generated after demethylation of T1D iPS cells, we performed immunofluorescence analysis of the Stage 5 cells to determine the expression of the pancreatic β-cell specific transcription factor Nkx6.1, which is critical for the maintenance of pancreatic β-cell function and identity[63,64]. We also determined the expression of C-peptide, which is a byproduct of proinsulin processing and is synonymous with *de novo* production of insulin[13,14,44,54,73,107]. In the dawn of pancreatic β-cell generation from ES cells, the first report of ES cell-derived insulin producing cells misrepresented their results[120] by showing that their cells express insulin when the insulin was actually derived from culture media components[121]. As such, using C-peptide expression as a metric for evaluating differentiated cells is important to conclusively demonstrate that the cells are producing insulin *de novo*[121]. As evidenced in Figure 25, T1D IPCs derived via demethylation show robust expression of C-peptide in the cytoplasm as well as strong nuclear expression of Nkx6.1. This confirms the flow cytometry results for Nkx6.1 and affirms our conviction that we have established a protocol that efficiently generates IPCs from T1D iPS cells that produce insulin *de novo* as determined by C-peptide expression by these cells.

T1D IPCs Possess Insulin Granules in Similar Quantities to Islets

Further analysis of the ultrastructure of these cells by Transmission Electron Microscopy (TEM) demonstrated a unique pancreatic β-cell like morphology of the granules contained in the T1D IPCs (Figure 26A). Insulin granules undergo various stages of maturation that are differentiated by the shape and darkness of the core[77,102]. The most mature insulin granules are angular due to the hexamer complexation of insulin with zinc, which creates a crystalline shape[122]. However, insulin granules universally possess a surrounding "halo" (which is an artifact of gluteraldehyde fixation) that is not found on any other hormone granule[122]. This feature is thus a unique and specific indication of β-cell like phenotype of differentiated cells.

As can be seen in Figure 26A, IPCs resemble islets in their possession of the three different insulin granules, all of which have the characteristic halo surrounding them. Additionally, the number of granules found in the IPCs is not statistically different from what we observed in primary human islets (Figure 26B). Thus, we have established a protocol for the generation of IPCs from T1D iPS cells that strongly resemble human islets in their ultrastructure in addition to their expression of insulin and other pancreatic β-cell specific markers.

The resemblance between the IPCs generated through this protocol and primary human islets is not limited to the intracellular features of the IPCs. As elaborated above, the overall appearance and size of the IPC clusters resembles that of islets. Counting the number of cells per cluster reveals that there is an average of 1372 cells per IPC cluster (Figure 27A), which is consistent with published reports of approximately 1500 cells per islet[123]. On average, our differentiations give rise to 300 IPC clusters per well of a 24-well plate (Figure 27B).

T1D IPCs Are Functional and Respond to High Glucose with Insulin Secretion

Until now, we suggested that demethylation promoted the selective generation of insulin-producing cells that are bound in tight clusters strongly resembling islets. Perhaps the most important criterion for defining the authenticity of the generated IPCs is to observe whether they exhibit glucose stimulated insulin secretion (GSIS), meaning that they will respond to high glucose challenge with insulin[45]. This characteristic β-cell property allows one to accurately gauge the true clinical application of the cells because it shows whether the cells are glucose-responsive and therefore, functional and suitable for therapy[45]. This is extremely important since these cells should respond to glucose spikes caused by food intake with insulin production[45]. Very recently, in late 2014, two reports emerged describing for the first time the generation of glucose-responsive cells from human ES cells[77,102]. However as of yet, the generation of functional, glucose-responsive IPCs from human iPS cells has not been demonstrated, much less using iPS cells of T1D patients.

To address the question of whether our method for generating IPCs from T1D iPS cells resulted in functional IPCs, we subjected the cell clusters to a GSIS assay, which involves exposing cells sequentially to low glucose (2.8 mM) and high glucose (28 mM) and comparing insulin content in the supernatant via ELISA. As evidenced in Figure 28A, clearly these IPCs are glucose-responsive in a manner that has never been published before for iPS cells, not even considering that these iPS cells are derived from T1D patients. However, we acknowledge that the amount of insulin secreted is significantly lower compared to islets (Figure 28B), indicating room for improvement. Remarkably, though, the fold-increase in insulin production by IPCs is higher than for islets (Figure 28C). The secretion of insulin by T1D iPS cell-derived IPCs after challenge with high glucose is a remarkable demonstration of the superiority of this protocol compared to prior reports[12-16,48] in generating authentic, functional IPCs.

Rapid Correction of Hyperglycemia in Diabetic Mice by T1D IPCs

To address the clinical utility of these cells in curing hyperglycemia *in vivo*, we transplanted the human T1D iPS cell-derived IPCs into completely immunodeficient Rag2$^{-/-}\gamma_c^{-/-}$ mice that were rendered diabetic (blood glucose levels of ≥300 mg/dL[104]) through a multiple low-dose regimen of streptozotocin (STZ), which is a toxin that selectively kills all mouse pancreatic β-cells[104]. Mice received 900 IPC clusters (~1.25 million cells) s.c. into the right shoulder flank[110] and their blood glucose levels were monitored weekly. Remarkably, the hyperglycemia plateaued and started to rapidly fall. Within 4weeks, all transplanted mice were either normoglycemic or achieved near normoglycemia (Figure 29A). None of the mice died or developed teratomas. Thus our data show rapid correction of hyperglycemia in diabetic mice using IPCs derived from T1D human cells. Compared to published timelines of 3 to 4 months[12-16,48], this rapid correction is promising testament to the superiority of our protocol in generating functional, mature IPCs *in vitro*. Excision of the transplanted cells after 8 weeks of s.c. transplantation revealed an organoid (Figure 29B) that showed glandular morphology evidenced by H&E staining (Figure 29C). The morphology of these cells was highly similar to H&E staining shown in one of the two seminal reports in the field published late last year (see Figure 7G of reference 77). In that reference, the organoids were derived from embryonic stem cell-derived IPCs that had been transplanted for 10 weeks under the kidney capsule[77].

Additionally, we subjected mice that showed stable correction of hyperglycemia to a glucose tolerance test, in which they receive a supraphysiological glucose bolus i.p. The management of this glucose spike is then assessed over a period of time in order to determine the kinetics of blood glucose regulation. Remarkably, in contrast to nontransplanted diabetic mice, which failed to return to normoglycemia and ultimately expired, IPC-transplanted mice completely recovered to normoglycemia in 4 hours (Figure 29D). This is evidence for how the IPCs endowed these formerly diabetic mice with the ability to tolerate and manage glucose spikes. However, we noted that the correction of hyperglycemia was significantly delayed compared to nondiabetic control mice, which is also evident by computing the “Area Under the Curve” for the three treatment groups

(Figure 29E), demonstrating that there is opportunity to further improve the function of the T1D iPS cell-derived IPCs.

iPS Cell-Derived IPCs are Poorly Antigenic and Do Not Stimulate NK Cell Killing Despite Poor MHC class I Expression

The success of this therapeutic modality in the clinical realm depends on how these cells fare in the inflammatory context of autoimmune disease that drives T1D. Insulin has been confirmed to be the chief autoantigen against which autoimmune responses are generated in T1D patients[124-126]. At first glance, this spells an enormous issue regarding the survival potential of iPS cell-derived IPCs since the expression of insulin by these cells is significant. However, the immunological equation of T1D is not as simple as guaranteed deletion of any cell that expresses insulin[4]. Instead, immunological recognition and subsequent deletion of insulin-expressing cells requires presentation of insulin on receptors called Major Histocompatibility Complexes (MHC)[4], of which there are two types: class I and class II. MHC class I is expressed on all nucleated cells and interacts with CD8 T cells[127]. MHC class II is only expressed by antigen presenting cells, such as B cells, Dendritic Cells (DCs) and macrophages, which scavenge protein “antigens” to present to CD4 T cells[128].

In T1D patients, insulin-specific autoreactive CD4 T cells escape deletion and orchestrate an autoimmune response after binding to insulin presented on MHC class II[4]. After scavenging and picking up insulin, DCs process the peptide and cross-present insulin (which is an exogenous antigen) on MHC class I[4]. After “kissing” autoreactive CD8 T cells targeting insulin, the DCs license the autoreactive CD8 T cells after providing them with particular costimulatory signals[4]. This eventually drives the activation and clonal expansion of insulin-specific autoreactive CD8 T cells[4]. These autoreactive CD8 T cells then migrate to and kill pancreatic β-cells by recognizing insulin bound on MHC class I that is expressed by the pancreatic β-cells themselves[4]. Thus, pancreatic β-cells are actively involved in their own demise by "shaking hands" with CD8 T cells that can only kill by "seeing" insulin on MHC class I[4]. Thus, if an insulin expressing cell does not express MHC class I, it cannot be lysed by an insulin-specific autoreactive CD8 T cell[4].

It is thus critical to define the immunological profile of iPS cell-derived IPCs and determine their expression of MHC class I. To this end, we determined the expression of MHC class I and class II on IPCs. We also assessed the expression of the T cell costimulatory molecules CD80 and CD86[42] by these cells. Undifferentiated iPS cells (which are famously poor expressors of these molecules[42] and thus regarded as "immunoprivileged") were utilized as negative controls in these experiments, whereas adult human peripheral blood mononuclear cells (PBMCs) served as positive controls[42]. As evidenced in Figure 30A, T1D IPCs poorly expressed MHC class I and MHC class II, as well as the T cell costimulatory molecules CD80 and CD86. We acknowledge that the expression of these molecules can be induced after their transplantation in the *in vivo* environment. This can be due to further maturation of the IPCs *in vivo*, or due to cytokine signals in the bloodstream that may upregulate MHC class I expression on these cells. However, what is presented here is quite promising because the lack of MHC class I by these cells *in vitro* makes these cells "invisible" to T cells and thus able to evade autoimmune destruction[42].

However, one important question we addressed following our finding that IPCs do not express MHC class I is to determine their susceptibility to Natural Killer (NK) cells. MHC class I is an inhibitory receptor for NK cells, which are a subset of lymphocytes that target MHC class I-negative cells, such as cancer cells or virus-infected cells[105]. Since IPCs do not express MHC class I, depending on their expression of other NK cell activating or inhibitory ligands, they could be suitable targets for NK cells. To address this, we performed a ^{51}Cr release assay using NK cells from human PBMCs activated with recombinant IL-2 as effector cells (killer cells) and cocultured them with ^{51}Cr-labeled IPCs as target cells. Release of radioactive ^{51}Cr suggests target cell death and allows one to make conclusions regarding the susceptibility of the target cells to NK effector cells. The positive control human K562 myeloma cells[42] were efficiently killed by NK cells, with the level of kill rising as the Effector:Target (E:T) cell ratio increased. In contrast, undifferentiated human iPS cells were not killed (Figure 30B), which os consistent with previously published data describing the paradoxical inability of NK cells to kill iPS cells despite their poor expression of MHC class I. Importantly, similar to their undifferentiated counterparts[42], IPCs are not recognized or killed by NK cells despite their poor expression of MHC class I (Figure 30B), which is consistent with prior reports regarding the poor susceptibility of undifferentiated ES cells to NK cell killing[129-132]. This suggests an immunoprivileged status for iPS cell-derived IPCs, which is promising for the clinical potential of these cells.

However, since these results are superficial and only telling of the *in vitro* quality of these cells, we cannot make any clear predictions on their immunological susceptibility or immunoprivilege after being transplanted. Further discussion of how these *in vitro* findings relate to our understanding of the immunological etiology and pathogenesis of T1D will be elaborated on further in the last section of Chapter V.

Summary

In Chapter III, we identified that the differentiation of T1D iPS cells into IPCs was impaired, the underlying basis of which was unclear. Gene expression data suggesting that the T1D culture did not express much *Pdx1* transcript suggested to us that there might have been epigenetic silencing which impaired the expression of critical genes such as *Pdx1* and ultimately negatively impacted the differentiation outcome. As such, we *hypothesized* that the poor IPC yield from the T1D iPS cells was due to epigenetic barriers preventing the expression of critical genes such as Pdx1. We further reasoned that the use of a demethylation agent might rescue this impairment by inducing a more labile, permissive state, and ultimately allow for enhanced cell responses to differentiation cues. In this series of experiments, we demonstrated correction of this impairment and robust Pdx1 expression using 5-aza-DC. This ultimately enhanced the differentiation of T1D iPS cells into islet-like IPC clusters that were compact and strongly expressed insulin but not glucagon. Additionally, these cells expressed other markers of pancreatic β-cells and resembled human islets in their possession of insulin granules. Finally, we demonstrated that these cells were glucose-responsive and rapidly corrected hyperglycemia in STZ-induced diabetic mice. To our knowledge, our studies are the first to efficiently generate functional IPCs from human iPS cells through a 3D culture platform. Additionally, we demonstrate that the differentiation of T1D iPS cells into IPCs is impaired relative to that of ND iPS cells and that we can correct this impairment using an epigenetic modifier. Indeed, we have demonstrated here a carefully optimized protocol by which we can efficiently convert T1D iPS cells into >95% Pdx1$^+$ cells and ~55% insulin$^+$ IPCs. Although, some features of these IPCs suggest that these cells need to further mature to become truly β-cell-like, we envision that improvements can be accomplished by coculture with cells comprising the islet niche, such as endothelial cells[33,133]. This will be elaborated on further in Chapter V.

Altogether our data demonstrate a highly efficient protocol for inducing directed derivation of IPCs from T1D patient-derived iPS cells. The success of a model in which iPS cells will one day be generated from T1D patients and used to generate IPCs will be highly dependent on the results of these current studies. We hope that these findings can one day translate into a patient-tailored, accessible cure for T1D.

Figure 15. Selection of a dose of 5-aza-DC to demethylate iPS cells while ensuring maximal cell viability

(A) Every cell type has a unique tolerance to 5-aza-DC, which is toxic at high doses. In order to identify an optimal dose of 5-aza-DC that would maintain integrity of the cells while demethylating effectively, we conducted a dose screen experiment on T1D iPS cells (*n* = 2), observing the quality of the colonies and degree of cell death over 4 days after 18h of treatment with various doses of 5-aza-DC. 30 nM of 5-aza-DC induced minimal toxicity (defined by thinning of colonies or loss of sharp colony edges), whereas we observed drastically compromised integrity of the cultures at 70 nM and 90 nM of 5-aza-DC. In order to ensure that the cultures will experience minimal toxicity, we utilized doses of 1 nM and 10 nM for future experiments, mostly focusing on 10 nM. **(B)** To confirm that those low doses would still demethylate cells, we performed a dot blot for 5-methylcytosine on gDNA isolated from untreated T1D iPS cells or iPS cells that were treated with 1 nM or 10 nM 5-aza-DC (*n* = 3). Untreated iPS cells possessed significant 5-methylcytosine content (leftmost column), evidenced by the dark spot where the DNA was blotted. As can be observed by lightening of the spots at the 1 nM and 10 nM doses, 5-aza-DC appeared to effectively demethylate the cells (1 minute or 5 minute represents the exposure time for the blot).

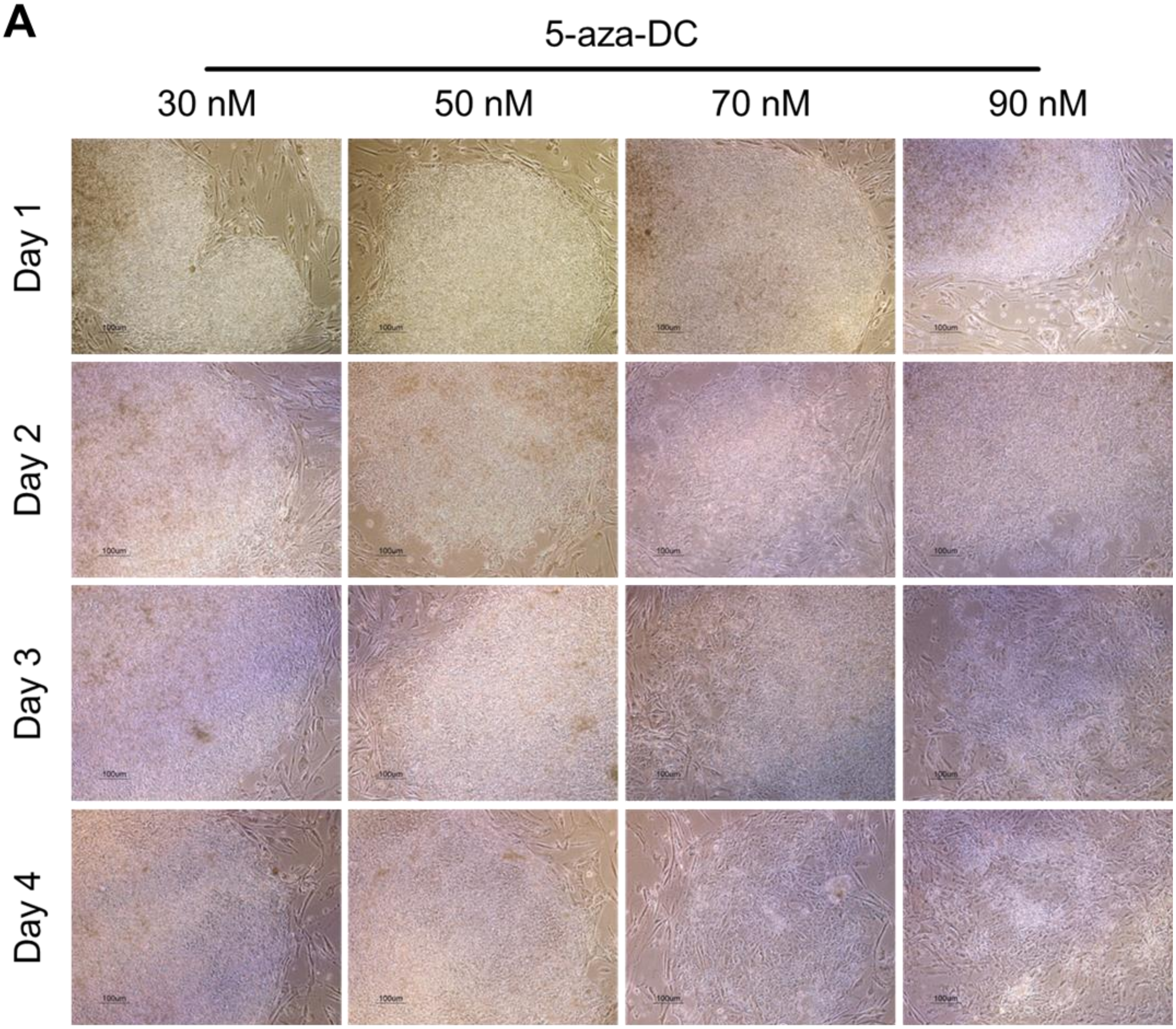
A
5-aza-DC
30 nM
50 nM
70 nM
90 nM
Day 1
Day 2
Day 3
Day 4
100um

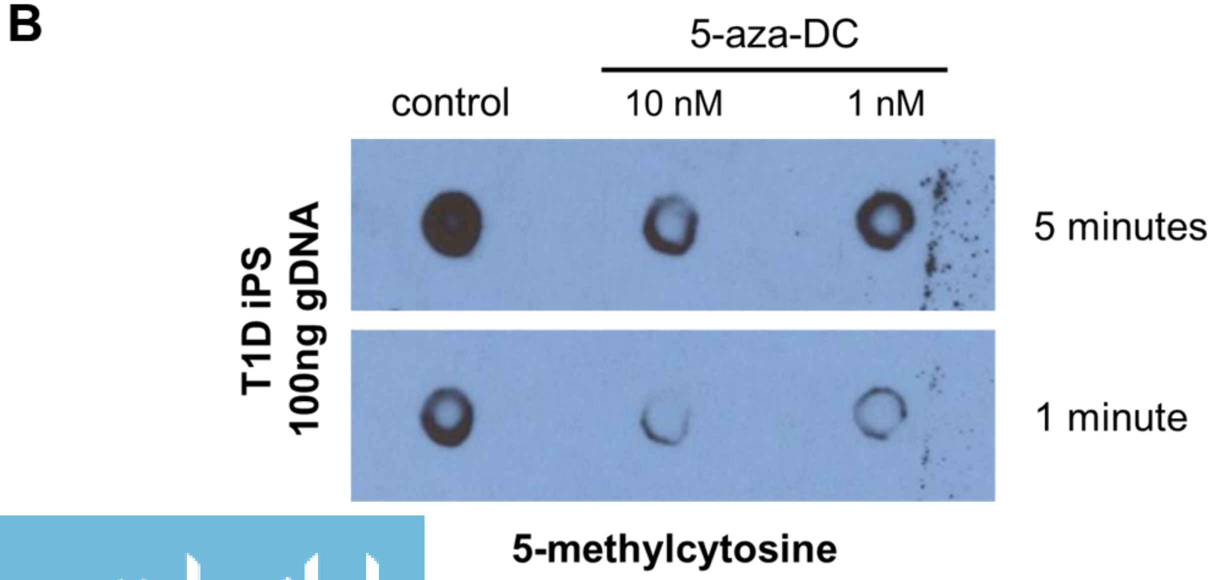
B
5-aza-DC
control
10 nM
1 nM
T1D iPS
100ng gDNA
5 minutes
1 minute
5-methylcytosine

Figure 16. Demethylation on D0 of differentiation arrests cells in a CXCR4$^+$ PDGFRα$^+$ Sox17$^-$ mesendodermal state

In order to identify the optimal time point at which demethylation should be initiated, we established two parallel differentiations of T1D iPS cells into DE cells. In one differentiation, the culture was exposed to 5-aza-DC on day 0 (which is the day that DE differentiation is initiated), whereas the other culture was demethylated at day 4 of differentiation (which is the last day of DE culture). At the end of the differentiations, we determined the efficacy of DE cell differentiation by determining the expression of CXCR4, PDGFR-α, and Sox17. Undifferentiated iPS cells (red plot) served as a negative control for all of these cell markers. Demethylation of the cells on day 0 of differentiation (green plot) resulted in cells that were CXCR4$^+$ PDGFR-α$^+$ Sox17$^-$, which represents the immature mesendodermal state. In contrast, demethylation of the cells on day 4 (blue plot) generated >90% CXCR4$^+$ Sox17$^+$ PDGFR-α$^-$ cells, representing true DE cells. This result motivated us to implement demethylation at the end of Stage 1 (on day 4), after generating DE cels, since demethylation at an earlier time point compromised the yield of DE cells. Thus, precise temporal control of the demethylation treatment is necessary to ensure optimal differentiation outcomes (n = 1).

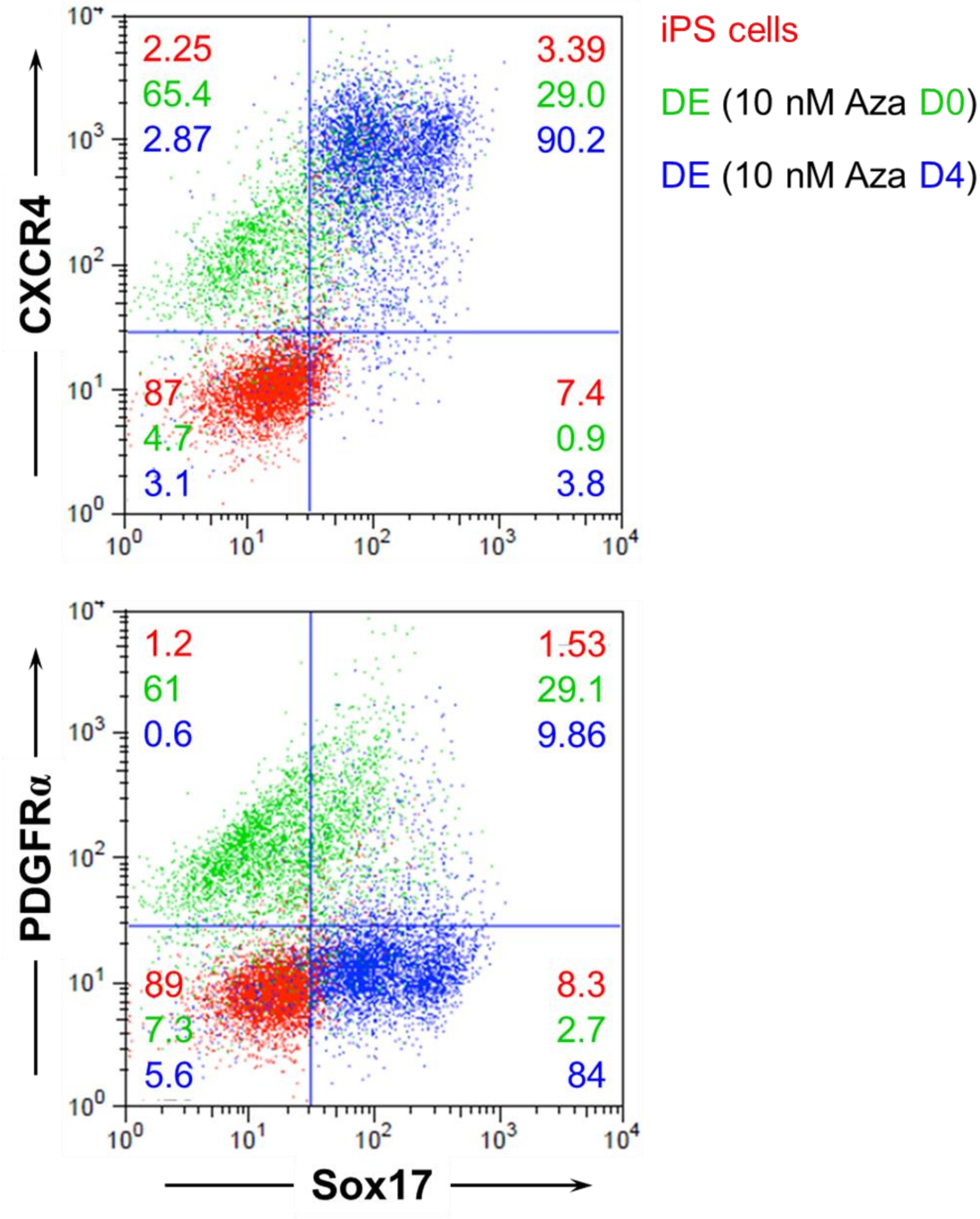
iPS cells
DE (10 nM Aza D0)
DE (10 nM Aza D4)
CXCR4
2.25
65.4
2.87
3.39
29.0
90.2
87
4.7
3.1
7.4
0.9
3.8
PDGFRα
1.2
61
0.6
1.53
29.1
9.86
89
7.3
5.6
8.3
2.7
84
10^0
10^1
10^2
10^3
10^4
Sox17

Figure 17. Demethylation of T1D DE cells uniformly gives rise to compact clusters that resemble islets

Morphological comparison of control and 5-aza-DC-treated cultures demonstrates the disparity between the treatment groups (*n* = 5). Whereas a regular differentiation of T1D iPS cells gives rise to a mixture of hollow cysts and compact spheroids, demethylation appeared to convert all of these T1D iPS cells into islet-like compact clusters.

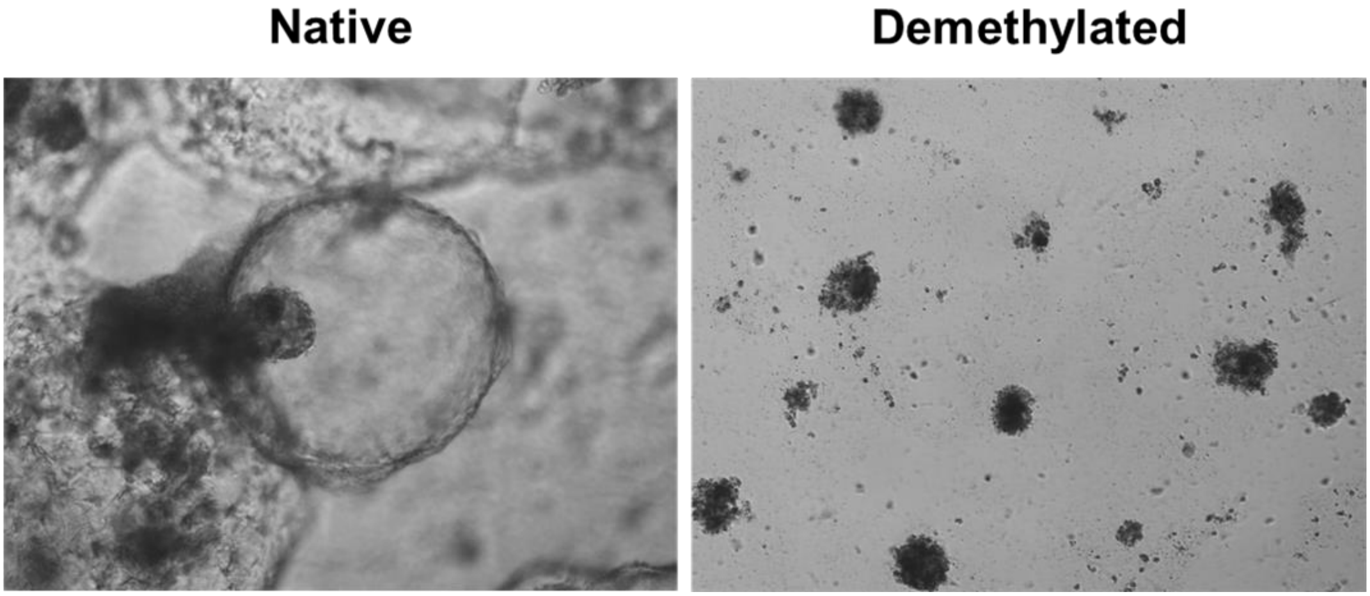

Native

Demethylated

Figure 18. T1D IPC clusters derived from demethylated DE cells stain strongly in dithizone solution in a manner similar to primary human islets

Treatment of T1D iPS cells with 5-aza-DC alters the morphology of the differentiated cells. Typically, T1D iPS cells give rise to a disorganized mix of cysts and spheroids (bottom half of leftmost column), with a dominant presence of hollow cysts. 5-aza-DC treatment instead promotes the formation of compact clusters that uniquely resemble human islets in both size and morphology. Dithizone staining (*n* = 4) reveals the strong red color of the compact clusters found in the 5-aza-DC treated cultures, which is reminiscent of islets. This is in contrast to what is observed in the untreated T1D IPC cultures, which stain brown in a manner similar to undifferentiated iPS cells.

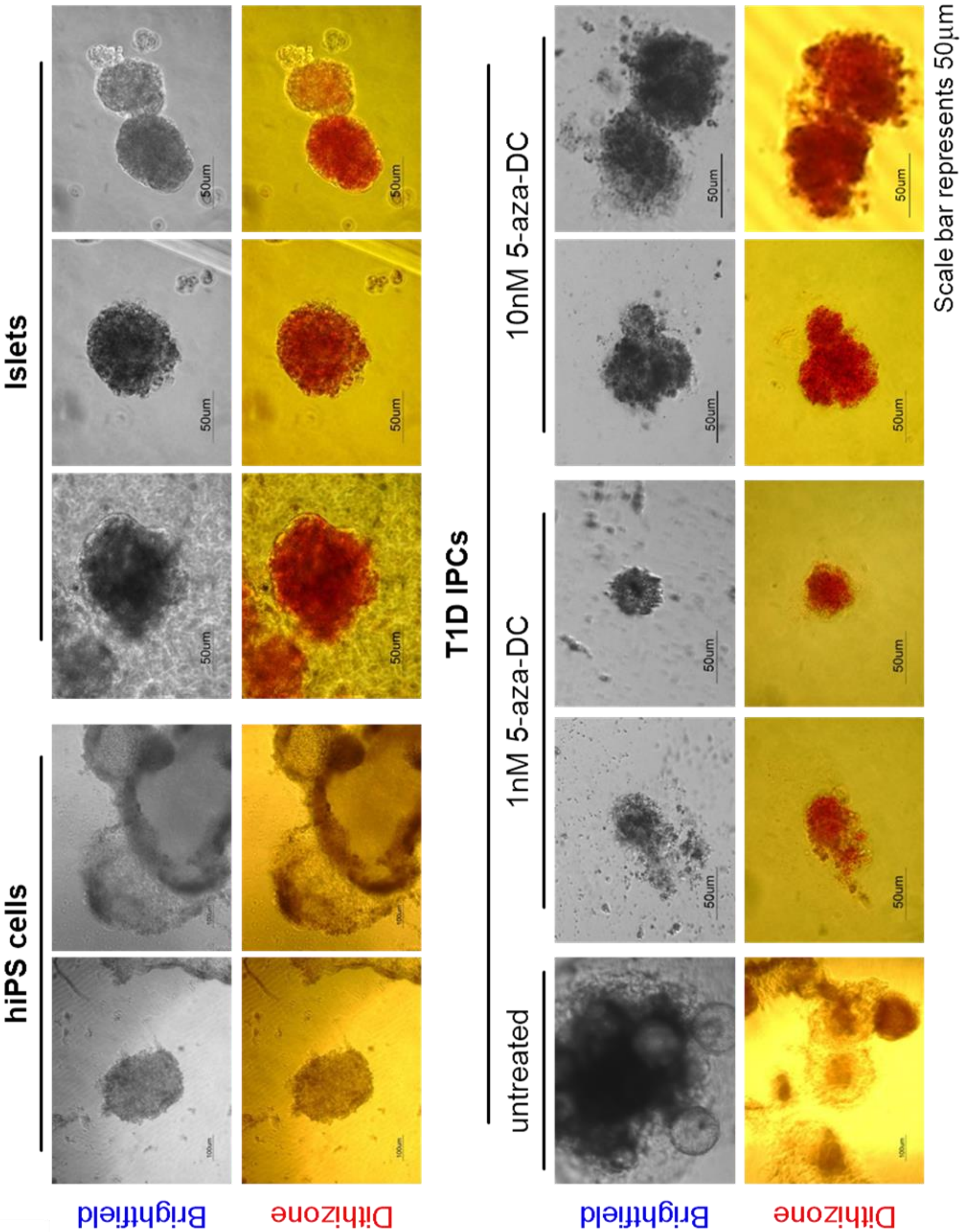
hiPS cells
Islets
T1D IPCs
untreated
1nM 5-aza-DC
10nM 5-aza-DC
Brightfield
Dithizone
100um
50um
Scale bar represents 50μm

Figure 19. Demethylation of T1D DE cells significantly improves the yield of Pdx1$^+$ cells

At the end of Stage 4, the yield of Pdx1$^+$ pancreatic progenitor cells form T1D iPS cells was poor (~12%), which translated into the impaired differentiation of the cells into insulin-expressing cells at the end of Stage 5 (Figure 11). Demethylation of T1D DE cells corrected this impairment and resulted in >95% Pdx1$^+$ cells at the end of Stage 4 (*n* = 4). Undifferentiated iPS cells served as a negative control, whereas the βTC3 mouse insulinoma cell line served as a positive control.

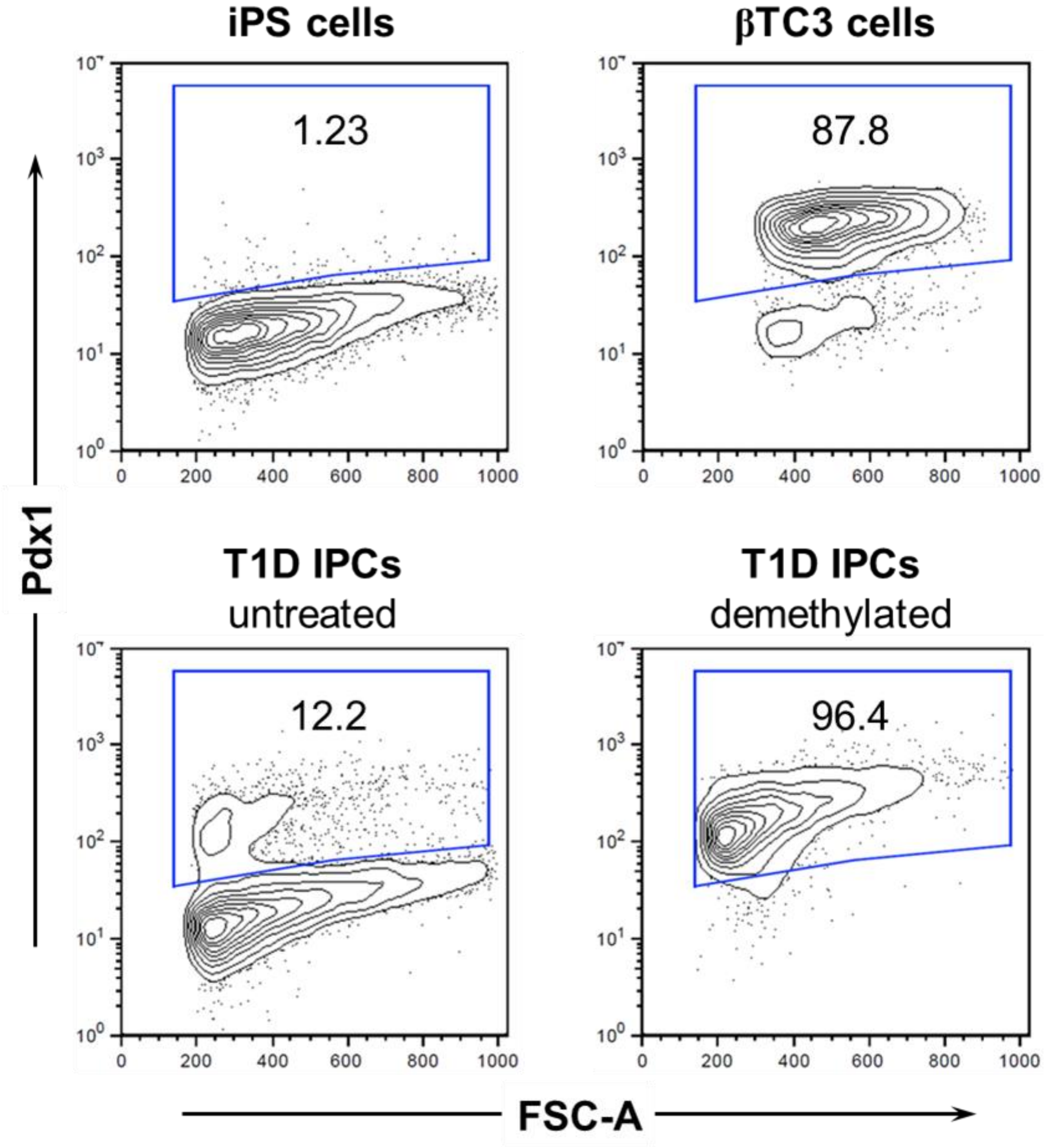
iPS cells
βTC3 cells
T1D IPCs
untreated
T1D IPCs
demethylated
1.23
87.8
12.2
96.4
Pdx1
FSC-A
10^0
10^1
10^2
10^3
0
200
400
600
800
1000

Figure 20. Range of Pdx1$^+$ Nkx6.1$^+$ cells derived from T1D iPS cells after transient demethylation treatment

(A) A significant proportion of the Pdx1$^+$ cells at the end of Stage 4 co-expressed the pancreatic β-cell specific transcription factor Nkx6.1 (*n* = 3). Undifferentiated iPS cells served as a negative control, whereas the βTC3 mouse insulinoma cell line served as a positive control. **(B)** As represented in this pooled collection of data from multiple experiments, we observed some variability in this yield at the end of Stage 4. Data are represented as mean ± SEM, *n* = 4 for Pdx1 staining, and *n* = 3 for Nkx6.1/Pdx1 double staining.

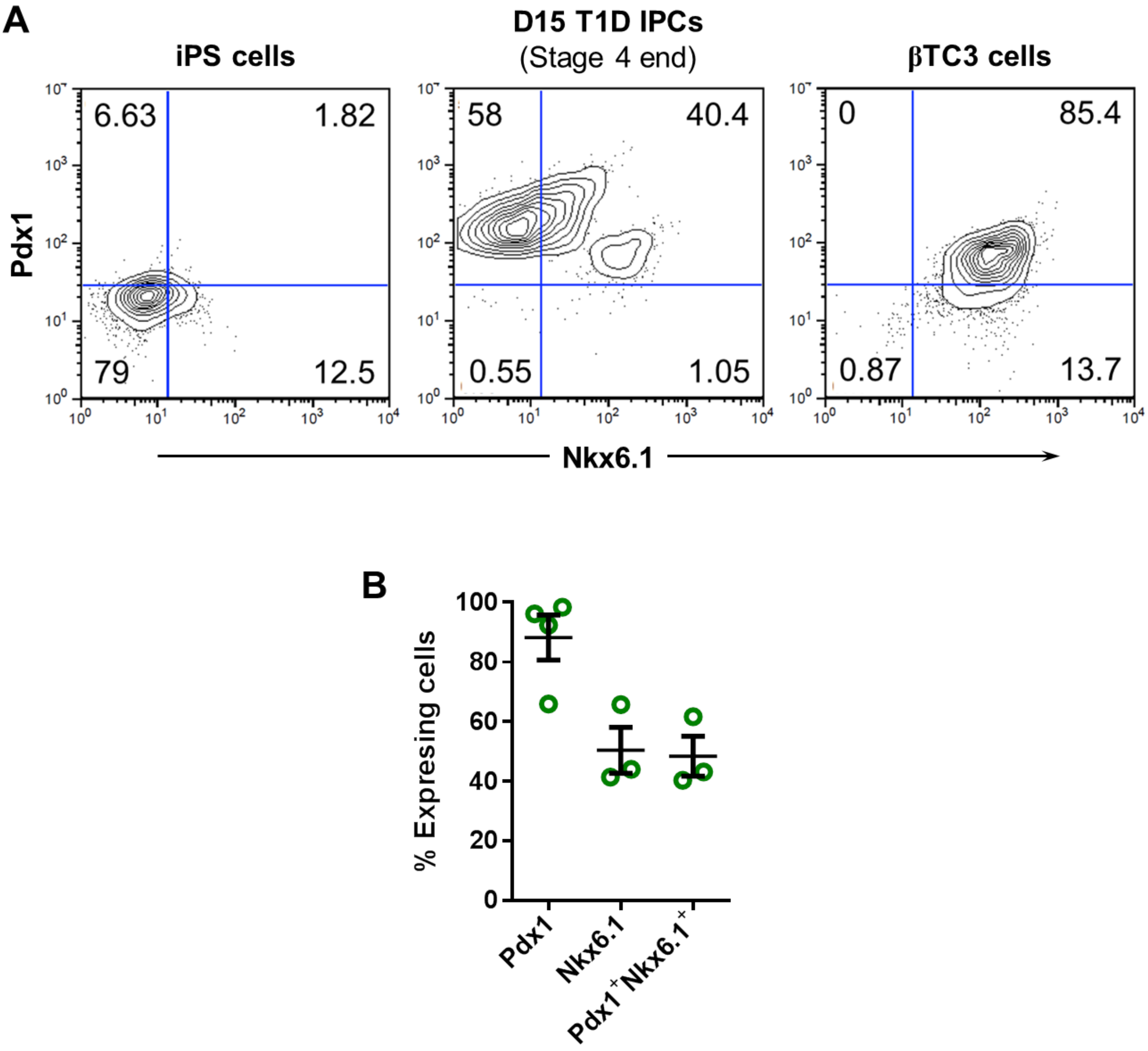
A
D15 T1D IPCs
(Stage 4 end)
iPS cells
βTC3 cells
Pdx1
Nkx6.1
6.63
1.82
79
12.5
58
40.4
0.55
1.05
0
85.4
0.87
13.7
10^0
10^1
10^2
10^3
10^4
B
% Expresing cells
100
80
60
40
20
0
Pdx1
Nkx6.1
Pdx1$^+$Nkx6.1$^+$

Figure 21. Demethylation of iPS cells significantly improves the yield of insulin$^+$ cells at the expense of glucagon$^+$ cells in a concentration-dependent manner

(A) Whereas untreated T1D iPS cells only yielded up to 13% insulin$^+$ cells, in cultures treated with 5-aza-DC, up to 56% of the cells were insulin-expressing (*n* = 5). In contrast, the greater emergence of insulin-expressing cells in the 5-aza-DC treated cultures was accompanied by a decline in the number of glucagon-expressing cells (*n* = 2) **(B)**, suggesting that 5-aza-DC directs iPS cells to form insulin secreting cells, rather than glucagon secreting cells. Controls for staining were iPS (negative) and βTC3 mouse insulinoma cells (positive). **(C)** The yield of insulin-expressing cells as opposed to glucagon-expressing cells proportionally improved in a concentration-dependent manner.

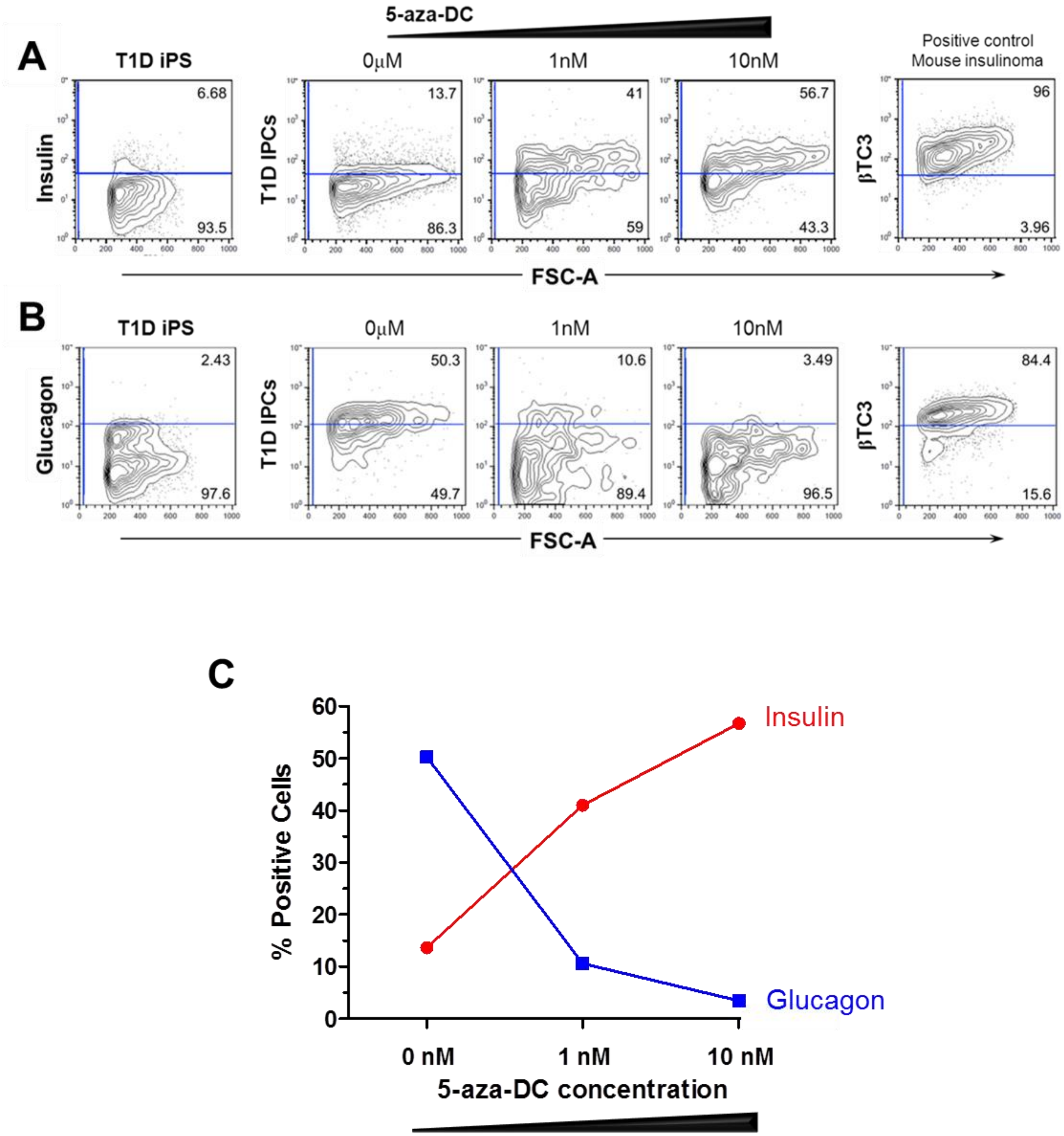
5-aza-DC
A
T1D iPS
0μM
1nM
10nM
Positive control
Mouse insulinoma
Insulin
T1D IPCs
βTC3
6.68
93.5
13.7
86.3
41
59
56.7
43.3
96
3.96
FSC-A
B
T1D iPS
0μM
1nM
10nM
Glucagon
T1D IPCs
βTC3
2.43
97.6
50.3
49.7
10.6
89.4
3.49
96.5
84.4
15.6
FSC-A
C
% Positive Cells
0
10
20
30
40
50
60
Insulin
Glucagon
0 nM
1 nM
10 nM
5-aza-DC concentration

Figure 22. Demethylation consistently yields a significantly higher yield of IPCs from T1D iPS cells

(A) We have obtained as many as 65% insulin-expressing cells from T1D iPS cells using this protocol. Controls for staining were iPS cells (negative) and βTC3 mouse insulinoma cells (positive). **(B)** Histogram depiction of these data reveals alignment of the robust insulin$^+$ peak of the T1D IPCs with that of the βTC3 cells. The negative peak aligned with that of the undifferentiated iPS cells. **(C)** A pooled representation from multiple experiments of the yield of insulin$^+$ cells from untreated ($n = 3$) and demethylated ($n = 5$) T1D DE cells shows that 5-aza-DC treatment consistently augments the yield of IPCs by nearly 4-fold, $^{***}p < 0.001$. Data are represented as mean ± SEM.

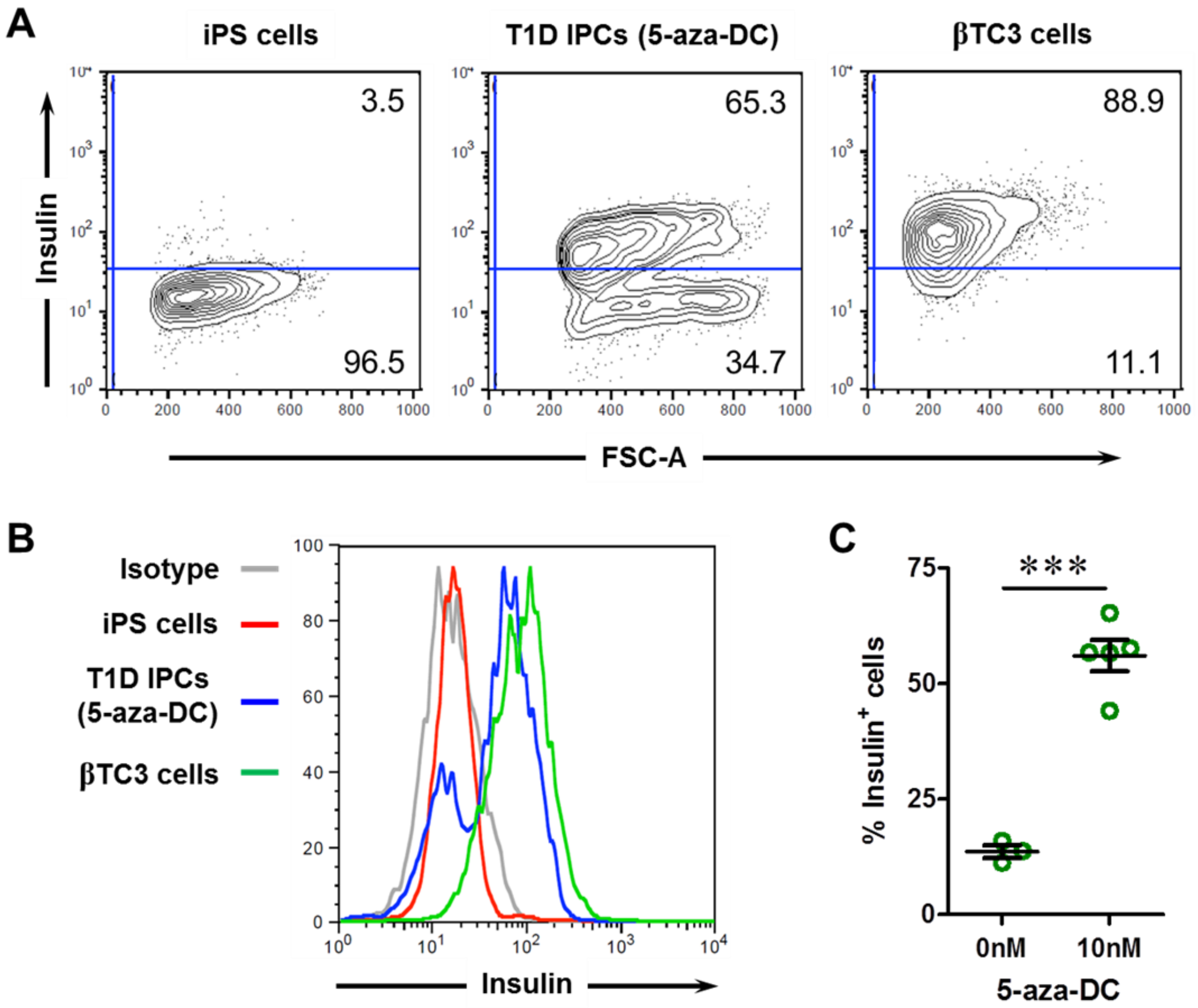
A
iPS cells
T1D IPCs (5-aza-DC)
βTC3 cells
Insulin
FSC-A
3.5
96.5
65.3
34.7
88.9
11.1
10^0
10^1
10^2
10^3
10^4
0
200
400
600
800
1000
B
Isotype
iPS cells
T1D IPCs (5-aza-DC)
βTC3 cells
0
20
40
60
80
100
Insulin
C
***
% Insulin$^+$ cells
0
25
50
75
0nM
10nM
5-aza-DC

Figure 23. 5-aza-DC converts T1D iPS cells into compact, islet-like clusters that consist almost entirely of insulin-expressing cells

iPS and ES cells typically give rise to a multihormonal pool of precursor cells that only acquire maturity and monohormonal expression of insulin after transplantation in mice. After utilizing 5-aza-DC to generate islet-like compact clusters, we sought to characterize the expression of insulin and glucagon within these cell clusters (*n* = 4). Consistent with the flow cytometry data, 5-aza-DC appears to promote the generation of unihormonal insulin-expressing cells while averting the formation of glucagon-producing cells. Human islets possess both insulin-expressing and glucagon-expressing cells. The scale bar represents 50 µm in all frames.

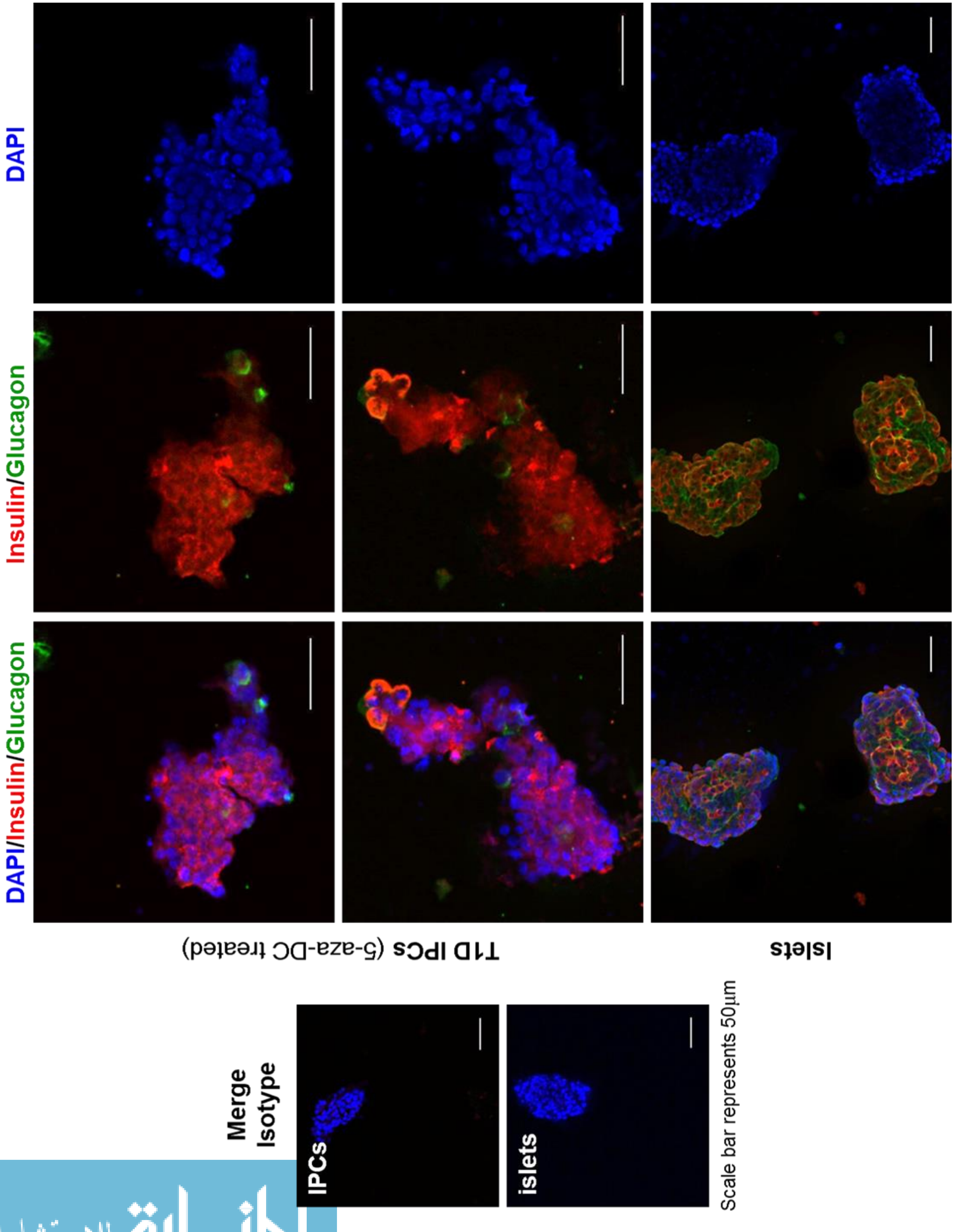
DAPI/Insulin/Glucagon
Insulin/Glucagon
DAPI
T1D IPCs (5-aza-DC treated)
Islets
Merge
Isotype
IPCs
islets

Scale bar represents 50μm

Figure 24. Demethylation of ND iPS cells does not significantly enhance the yield of insulin$^+$ cells and Pdx1$^+$ cells

To address whether demethylation enhances the yield of Pdx1$^+$ cells and insulin$^+$ cells from ND iPS cells, we established parallel differentiations of ND iPS cells, treated with and without 10 nM 5-aza-DC for 18h on day 4 of differentiation (*n* = 2). Controls for staining were iPS cells (negative) and βTC3 mouse insulinoma cells (positive). **(A)** The yield of Pdx1$^+$ cells was not significantly different between untreated and 5-aza-DC treated ND IPC cultures, and this translated into **(B)** equivalent yield of insulin-expressing cells from the two culture conditions. Thus, demethylation enhances the differentiation into IPCs of specifically T1D iPS cells but not ND iPS cells. This is likely because there are specific gene loci on T1D cells that are aberrantly methylated, which is corrected by transient 5-aza-DC treatment.

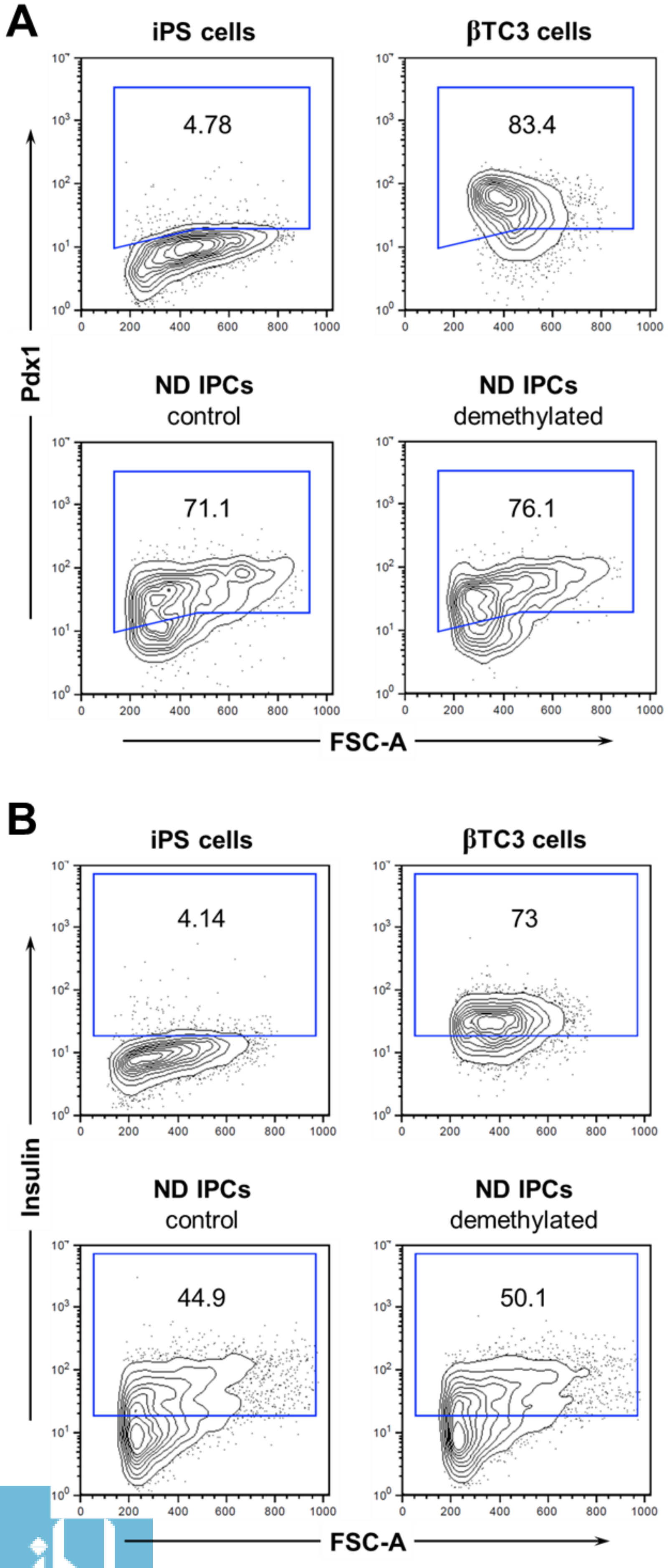
A
iPS cells
4.78
βTC3 cells
83.4
ND IPCs
control
71.1
ND IPCs
demethylated
76.1
Pdx1
FSC-A
10⁰
10¹
10²
10³
10⁴
0
200
400
600
800
1000
B
iPS cells
4.14
βTC3 cells
73
ND IPCs
control
44.9
ND IPCs
demethylated
50.1
Insulin
FSC-A

Figure 25. T1D IPCs express C-peptide in addition to the pancreatic β-cell specific transcription factor Nkx6.1

We further characterized the IPCs for expression of C-peptide (*n* = 3), which a byproduct of insulin processing, and the pancreatic β-cell specific transcription factor Nkx6.1 (*n* = 2). We observed robust cytoplasmic C-peptide staining in these clusters, confirming *de novo* production of insulin in the T1D IPC clusters. Additionally, these cells expressed Nkx6.1 largely in the nucleus, although there was some cytoplasmic staining as well. The scale bar represents 10 μm in all frames.

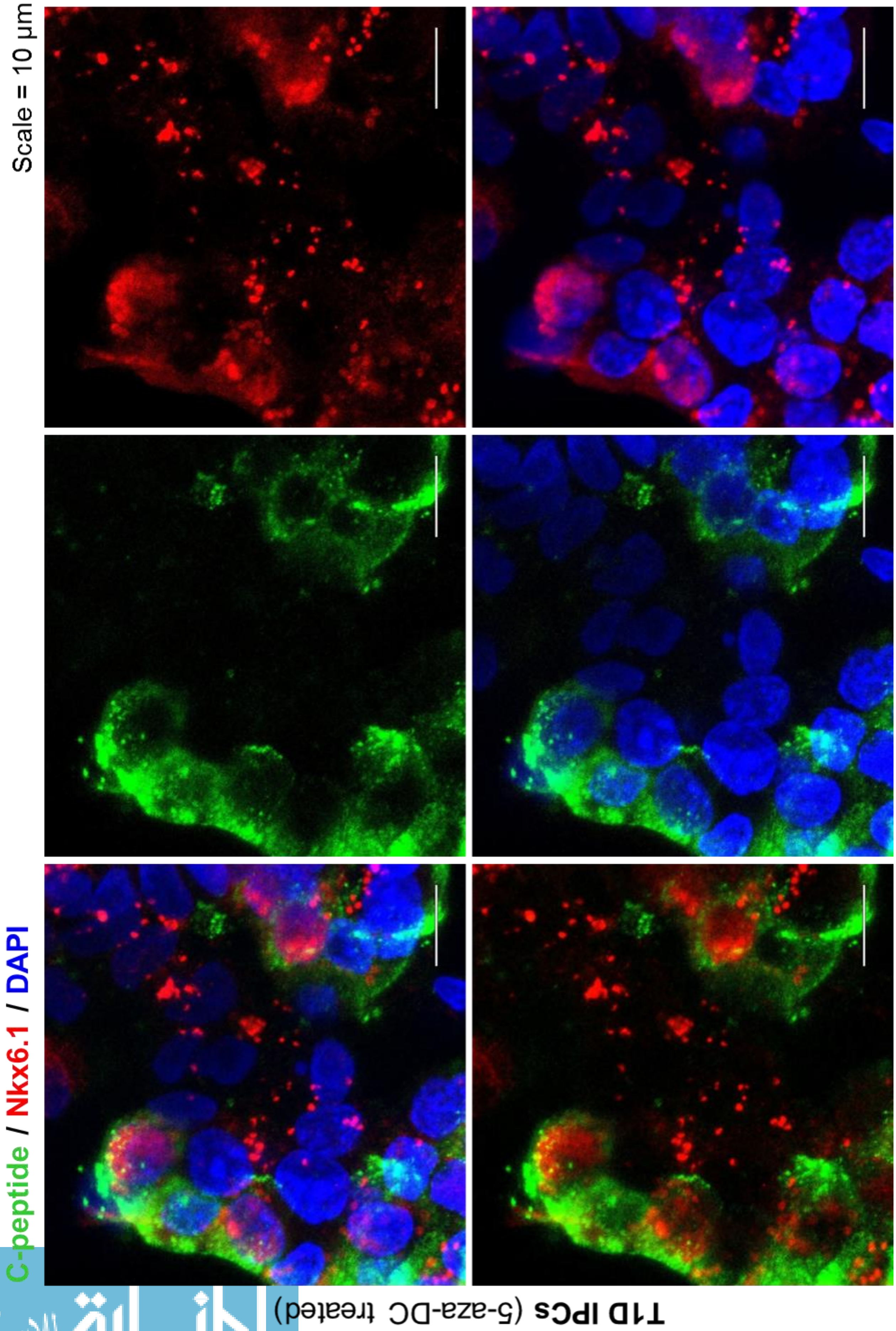
Scale = 10 µm
C-peptide / Nkx6.1 / DAPI
T1D IPCs (5-aza-DC treated)

Figure 26. T1D IPCs resemble islets in their ultrastructure and possess insulin granules of various maturities

(A) Human islets (top panel) possess insulin granules of various maturities that are differentiated by the color and shape of the core granule. However, all granules possess a characteristic “halo” surrounding them, which is very specific to the insulin granule. Similar to islets, T1D IPCs derived from this protocol (bottom panel) possess insulin granules of various maturities, confirming their authenticity and similarity to human islets (*n* = 3 experiments). **(B)** Comparison of the number of granules per cell in islets and IPCs reveals a nonsignificant difference between the two cell types. Data are represented as mean ± SEM, *n* = 57 IPCs and 28 islet pancreatic β-cells counted.

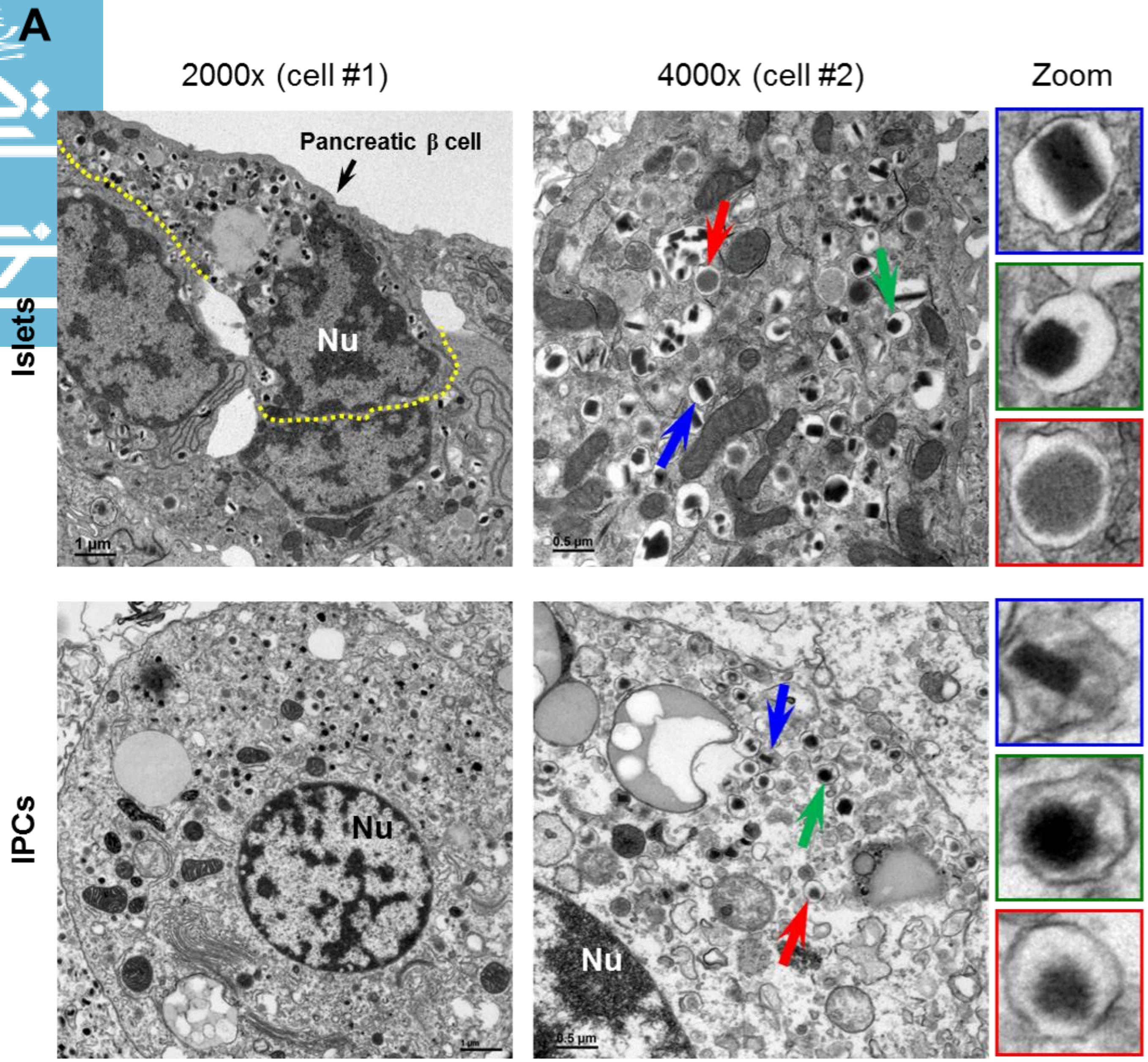
A
2000x (cell #1)
4000x (cell #2)
Zoom
Islets
Pancreatic β cell
Nu
1 μm
0.5 μm
IPCs
Nu
1 μm
Nu
0.5 μm

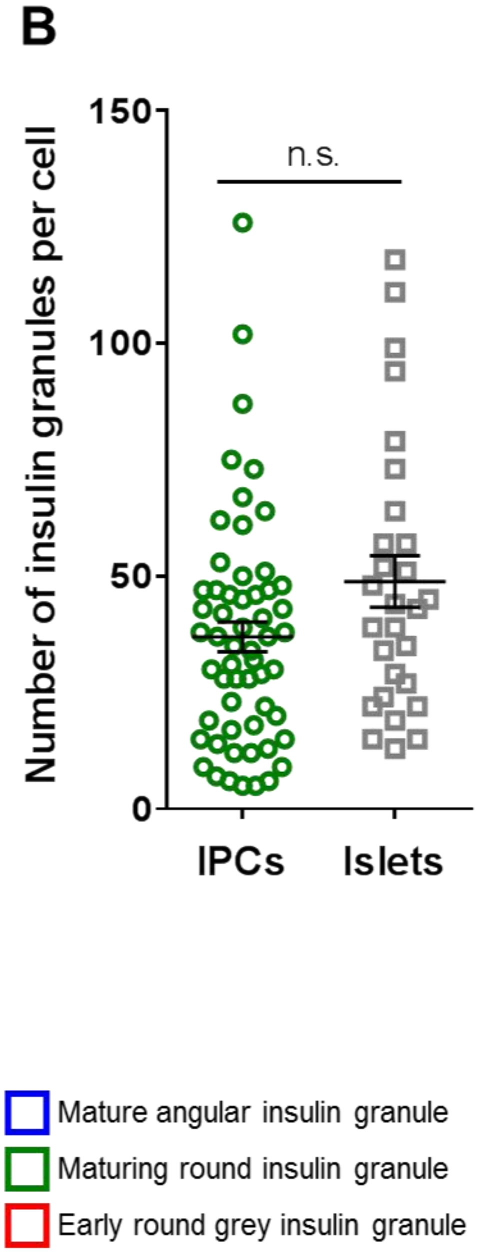
B
Number of insulin granules per cell
150
100
50
0
n.s.
IPCs
Islets
Mature angular insulin granule
Maturing round insulin granule
Early round grey insulin granule

Figure 27. The average number of cells per IPC cluster resembles published findings on the number of cells per islet

The average number of cells per IPC cluster is similar to what has been described for human islets, and this data is depicted in **(A)**. The average number of IPC clusters per well is depicted in **(B)**. Data are represented as mean ± SEM, $n = 4$.

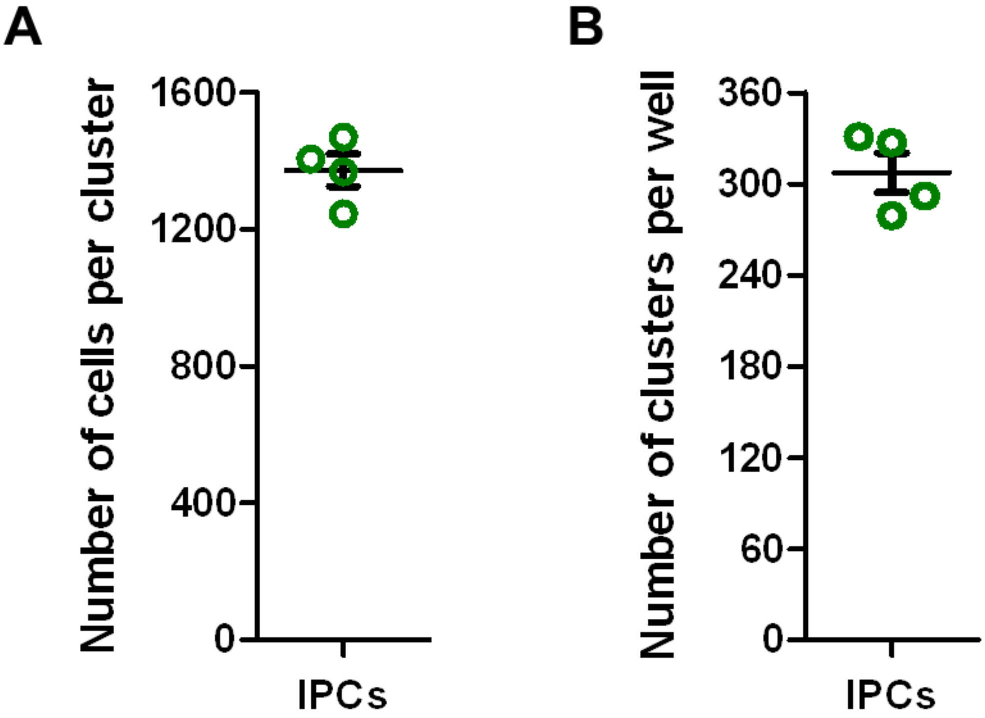
A
Number of cells per cluster
1600
1200
800
400
0
IPCs
B
Number of clusters per well
360
300
240
180
120
60
0
IPCs

Figure 28. T1D IPCs are functional and glucose-responsive

To determine if T1D iPS cell-derived IPCs are functional and respond to high glucose with insulin secretion, we subjected IPCs and human islets (positive control) to a GSIS assay. The variation in cell number across the wells was normalized by total protein content per well. After baseline equilibration in 2.8 mM glucose solution (low glucose or LG), exposure to 28 mM glucose (high glucose or HG) resulted in significant increase in insulin secretion by both IPCs **(A)** and islets **(B)**. However, the amount of insulin secreted was significantly lower in IPCs than what was observed for human islets. Still, the fold-increase in insulin secretion is higher for IPCs than for islets **(C)**, *n* = 4 (two experiments of duplicates), $^{**}p < 0.01$, $^{***}p < 0.001$, $^{****}p < 0.0001$.

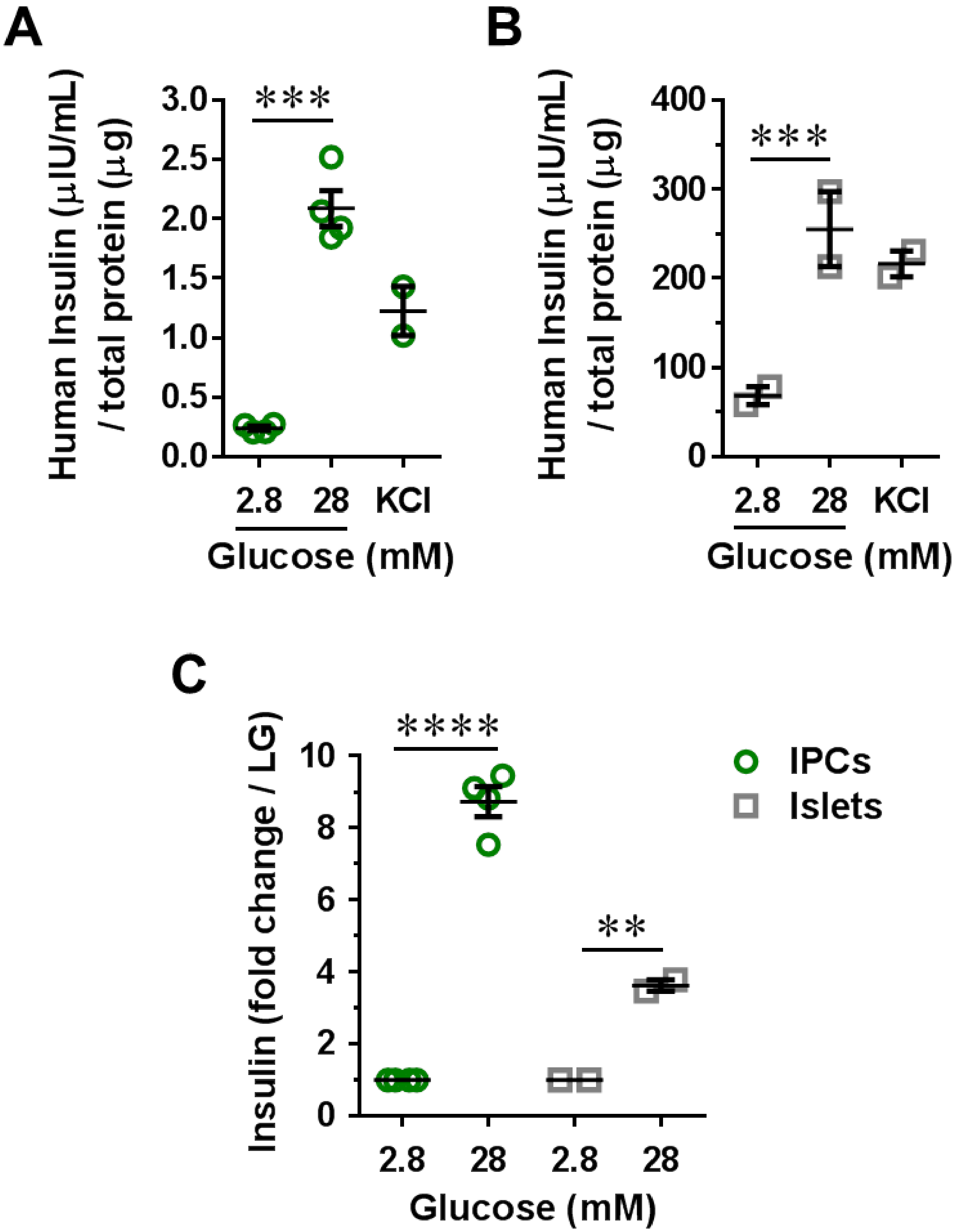
A
Human Insulin (µIU/mL) / total protein (µg)
3.0
2.5
2.0
1.5
1.0
0.5
0.0
***
2.8
28
KCl
Glucose (mM)
B
Human Insulin (µIU/mL) / total protein (µg)
400
300
200
100
0
***
2.8
28
KCl
Glucose (mM)
C
Insulin (fold change / LG)
10
8
6
4
2
0
****
**
2.8
28
2.8
28
Glucose (mM)
IPCs
Islets

Figure 29. Rapid correction of hyperglycemia in diabetic mice by T1D IPCs

(A) STZ-induced diabetic mice (blood glucose levels of ≥300 mg/dL) show rapid correction of hyperglycemia after transplantation with IPCs (*n* = 5). All of the mice show complete and consistent normalization of blood glucose levels within 28 days of IPC-transplant.

(B) Excision of the transplanted cells 8 weeks post-transplantation reveals the presence of an organoid-like structure.

(C) H&E staining shows glandular morphology of the cells. Image scale bar = 50 µm and inset scale bar = 10 µm.

(D) When subjected to supraphysiological glucose challenge, T1D IPC-injected mice (showing 5 weeks of stable correction) show effective management of the glucose bolus (2 mg/kg i.p.) by recovering to the baseline normoglycemic state within 4 hours. In contrast, nontransplanted diabetic mice do not recover from severe hyperglycemia. Nondiabetic mice recover to normoglycemia more quickly than IPC-transplanted mice.

(E) Computation of the “Area Under the Curve” (AUC) for the three treatment groups demonstrates that while IPC-injected mice show superior glucose correction kinetics compared to nontransplanted diabetic mice, they show poorer kinetics compared to nondiabetic control mice. This suggests room for improvement of T1D iPS cell-derived IPCs.

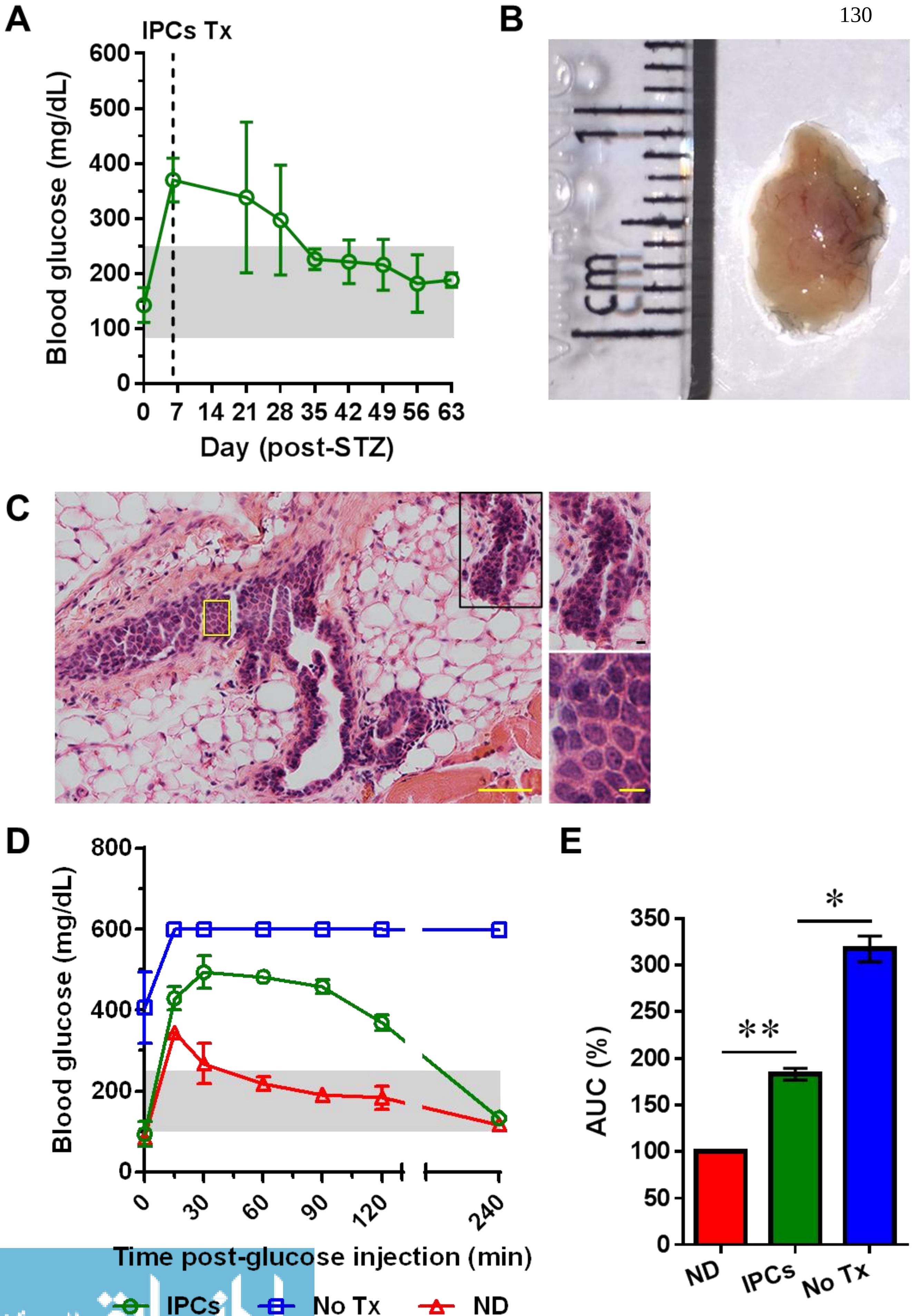
A
IPCs Tx
Blood glucose (mg/dL)
600
500
400
300
200
100
0
0
7
14
21
28
35
42
49
56
63
Day (post-STZ)
B
cm
1
C
D
Blood glucose (mg/dL)
800
600
400
200
0
0
30
60
90
120
240
Time post-glucose injection (min)
IPCs
No Tx
ND
E
AUC (%)
350
300
250
200
150
100
50
0
**
*
ND
IPCs
No Tx

Figure 30. T1D DE cells and IPCs are poorly antigenic and are not susceptible to NK cell-mediated killing *in vitro*

(A) As a parameter to preliminarily define the immunological profile of iPS cell-derived IPCs, we used flow cytometry to determine the expression of MHC class I, MHC class II, and the T cell costimulatory molecules CD80 and CD86. Undifferentiated iPS cells served as a negative control for all of these markers, whereas human peripheral blood mononuclear cells (hPBMCs) served as a positive control. As expected, all PBMCs expressed MHC class I, and a subset of the cells, which are antigen presenting cells, expressed MHC class II. Some PBMCs expressed CD86, and although we didn’t observe CD80 staining in these cells, this could be due to the fact that the PBMCs used for these experiments were naïve and not activated. Similar to their undifferentiated counterparts, IPCs did not express any of these markers ($n = 2$), which likely means that they will be able to evade autoimmune destruction unless their immunological profile changes post-transplantation. **(B)** Poor MHC class I expression by IPCs makes them potentially susceptible to NK cell attack, depending on their expression of other NK cell activating or inhibitory ligands. To determine the susceptibility of IPCs to NK cells, we performed a ^{51}Cr release assay using radioactive ^{51}Cr-labelled IPCs as target cells. IL-2 lymphokine-activated hPBMCs, of which 15% of the cells are NK cells, were used as effector cells. Undifferentiated iPS cells (negative control) and the NK cell-sensitive K562 leukemia cells (positive control) were also used as target cells. The effector and target cells were incubated for 4h at various Effector:Target cell ratios and ^{51}Cr release was determined. IPCs, similar to their undifferentiated precursors, were not susceptible to NK cell killing *in vitro*, despite their poor expression of MHC class I.

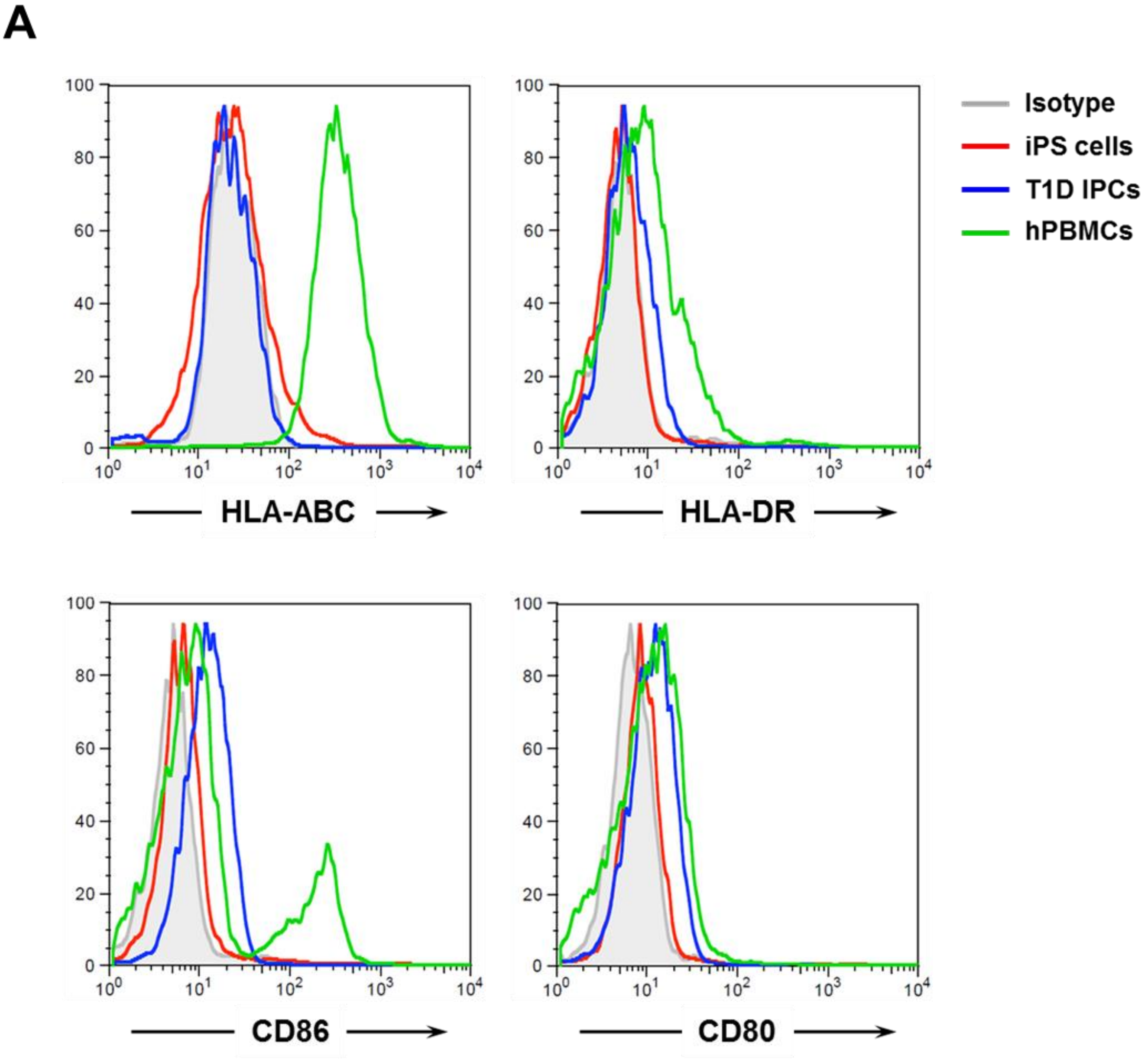
A
100
80
60
40
20
0
10^0
10^1
10^2
10^3
10^4
HLA-ABC
HLA-DR
CD86
CD80
Isotype
iPS cells
T1D IPCs
hPBMCs

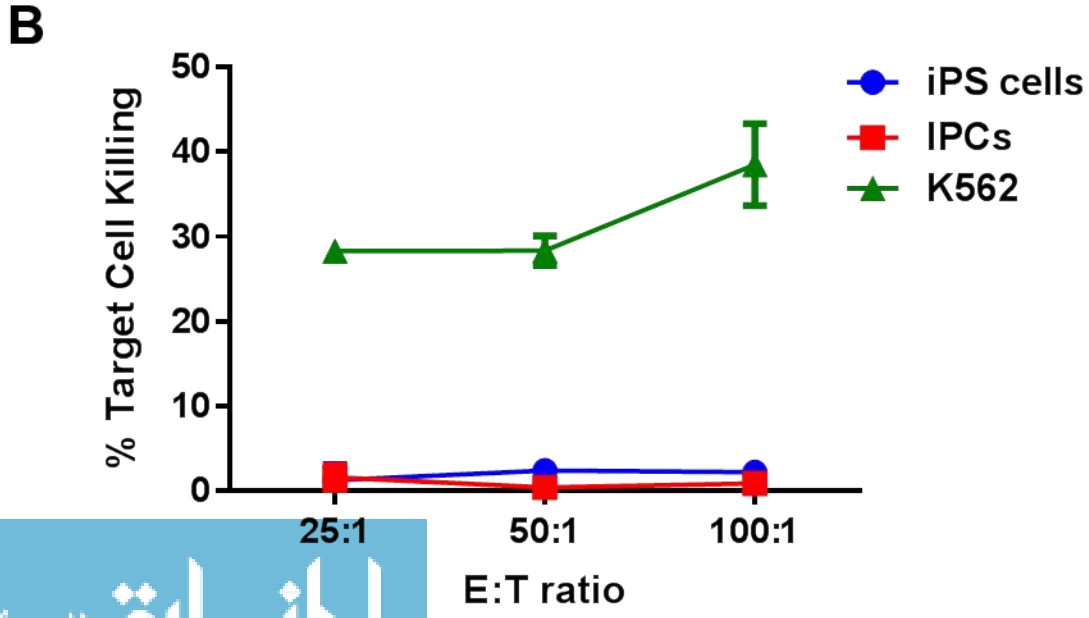
B
% Target Cell Killing
50
40
30
20
10
0
25:1
50:1
100:1
E:T ratio
iPS cells
IPCs
K562

CHAPTER V

DISCUSSION

The Differentiation of T1D iPS Cells into IPCs is Impaired

The use of pluripotent stem cells for the treatment of T1D has met reasonable success if assessed by reports indicating *in vivo* correction of hyperglycemia upon transplantation of pluripotent stem cell-derived endocrine precursor cells into diabetic mice[13,15,16]. Pancreatic endocrine progenitors derived from human ES cells, in particular, have been widely demonstrated to adopt a competent β-cell identity *in vivo*[13,15,16]. However, the inefficient differentiation of pluripotent stem cells into insulin-expressing cells[12-16,48], coupled with the fact that these cells are not glucose-responsive *in vitro*[12-16,48], is disappointing and leaves much to be desired.

Here, we have established a novel 3D culture platform using the bioactive substrate matrigel for inducing highly efficient directed differentiation of iPS cells into IPCs. Inspiration underlying the finer details of this protocol has been drawn from macroscopic organization of cells in clusters similar to endocrine islets of the pancreas[1,87], as well as from microscopic signaling processes governing cell differentiation[47]. By employing an innovative 3D platform and fine-tuning lineage choices with well-reasoned differentiation cues, we have established an outstanding protocol that improves on previous differentiation efficiencies[12,13,15,16] from ND iPS cells by 4-5 fold.

However, we showed in Chapter III that the effective differentiation of ND iPS cells does not translate for T1D iPS cells. Although the early differentiation of T1D and ND iPS cells into DE cells is equivalent, downstream differentiation of the cells reveals striking disparities. This was first observed in morphological differences between T1D and ND differentiating cultures, whereby the T1D culture yielded ~85% insulin-negative hollow cysts and 15% insulin-expressing compact clusters, but the ND culture gave rise to a 50:50 mixture of the two cluster types. This translated in a very consistent manner to the percentage of insulin$^+$ cells as determined by flow cytometry. Indeed, as determined through several parameters, we have shown that the differentiation of T1D iPS cells into IPCs is impaired, and that this impairment manifests as early as Stage 3, when Pdx1 expression should be initiated. Remarkably, this observation is consistent with data that was briefly introduced in another report that utilized T1D iPS cells as a negative control for generating Pdx1$^+$ pancreatic progenitor cells[106]. Our studies advance several steps ahead of this report since we 1) compared the differentiation of ND and T1D iPS cells all the way to Stage 5 using a robust 3D differentiation protocol, and 2) we specifically sought to correct the differences in the differentiation of T1D and ND iPS cells.

Our finding is highly significant since iPS cell-based therapy for T1D will, in all likelihood, involve the patient's own somatic cell-derived iPS cells[6,9]. With all prior reports using human ES cells or iPS cells derived from healthy subjects[12-16], this finding demands a better understanding of the influence of the disease state of the patient from which iPS cells are derived on the differentiation of these iPS cells into IPCs. Indeed, our studies underscore the need to address inadequacies in the differentiation of T1D iPS cells into IPCs before such therapy is hastily translated into the clinic only to yield disappointing results after expensive pharmaceutical development[6].

We concluded in Chapter III that the differentiation of T1D iPS cells into IPCs was impaired. After obtaining the gene expression data showcasing the impaired expression of *Pdx1* mRNA transcript in T1D differentiating cells, we reasoned that there were epigenetic barriers that hindered the expression of critical genes for pancreatic β-cell specification, such as *Pdx1*. Thus, we *hypothesized* that using epigenetic modifiers such as 5-aza-DC would allow for the expression of *Pdx1* and downstream genes, which altogether would ultimately improve the differentiation outcome and result in a high yield of insulin$^+$ IPCs from T1D iPS cells.

An Epigenetic Modifier Enhances the Generation of Functional, Glucose-Responsive IPCs from T1D iPS Cells

Following this hypothesis, we thus treated the T1D culture with 5-aza-DC after the generation of DE cells, which is the time point after which impaired differentiation is observed. This resulted in >95% Pdx1$^+$ pancreatic progenitor cells from T1D iPS cells at the end of Stage 4, which eventually gave rise to >50% insulin-expressing IPCs. This yield is comparable to what we observed in human islets and in the ND differentiating cultures. Curiously, demethylation did not improve the yield of IPCs from ND iPS cells, suggesting that the differentiation impairment due to methylation was specific to T1D differentiating cells. When we determined the proportion of insulin$^+$ cells vs. glucagon$^+$ cells in the cultures, we found that 5-aza-DC improved the yield of IPCs in a concentration-dependent manner while averting the generation of glucagon-expressing cells. This suggested to us that demethylation was making the differentiating cells more receptive to differentiation cues designed to generate specifically insulin-expressing cells. Further analysis of the cells by immunofluorescence and TEM analysis demonstrated that demethylation of T1D DE cells generated authentic pancreatic β-cell-like IPCs that expressed characteristic markers and possessed insulin granules of similar quality and in comparable quantities as primary human islets. Next, we demonstrated for the first time that these IPCs derived from T1D iPS cells are functional, meaning that they responded to high glucose stimulation with insulin secretion. Finally, transplantation of the cells s.c. into STZ-induced diabetic mice resulted in rapid correction of hyperglycemia in 4 weeks, demonstrating strong clinical potential of these cells. When these mice were subjected to glucose challenge, the mice fully recovered to normoglycemia in 4 hours, unlike nontransplanted diabetic mice. However, correction was significantly delayed compared to nondiabetic mice, demonstrating room for improvement.

To introduce more consistency and create a superior environment to support the transplanted cells, in our future studies, we will be transplanting induced pluripotent stem cell-derived IPCs under the skin of mice with minimal surgery after creating a vascularized pocket induced by a foreign body reaction[134]. This procedure is more reliable than simple s.c. infusion of cells by ensuring that the cells remain localized in a defined pocket, and by providing a cell-supporting vascularized matrix. It is also significantly less invasive than subcapsular kidney transplantation while remaining strongly effective for islet transplantation, and thus has strong clinical potential. This method is designed to harness the natural foreign-body response elicited by medically approved vascular catheters to transform the tissue under the skin from a hypoxic, avascular space into a densely vascularized cellular graft-supporting matrix. Hopefully, this will enhance the function of our transplanted cells, which already demonstrate excellent clinical promise for the cure of T1D.

Altogether, these data show that epigenetic modifiers such as 5-aza-DC promote greater efficiency of differentiation of uncooperative T1D iPS cells into functional IPCs that resemble pancreatic islets.

Current Shortcomings of the Differentiation Procedure

Despite our success with this protocol in generating functional IPCs from T1D iPS cells, we have several areas in which we can foresee improvements so as to generate a higher yield of IPCs that are superior in function and safer to use for therapy. Indeed, the shortcomings perceived in our protocol in its current state is 1) the relatively low yield of IPCs from the number of iPS cells first used in the differentiation procedure, 2) the use of a harsh demethylation agent with broad impact on the epigenome[111], which carries the risk for inducing the activation of oncogenes, and 3) the significantly poorer glucose-responsiveness of these IPCs compared to primary human islets.

Regarding the yield of IPCs from iPS cells, we generally transfer 2 wells of iPS cells in a 6-well plate into 1 well of a 24-well plate containing matrigel. Our typical differentiations start with 18 wells of iPS cells in a 6-well plate, which contain approximately 18 million cells. After the transfer into 3D cultures, the cells are transferred to 10 wells of a 24-well plate. At the end of the differentiation, we obtain an average of 300 clusters per well, with an average of 1370 cells per cluster. This means that in 10 wells, we have 4.2 million cells at the end of Stage 5. Even though 50% of the cells might be expressing insulin, the efficiency of differentiation is thus 20% when one accounts for cell numbers. This is much higher than for other protocols, and the cells we generate are functional, but clearly there is room for improvement so that we can not only generate functional IPCs but generate them in high quantities. For this purpose, it is prudent to investigate other culture platforms that are more suited for the scalable differentiation of iPS cells into billions of IPCs.

Besides our concerns regarding the yield of these cells in actual cell numbers, we have concerns regarding the safety of these cells if they are eventually translated into the clinic. The use of a broad spectrum and harsh demethylating agent such as 5-aza-DC has safety concerns and may potentially activate the expression of oncogenes[111]. However, this risk is reduced because the treatment is very transient and the cells quickly reacquire methylation within a few days[110]. Still, this topic demands attention, and so we should aim to identify other epigenetic modifiers that may be milder and have more specific effects, which would make these IPCs safer for use in therapy.

Lastly, we will discuss strategies that can be implemented in the protocol to enable the generation of functionally superior IPCs that are equivalent to islets in their glucose-responsiveness *in vitro*. So far, the struggle has been how to generate IPCs in high efficiency, and these cells were not functional at all. Even if those cells expressed insulin, they were incapable of secreting it in a glucose-responsive manner. Thus is because the acquisition of insulin secretory machinery is the most terminally gained characteristic in the generation of pancreatic β-cells[15,45]. Here, we demonstrate the generation of IPCs that strongly resemble islets in their expression of pancreatic β-cell specific markers and possession of insulin granules. Additionally, we show that these IPCs are indeed glucose-responsive in a manner that has never been reported before for iPS cells. Thus, our IPCs have acquired insulin secretory machinery. However, we readily acknowledge that the amount of insulin produced is lower than it is for islets. Thus, these cells still need to further mature in order to become functionally superior and equivalent to pancreatic β-cells. Prior reports utilizing pancreatic endocrine progenitor cells (which were far more immature than the cells we demonstrate here) showed that their cells acquired full functional capacity that was similar to islets only after transplantation[12,13,15,16]. We expect our cells to behave similarly upon transplantation, but because they will need less time to develop since they are already quite mature, this process will be more rapid. we However, generating IPCs that are functionally equivalent to islets *in vitro* is advantageous for accelerating the process of correcting hyperglycemia even further. Moreover, if these cells resemble islets more in their functionality, they may be an excellent source of cells for drug testing and pharmaceutical development by serving as a significantly less expensive bridge between the bench and bedside[9]. Altogether, we envision that several improvements can be made in the protocol to yield not only functional IPCs, but allow further maturation to generate IPCs that are functionally equivalent to human islets. In order words, the future goal of this project is no longer simply to make functional IPCs; it is now to make IPCs that are *functionally equivalent* to human islets.

Selection of an Optimal and Scalable Differentiation Platform to Improve the Functionality and Yield of IPCs from iPS Cells

We believe that utilizing a 3D spinner flask culture system will best address the first issue and allow for a scalable and equally, if not more, effective protocol for the generation of billions of IPCs[102,135]. Bioreactors included in these systems have enabled manipulation of microenvironment by providing the means to precisely modulate the temperature and diffusion of nutrients and oxygen via perfusion systems[136] (Figure 31A). The use of spinning flask cultures, in which the agitation promotes cell clustering, has been used to make cerebral organoids, the cellular organization of which strongly resembled native brain tissue and was much better than the organoids resulting from static 2D cultures[38]. Additionally, these culture systems have been used to make pancreatic endocrine progenitor cells[135], and late last year, they were used as the platform for the generation of functional IPCs from human ES cells[102]. Indeed, they claimed that this culture system allowed them to generate “billions” of IPCs using this highly scalable approach that promotes 3D clustering[102]. Furthermore, the shear and flow of fluid as the cells are swimming in these spinning flasks may better mimic the *in vivo* microenvironment of islets, which encounter blood flow in a manner that cannot be replicated in a stationary 3D matrigel scaffold system[135]. This may thus enhance the maturity and functionality of IPCs by better reproducing the native islet niche *in vivo*. Thus, progress in this project should entail differentiating iPS cells into IPCs using this platform so that we can make the protocol more scalable and efficient.

Another approach that was recently utilized to generate IPCs in a 3D format was the air-liquid interface (ALI) culture system[77]. In this culture system, cells growing on basements membranes *in vivo* are exposed to air on one side and differentiating media on the other side[77,137] (Figure 31B). Although this culture system is not practical or high-yielding as the as the scalable spinner-flask cultures, ALI cultures possess the advantage of being able to re-create the microenvironment required to establish cell polarity[77,137]. Cell polarity involves cells acquiring a sense of "direction" across the apico-basal axis[138]. During embryogenesis, the pancreas is formed by the differentiation of pancreatic epithelium, which involves branching and morphogenesis[139]. The remodeling of cells and the subsequent cell specification requires cell polarity changes[139]. In one report, it was shown that the loss of Cdc4-2, a Rho-GTPase that is required for cell polarity, impaired the process of specification to pancreatic endocrine cells, which indicates the importance for the establishment of cell polarity for endocrine cell formation[140]. Moreover, it was shown that the loss of Celsr2 and Celsr3, which are critical for maintenance of cell polarity, in pancreatic progenitors led to reduced differentiation towards pancreatic β-cells[141], which underscores the necessity to promote cell polarization during differentiation to generate pancreatic β-cells *in vitro*. Thus, to recreate the phenomenon of cell polarity in our differentiating cells, ALI cultures may be beneficial[77]. Exploiting this culture platform may address the third concern we have with our current protocol and may allow for the generation of superior IPCs that are more mature and functionally equivalent to islets[77].

Another culture platform that may accomplish similar goals is decellularization and re-seeding of native pancreatic tissue with IPCs in order to enhance their maturity and function. This is one of the novel techniques currently trending in the field of regenerative medicine since it provides a native 3D scaffold for re-seeding of cells[142]. In essence, decellularization would create a pancreas-specific extracellular matrix (ECM) that can function either as a tissue bed, or if concentrated, as a “pancreatic matrigel”[142]. This may be superior compared to regular matrigel because of its possession of pancreas-specific ECM proteins that may positively influence the differentiation of stem cells into the pancreatic lineage. In this procedure, the organ is first decellularized using detergent to remove all cellular and nuclear material, washed extensively to remove the detergent, and re-seeded afterwards with new cells to support the underlying ECM[142] (Figure 31C). Decellularized organs are thought to provide a ready-made perfusable vascular tree, maintain important ECM components, and include a “blueprint” for the intricate *in vivo* microenvironment that may together enable superior functional development of seeded stem cells[142]. Reports of decellularization of the heart, kidney and lung have shown convincing return of functionality in the recellularized natural scaffold[143-153]. A recent study showed the increase in expression of INS1 in pancreatic cells reseeded onto the decellularized pancreas[142]. Studies have also demonstrated enhanced islet cell attachment and β-cell proliferation when the cells were seeded on endothelial cell-derived ECM[154]. This not only shows a key role for the *in vivo* microenvironment but also displays the necessity of multi-cellular interaction for enhanced cellular functionality. Similarly, the seeding of human islets onto decellularized small intestinal mucosa improved the function of islets when maintained *in vitro*[142,155,156]. Interestingly, increased islet functionality was observed when islets were seeded onto pancreatic ECM as opposed to liver ECM, suggesting organ-specific features of the pancreatic ECM that better support pancreatic cells[142]. Islets seeded on a decellularized pancreatic scaffold encapsulated in PLGA better facilitated insulin independence in diabetic rats[157]. These results, however compelling, demand future studies on the impact of decellularized scaffolds in the maintenance and differentiation of iPS cell-derived IPCs. Although this field is still in its infancy, future developments in this area are highly anticipated and promise to be exciting.

Manipulation of our differentiation protocol to include novel cell culture techniques such as spinning flask 3D cultures, ALI culture, and decellularization of organs should be investigated to augment the yield of cells and provide a more native microenvironment that may enhance the maturity and function of the differentiated cells. 3D spinning flask cultures coupled with bioreactor support is especially helpful in providing a reliable platform for the scalable generation of iPS cell-derived IPCs[102,135]. Clearly, the combination of refining signaling pathway modulation and implementing novel bioengineering strategies is necessary to provide a successful and practical iPS cell-based strategy for therapy of T1D.

The Role of Epigenetics in the Differentiation of T1D vs. ND iPS Cells

We have shown in this manuscript that the differentiation of a T1D iPS cell line into IPCs is impaired. Subsequently, we demonstrated that this impairment can be corrected after transient treatment with a demethylating agent. We additionally demonstrated that this enhancement did not manifest in ND iPS cells and was specific to T1D iPS cells. This suggests that there are specific epigenetic aberrancies in T1D iPS cells that intrinsically impair their differentiation into IPCs, which is likely why only they are responding positively to transient demethylation.

However, while we can comfortably conclude that the mechanism for this phenomenon is indeed rooted in epigenetics, it remains to be determined what particular gene loci are specifically derepressed to allow β-cell specification upon 5-aza-DC treatment. A critical question that arises from our studies is the mechanism by which 5-aza-DC promotes the generation of IPCs from iPS cells. We hypothesize that 5-aza-DC demethylates and hence facilitates the expression of genes, such as *Pdx1*, that are critical for pancreatic β-cell specification in response to differentiation stimuli, thus enhancing the effect of these differentiation cues. For example, 5-aza-DC may remove the aberrant methylation marks on promoters of genes such as *Pdx1, Ngn3, Nkx6.1, MafA, Nkx2.2,* and *Insulin*. We specifically think these genes may be of interest because of their pivotal role in orchestration of the pancreatic β-cell fate[46,77]. However, we think that it is entirely possible that the only aberrantly methylated gene in T1D differentiating cells is *Pdx1*, and that correction of this impairment alone is what results in the drastically improved differentiation outcomes.

The ideas presented above are highly speculative and demand rigorous methylome analyses to assess the influence of demethylation in the differentiation of T1D iPS cells into IPCs. Garnering an understanding of the specific gene loci that are aberrantly regulated in T1D cells would facilitate the development of targeted strategies to re-express specifically those genes that are abnormally expressed. We propose that Reduced Representation Bisulfite Sequencing (RRBS) may be a useful tool for addressing this question, since it would allow for the capture of methylation rich CpG islands[158,159] in the DNA of T1D iPS cells, which would be subjected to analysis to identify the aberrantly methylated loci in genes critical for specification of the pancreatic β-cell fate, such as *Pdx1*.

In our studies, it is important to note that because the demethylation treatment is transient, methylation in the genome eventually reappears within a few days of the short-term treatment[110]. However, we think that the differentiation cues ultimately impact gene expression and turn on genes such as *Pdx1* or *Nkx6.1*, keeping them in a nonmethylated state even while the rest of the genome is being appropriately remethylated. This would explain why the demethylation treatment results in long-term improvement of the differentiation outcome. Regardless, methylome analyses will offer mechanistic insight into the impaired differentiation of T1D iPS cells into IPCs, which will inform the development of safer and more therapeutically suitable strategies to enhance the differentiation of iPS cells into IPCs.

Identifying a Suitable and Minimally Disruptive Epigenetic Modifier to Safely Derive IPCs from T1D iPS cells

Our data suggest that the demethylating agent 5-aza-DC significantly improves the yield of IPCs from T1D iPS cells. However, the impact of this agent is very general[111,116], and the dose screening experiment was confirmation to us that this compound is quite potent and toxic at high doses. Since 5-aza-DC is a particularly strong demethylating agent[111,116], it might be prudent to investigate the impact of milder demethylating agents as well as other classes of epigenetic modifiers, such as histone deacetylases. This will address our second concern with the current differentiation procedure, regarding safety of the cells derived using 5-aza-DC as the demethylating agent.

Vitamin C is a TET-dependent DNA demethylating agent[160], and it is an especially attractive candidate because it is mild. This is because Vitamin C promotes hydroxymethylation[160], as opposed to transiently stripping the entire DNA of methyl groups, which is how 5-aza-DC operates. Another demethylation agent that may be investigated for enhancing the generation of IPCs is the small molecule RG108, which only inhibits Dnmt1[161], unlike 5-aza-DC, which inhibits both Dnmt1[162] and Dnmt3a[163]. Thus, the more limited scope of the inhibition by RG108 may make it a safer and more tolerable demethylating agent compared to 5-aza-DC.

There is a strong case to be made regarding the impact of histone packaging in affecting cell differentiation and lineage commitment[109]. As described in the Introduction of Chapter IV, a recent report demonstrated the significance of aberrant Polycomb group (PcG)-mediated accumulation of repressive H3K27me3 marks in differentiation of human ES cells into pancreatic endocrine cells[15]. These data suggested that the incomplete chromatin remodeling of critical β-cell genes during *in vitro* differentiation may underlie the suboptimal function and immature properties of IPCs generated so far[15]. This phenomenon may translate into our own observations with the impaired differentiation of T1D iPS cells into IPCs.

In this manuscript, we have only investigated the impact of methylation on the differentiation of T1D iPS cells. However, histone modifications represent an entirely new and highly significant epigenetic realm[109] that may be aberrantly modulated in T1D iPS cells, and this facet of epigenetics thus merits active future investigation. Based on the earlier report on aberrant function of PcG proteins ultimately influencing cell differentiation[15], we speculate that inhibiting the PcG complex during the differentiation of T1D iPS cells into IPCs may enhance the yield of mature IPCs by instating appropriate histone marks on relevant genes involved in pancreatic β-cell specification. To accomplish this, one can utilize Prt4165, a small molecule inhibitor of the PcG complex[164], as a reagent to enhance the yield of IPCs from T1D iPS cells.

Alternatively, other histone modifiers (unrelated to regulation of the PcG proteins), such as histone deacetylase (HDAC) inhibitors[165,166] may be utilized to alter histone packaging and ultimately influence cell differentiation. HDAC inhibitors, such as sodium butyrate[165], may promote the expression of silenced genes and have been used to enhance the yield of iPS cells during reprogramming from somatic cells[167]. We suggest that these reagents may also enhance the downstream differentiation process by fine-tuning epigenetic profiles according to differentiation stimuli. For this purpose, one can also consider Valproic Acid (VPA), which is also a very weak demethylating agent[166,168].

Other small molecules have been demonstrated to exert potent effects in augmenting pancreatic differentiation of human pluripotent stem cells. Most intriguingly, transient Dimethyl Sulfoxide (DMSO) treatment was shown to robustly enable pancreatic endocrine lineage commitment even among the most uncooperative pluripotent stem cell lines, including a T1D iPS cell line[106]. Although the entire mechanism has yet to be elucidated, preliminary analyses show that DMSO induced reversible arrest of the cells in the G1 phase of the cell cycle and promoted expression of hypophosphorylated Retinoblastoma (Rb) protein in a cell-cell contact dependent manner[106]. It is tempting to speculate that the activity of epigenetic modifiers may be modulated by DMSO treatment, somehow enhancing the impact of stage-specific stimuli applied to induce activation of the pancreatic β-cell differentiation program. Supporting this idea, DMSO has been reported to control DNA methylation and hydroxymethylation by regulating levels of epigenetic scribes, including Dnmt3a, Dnmt1 and TET[169]. If the mechanism for this phenomenon is indeed rooted in epigenetics, it remains to be determined what specific role DMSO plays in derepression of particular gene loci associated with mature pancreatic β-cell specification.

Altogether, these discussions emphasize a need to better understand the role of epigenetics underlying the impaired differentiation of T1D iPS cells into IPCs. In particular, histone-based modulation of β-cell gene expression must be investigated since it plays a crucial role in cell differentiation[15,109]. Thus, future development of this project demands involving these three classes of reagents (PcG inhibitors, HDAC inhibitors and other demethylating agents) and defining their impact on the yield of IPCs from iPS cells.

The Natural Islet Endocrine-Endothelial Cell Axis May Be Exploited to Enhance Differentiation and Maturity of iPS Cell-Derived IPCs

When considering how to enhance the maturity and function of differentiating cells derived from stem cells, it is critical to remember that *in vivo* development of ES cells occurs in a systemized manner involving units of tissues influencing the differentiation of other tissues. In other words, the process of organogenesis entails many tissues that are not isolated from each other. Instead, these tissues function and differentiate as a unit. This notion is supported by a striking report that recently emerged in which 3D liver buds were generated *in vitro* from iPS cells by a logical co-culture scheme[32,33]. Cocultures were generated between iPS cell-derived hepatic-specified endoderm cells with human umbilical vein endothelial cells (HUVECs) and mesenchymal stem cells[32,33]. After just 3 days of cultivation, the resulting self-organizing organoids showed evidence of endothelial cell network formation *in vitro*, and became fully functional liver tissue *in vivo*, even establishing vasculature connections with host vessels in as little as 48 hours post-transplantation[32,33]. The enormous success of this differentiation scheme was in part due to its macroscopic focus on recapitulating liver organogenesis, which depends on the complex and dynamic interplay between newly-specified hepatic cells and stromal cell pools, such as endothelial cells and mesenchymal cells[32,33].

This mindset should be translated into differentiation protocols designed to generate pancreatic β-cells. The critical roles for the pancreatic mesenchyme in orchestrating the expansion of pancreatic progenitors and regulating the balance between the exocrine and endocrine arms of the embryonic pancreas are well established[52,170,171]. Recent evidence suggests that pancreatic mesenchymal co-culture preserves pancreatic progenitor cell pools through the endowment of prolonged proliferation and self-renewal capabilities, while averting their further differentiation[172]. These data recapitulate what is observed in pancreatic development *in vivo*, where the pancreatic mesenchyme produces FGF10 that promotes expansion and maintenance of pancreatic progenitor cells while hindering their further differentiation through activation of Notch signaling[52,53]. These findings underscore the importance of incorporating organ-matched niches and microenvironments into differentiation protocols so as to mimic organogenesis *in vitro*.

Yet, despite these promising leads, most differentiation schemes completely fail to address such pertinent players in organ development. Here, we examined a bigger picture of islet homeostasis and identified a component of extrinsic signaling to pancreatic β-cells contributed to by intra-islet endothelial cells (ECs), which appears to be critical in the maintenance of islet size, proliferation and regenerative capabilities[173,174]. During murine pancreatic embryogenesis, the vasculature provides instructive signals and is essential for insulin expression in the endoderm that derives the pancreas[133]. In both rodents and humans, vascular ECs and islets are intimately associated with each other in the adult pancreas[98]. In fact, approximately 10% of the blood flow entering the pancreas is received by the highly vascularized islets, which remarkably only constitute 1-2% of the pancreatic tissue mass[98]. This vast network of conduits allows for rapid dissemination of hormones produced by the islets into the bloodstream[99]. In addition to these generic roles, intra-islet ECs support islet survival and proliferation indirectly by producing laminins and other components of the ECM[99], as touched upon earlier in Chapter I. Furthermore, intra-islet ECs have been shown to enhance insulin production by pancreatic β-cells, as well as directly promote their survival and proliferative capacities via secretion of soluble factors[98]. This is primarily mediated through bidirectional, synergistic crosstalk along the pancreatic β-cell-endothelial cell axis.

The essence of cooperative signaling between pancreatic β-cells and their associated ECs revolves around Vascular Endothelial Growth Factor (VEGF) secreted by islets, and Hepatocyte Growth Factor (HGF) produced by ECs[98,174] (Figure 32A). Islets are known to express the EC mitogen VEGF-A in large quantities throughout development and life[175], supporting native vasculogenesis, as well as promoting endothelial cell proliferation and survival through Akt, MAPK, and NO signaling[176]. This in turn induces the secretion of paracrine factors by VEGF-stimulated ECs, which produce mainly HGF[174], but also FGF and endothelin-1[98]. HGF then orchestrates downstream proliferative and survival signaling cascades by binding to its high-affinity receptor, c-Met, expressed by pancreatic β-cells[177].

The endocrine-EC axis has been implicated in the marked increase in proliferation of both intra-islet ECs and pancreatic β-cells in pregnant animals[174]. Blockade of HGF in EC pre-conditioned culture media abolished the proliferative response on pancreatic β-cells induced by the medium alone[174]. Additionally, targeted ablation of c-Met in pancreatic β-cells in mice resulted in impaired glucose tolerance, mild hyperglycemia, decreased Glut2 expression, reduced islet size, and lower insulin content within the islets[173]. Another report has emerged with similar findings, demonstrating evidence of significant reduction in Glut2 expression, impaired glucose-stimulated insulin secretion, and the predominance of smaller islets without accompanying variations in total β-cell mass[177]. Islets overexpressing

HGF are more resistant to apoptosis following transplantation[178] and conversely, disruption of pancreatic HGF signaling confers greater susceptibility to STZ-induced hyperglycemia in mice[179].

In order to adapt this critical aspect of islet homeostasis into differentiations in vitro, it may be beneficial to cultivate the differentiating cells with HUVECs during the last stage of differentiation. Moreover, it may be productive to model the endocrine-EC axis *in vitro* through stepwise generation of conditioned media[174] (Figure 32B). First, islets are placed in fresh islet media and the conditioned media is harvested after 24 hours. This media, now containing islet-secreted factors such as VEGF-A, is then exposed to endothelial cells, which respond to VEGF-A and reciprocate with production of islet mitogens such as HGF and FGF. This doubly-conditioned media can be utilized as a supplement for IPC differentiations, with the intention of increasing insulin expression, inducing proliferation, maintaining survival of these cells, and facilitating the organization of machinery requisite for glucose stimulated insulin secretion. This would thus address the third concern with our current differentiation procedure and allow for the generation of more mature IPCs of superior functionality. We do not plan to integrate pancreatic mesenchymal cells in our differentiations since the mesenchyme appears to hinder further differentiation and is instead ideal for sustaining pancreatic progenitors rather than yielding IPCs with mature β-cell characteristics[172]. The important nature of this axis *in vivo* may yield striking effects if incorporated into IPC differentiations *in vitro*.

From Bench to the Bedside: Challenges and Concerns that Need to Be Addressed Before Translating this Technology into the Clinic

Generating IPCs from autologous iPS cells with the aim of administering these cells into patients requires careful consideration of the technical and financial challenges that must be overcome before translating these cells toward clinical application[180]. Using iPS cells to generate IPCs has several advantages in the clinical realm compared to generating other cell types since only one cell type needs to be generated (the β-cell), and the route of transplantation is well-established based on longstanding experience with cadaveric islets[102]. However, several obvious concerns with utilizing iPS cells to cure T1D remain relevant.

A principal issue regarding the use of iPS cells in the clinic is their derivation using reagents and supportive matrices that are derived from animals[181]. This xenogenic contamination carries the risk that the stem cells and differentiating cells may become immunogenic. More condemning, especially regarding nonhuman feeder cells that are often used to maintain the stem cells, is the risk that these cells may harbor viruses that may compromise product integrity or worse, pose a risk to human health[55]. In order to avoid these issues, several modifications can be made to the differentiation procedure to enable the generation of GMP-grade IPCs that are therapeutically suitable and safe for clinical application.

First, in iPS cell culture, the use of mouse embryonic fibroblasts, which serve as feeder cells, or diluted matrigel, must be eliminated. In place of that, a synthetic animal-free matrix can be utilized, such as vitronectin. For 3D cultures, matrigel cannot be used despite the fact that it will be washed out prior to transplanting the cells. Instead, suspension-based culture systems should be used, not only because this initiative would eliminate the requirement of animal-based matrices, but because this is also a more scalable platform and enables significant scale-up of IPC generation[135]. GMP-grade growth factors, kits, and non-animal based cell dissociation reagents must be used in the maintenance and culture of cells[181]. Animal serums must be substituted for defined synthetic counterparts to ensure reproducibility of differentiation batches and eliminate the risk of xenogenic contamination[181].

However, with all of these progressive GMP reforms comes a significant increase in the financial expenditure involved in generating IPCs, the production of which is already relatively exorbitant[182]. Just the generation of patient-tailored iPS cells using GMP-practice alone has been estimated to cost several hundred thousand dollars, which is an enormous obstacle toward pharmaceutical development and application[182]. Thus, pharmaceutical companies collaborating with laboratories such as Joseph Wu's in Stanford have posited that patient-tailored iPS cell therapy is an impractical venture (firsthand account). Instead, MHC-matched iPS cell banks must be established to allow for a sort of "one size fits all" approach that is much more commercially viable[182]. In light of this, the immunological edge of using iPS cells as a patient-tailored therapy will diminish, but the immunoprivilege inherent to iPS cells, as well as their ethically unrestricted derivation and their unlimited availability, will remain significant advantages.

Despite their therapeutic promise, another obstacle that must be addressed before iPS cells are translated for clinical application is their potential risk for tumorigenicity[183]. This risk is significantly reduced using iPS cells generated nowadays by eliminating the use of oncogenic transgenes for the dedifferentiation process, and more importantly, using entirely nonintegrative reprogramming approaches, such as small molecules or proteins[9]. However, intrinsic to the quality of being pluripotent is the property of unlimited self-renewal, which unfortunately predisposes these cells to give rise to tumors *in vivo*. This was especially evident upon transplantation of "differentiated" cells derived using past rudimentary protocols that attempted to differentiate ES and iPS cells into downstream lineages[183]. That is because those primitive protocols were incredibly inefficient at convincingly differentiating the pluripotent stem cells into even progenitor cells, much less end-stage cells, and there was overwhelming heterogeneity in the developmental maturity of the cells resulting from those rudimentary protocols[183]. Thus, a significant majority of the cells either remained pluripotent or reverted from progenitor cells into a proliferative multipotent stem cell that ultimately gave rise to tumors. However, as is evident in the field of cardiac differentiation of iPS cells, recent advances to mainstream protocols have increased the yield of truly mature cardiomyocytes from 5% to >95%, and this has been accompanied by a complete absence in the occurrence of tumors in transplanted mice[36,183]. With regard to IPCs, two recently published reports noted that there was no evidence of tumorigenicity[77,102], which is not unbelievable considering that even the Pdx1$^+$ pancreatic progenitor cell is far removed from the developmental peak occupied by the pluripotent stem cell. In our own studies, we have not observed any tumor formation, and this is likely because we are able to generate >90% DE cells and ~97% Pdx1$^+$ cells from most differentiation batches. By the time the cells become IPCs, the presence of residual pluripotent stem cells is highly unlikely in light of our data and considering their delicate nature and selective culture conditions. Still, it is crucial to address this risk with participants of clinical trials and to be proactive regarding the development of potential tumors from the transplanted cells.

Altogether, the field of using of iPS cells as a therapeutic intervention for T1D remains in its infancy. Yields of IPCs can be improved using scalable suspension-based culture systems, which are well-established in this field[135], and so availability of the cells should not be an issue. Still, the extreme financial burden of generating iPS cell-derived IPCs, as well as the significant reforms that must be made in order to make these cells GMP-grade, will serve as major impediments to clinical application of these cells. At this point in time, the use of iPS cells to generate IPCs may not be practical. However, as years pass and GMP-based methodologies for differentiating iPS cells into IPCs become more efficient, mainstream, and economical, the use of iPS cells for the cure of T1D may be more worthwhile and this research will ultimately be valuable to the field.

Consideration of the Immunological Interplay of iPS Cell-Derived IPCs in the Context of Autoimmune Disease

A critical question that remains to be answered is whether the IPCs derived from these iPS cells will be immune to destruction by autoimmune attack post-transplantation, and hence whether graft function will be preserved long-term. Currently, the transplantation of cadaveric islets confronts formidable barriers before this form of therapy is standardized, not only because of their scarcity but also due to the possible occurrence of recurrent autoimmune rejection[184]. As such, encapsulation modalities are being widely investigated in their ability to protect the islet grafts from immune cell infiltration while allowing nutrients, waste, and insulin to pass to and from circulation[185]. Additionally, the reinstatement of tolerance toward insulin, the antigen that incites autoimmune disease in T1D, is being investigated[124-126].

It is well established that the immunodominant epitope that triggers immunological rejection is in fact insulin[4,186,187], which is presented by Major Histocompatibility Complex (MHC) class II to high-affinity binding CD4 autoreactive T cells that ultimately orchestrate a nonpathogenic humoral and pathogenic CD8 T cell autoimmune responses targeting pancreatic β-cells[4,187,188]. Certain MHC II alleles, primarily HLA-DR4, HLA-DR3 and HLA-DQ8, have shown bias with regard to their association with the development of T1D[188]. Progression from this inductive phase toward a destructive state, characterized by widespread insulinitis and clinical dysfunction, occurs due to epitope spreading, where autoimmune responses are mounted against other β-cell-associated "neoantigens"[187,189]. These neoantigens include Znt8, IGRP, IA-2 and GAD, liberated via primary destruction of the first few pancreatic β-cells during the inductive phase of T1D[187,189].

The presence of these T1D-associated antigens, particularly insulin, is likely to be significant on iPS cell-derived IPCs, especially after their transplantation and establishment as bona fide pancreatic β-cell replacements. It is concerning to consider that the immune system of the same T1D patient that originally destroyed his own pancreatic β-cells will be transplanted with similar substitutes. However, it must be stressed that the antigenicity and hence the immunogenicity of IPCs is likely to be uniquely poor compared to that of their primary human counterparts, owing to their derivation from famously immunoprivileged pluripotent stem cells[42,132].

These speculative considerations were confirmed in preliminary data documented in Figure 30, where we showed that the IPCs poorly express MHC class I and II, as well as the T cell costimulatory molecules CD80 and CD86. Additionally, we showed that IPCs are not susceptible to NK cell killing despite their poor expression of MHC class I, demonstrating an immunoprivilege characteristic of these cells that is similar to what is observed for undifferentiated iPS cells[42,130]. Moreover, these results are consistent with our extensive studies on mouse and human ES and iPS cell-derived hematopoietic progenitor cells (HPCs)[42,190,191]. For instance, previous reports in our lab have confirmed that, similar to their pluripotent precursors, mouse and human iPS cell-derived HPCs poorly express MHC class I and do not express MHC class II[42,190,191]. In addition, the lack of expression of T cell costimulatory molecules by these cells ultimately manipulates the immune system to induce antigen-specific T cell anergy and dysfunction[42,191]. Such findings are highly significant in their implication for the unique position occupied by iPS cell derived tissues in replacing cells destroyed due to autoimmune reactions.

However, we acknowledge that these features of iPS cell-derived IPCs may change post-transplantation. We propose the following model by which one can determine the immunological susceptibility of iPS cell-derived IPCs to autoimmune attack upon transplantation (Figure 33). In order to address this very important topic, one will have to generate a humanized mouse model in which the hematopoietic system is derived from the T1D patient. This would endow the mouse with T cells targeting insulin-expressing cells. These mice should then be transplanted with IPCs, and the function and survival of the graft should be assessed by measuring the presence of human insulin in the blood of these mice. Several weeks later, the mice should be sacrificed and immune cell infiltration into these grafts should be determined. This model would conclusively allow one to make predictions regarding the immunological susceptibility of IPCs to autoimmune attack.

There are several possible reasons that IPCs may lose immunoprivilege upon transplantation. For example, it is possible that the exposure to a cytokine milieu *in vivo* may upregulate MHC class I expression on these cells, which will ultimately make them susceptible to autoreactive CD8 T cell recognition and killing. If this is the case, immunoprotection modalities may be investigated in the form of cell encapsulation[185] so as to allow release of insulin and exchange of nutrients while abrogating immune cell infiltration. Still, the advantage of using IPCs over cadaveric islets are evident in 1) their unlimited availability and 2) the definite lack of allogeneic immune responses, since the IPCs will be autologous and designed as a patient-tailored therapy[6].

Summary and Future Directions

Altogether, we have demonstrated here a highly effective 3D culture-based protocol that uses an epigenetic modifier and well-reasoned signaling cues for the generation of authentic and functional IPCs from T1D iPS cells. Using this carefully optimized protocol, we can efficiently convert T1D iPS cells into >90% CXCR4$^+$ Sox17$^+$ PDGFR-α$^-$ definitive endodermal cells and eventually >95% Pdx1$^+$ pancreatic progenitor cells. The yield of insulin$^+$ cells is consistently and remarkably high in these differentiations (>50%), and these IPCs strongly resemble pancreatic β-cells in their expression of pancreatic β-cell specific markers and possession of insulin granules. Finally, these IPCs are glucose-responsive and capable of superior, rapid and efficient correction of hyperglycemia in diabetic mice, endowing them with the ability to effectively regulate blood glucose levels after supraphysicological glucose challenge. Because of their noncontroversial derivation, unlimited availability, patient-tailored utility, and potential ability to evade immune detection and likelihood to remain functional despite autoimmune presence, iPS cell-derived IPCs are likely to be a prime therapeutic tool for the cure of T1D in the future.

Figure 31. Novel culture platforms for differentiating iPSCs into IPCs

(A) 3D differentiation better mimics physiological differentiation of embryonic stem cells during embryogenesis, and may thus be a more suitable platform for differentiating iPSCs into mature, functional IPCs *in vitro*. This may be achieved via either static 3D cultures (top panel), which incorporate a bioactive scaffold in which cells are embedded, or dynamic suspension 3D cultures (bottom panel), in which cell clusters may be maintained in rotating spinning flasks to provide improved oxygenation and diffusion of nutrients to the cells. In addition, cell clusters may be encapsulated in growth-supporting matrices or maintained in mechanically controlled bioreactors to precisely manipulate the cell culture conditions. **(B)** To induce apical-basal polarity in differentiating cells, they may be cultured in an Air-Liquid Interface (ALI) culture system. Here, cells are positioned on top of a pore-laced membrane under which the media is placed, while at the top end the cells are exposed to air. The ALI culture configuration facilitates the acquisition of cell polarity, which is a feature found on mature cell types and may improve the functionality and efficiency in deriving differentiated cells, such as IPCs. **(C)** A natural scaffold for seeding IPCs can be generated by decellularization of the pancreas with detergent to strip the organ of cellular and nuclear material, leaving only the native ECM and vascular architecture intact. After thoroughly washing away the detergent, the organ can then be re-seeded with iPSC-derived IPCs. The potential use of decellularized organ scaffolds for improved IPC differentiation and functionality post-transplantation is promising due to the provision of critical ECM components in the decellularized template, existing microvasculature, and homing signals in the natural microenvironment that may improve cell survival and function.

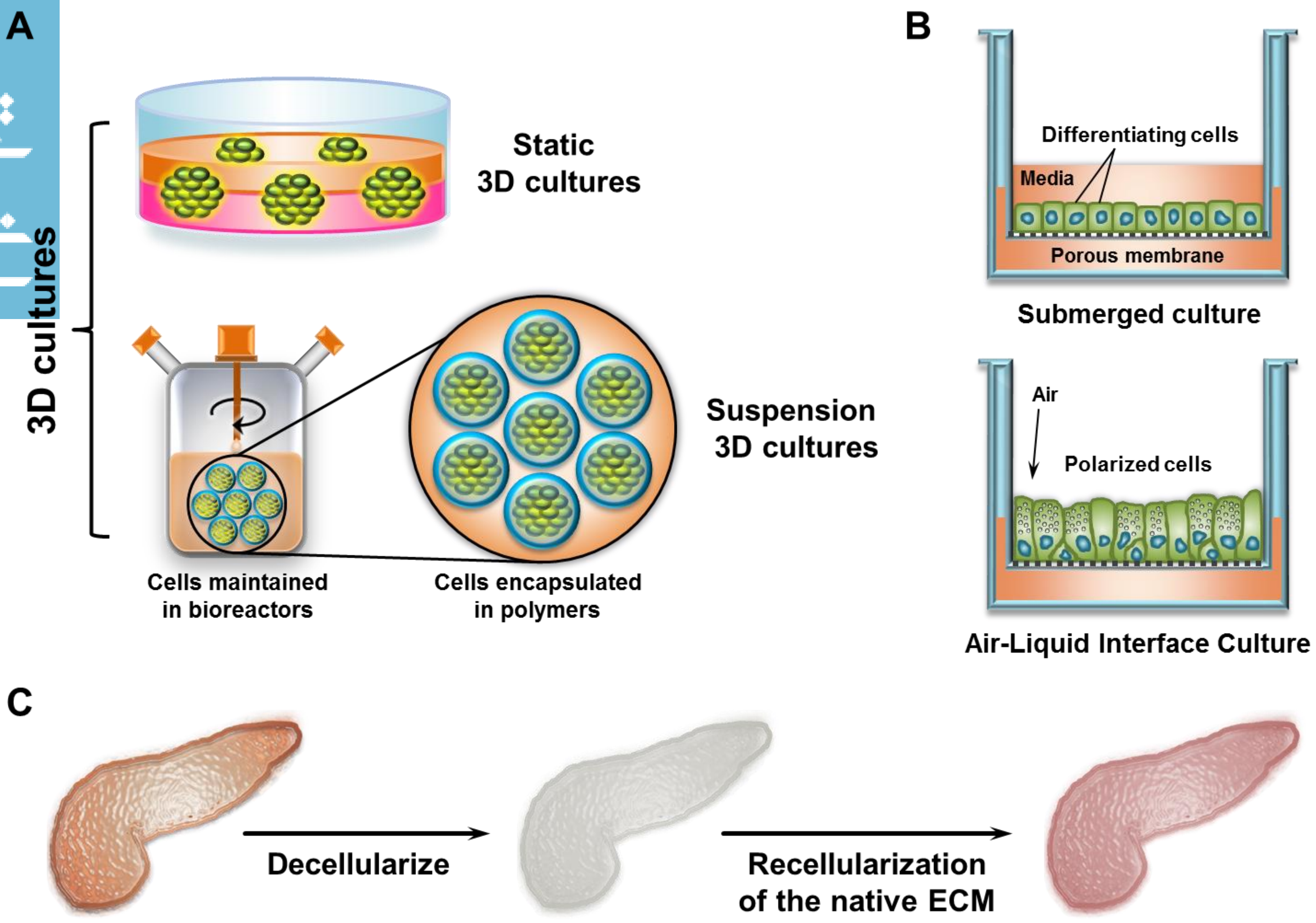
A
3D cultures
Static
3D cultures
Suspension
3D cultures
Cells maintained
in bioreactors
Cells encapsulated
in polymers
B
Differentiating cells
Media
Porous membrane
Submerged culture
Air
Polarized cells
Air-Liquid Interface Culture
C
Decellularize
Recellularization
of the native ECM

Figure 32. Cooperative signaling along the endothelial-endocrine axis may enhance survival, maturation and function of iPS cell-derived IPCs

(A) Secretion of VEGF by pancreatic islets supports endothelial cell survival and proliferation through activation of pathways involving (but not limited to) Akt and Nitric Oxide (NO), which induce survival and proliferation, respectively. These endothelial cells reciprocate by producing HGF, which binds to the receptor c-Met expressed by islet cells and promotes their own survival and proliferation through activation of the Akt and MAPK signaling pathways. Thus, cooperative signaling along the endothelial-endocrine axis within pancreatic islets activates downstream signal transduction contributing to mutual survival and proliferation. **(B)** This is the schema for generating endothelial cell-conditioned islet media pre-conditioned by human islets. Islets cultured in islet medium (IM) over 24 hours secrete growth factors such as VEGF that remain in the conditioned media when islets are pelleted. Endothelial cells exposed overnight to the islet-conditioned medium will respond to the islet-secreted VEGF and produce their own cocktail of growth factors, such as HGF, which in turn supports islet proliferation. After pelleting residual endothelial cells, the resultant bi-conditioned media is suitable for supplementation into IPC differentiation media.

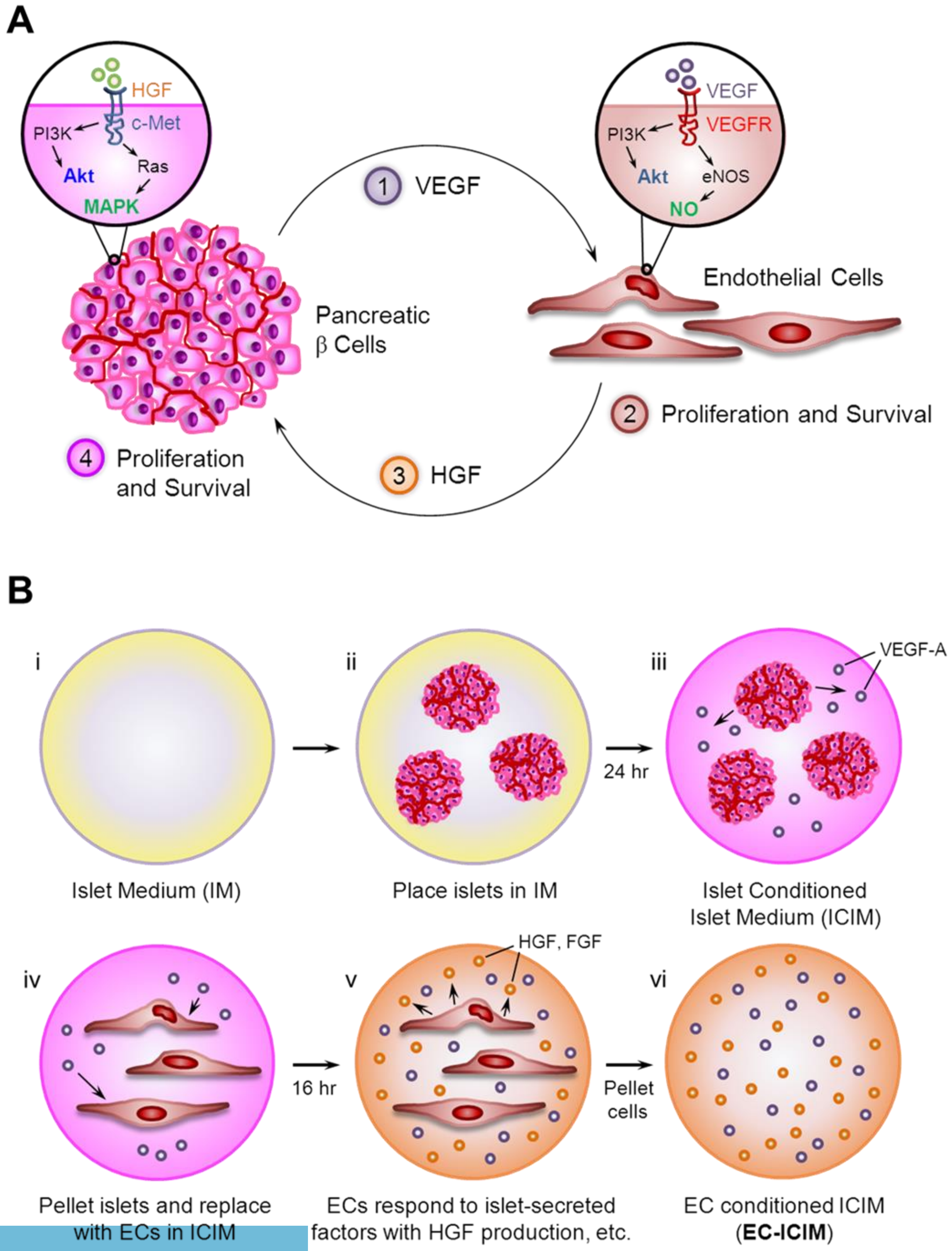
A
HGF
c-Met
PI3K
Akt
Ras
MAPK
VEGF
VEGFR
PI3K
Akt
eNOS
NO
1 VEGF
Endothelial Cells
Pancreatic β Cells
2 Proliferation and Survival
3 HGF
4 Proliferation and Survival
B
i
ii
iii
VEGF-A
24 hr
Islet Medium (IM)
Place islets in IM
Islet Conditioned Islet Medium (ICIM)
iv
v
vi
HGF, FGF
16 hr
Pellet cells
Pellet islets and replace with ECs in ICIM
ECs respond to islet-secreted factors with HGF production, etc.
EC conditioned ICIM (EC-ICIM)

Figure 33. A humanized mouse model to investigate the autoimmune susceptibility of iPS cell-derived IPCs *in vivo*

To investigate the autoimmune susceptibility of iPS cell-derived IPCs *in vivo*, one must utilize a humanized mouse model in which the immune system is derived from a T1D patient (and thus has the autoreactive T cells that mediate the pathogenesis of T1D). The proposed model for this experiment entails preparing iPS cells from fibroblasts of the T1D patient, and differentiating these iPS cells into IPCs, as well as isolating peripheral blood cells from the same patient in order to derive the immune system and thereby generate the humanized mouse model for T1D. After reconstituting the hematopoietic system in the immunodeficient mouse with the T1D patient's hematopoietic cells, the presence of autoreactive T cells against insulin must be confirmed using tetramer technology. Subsequently, the mouse must be transplanted with the iPS cell-derived IPCs. The survival and function of this grant must be monitored, and after several weeks of transplantation, the graft should be harvested and immune cell infiltration assessed. Additionally, determining the expression of MHC class I and T cell costimulatory molecules might be informative. This model should hopefully provide some insight into the ability of iPS cell-derived IPCs to evade autoimmune T cell recognition and attack in the context of T1D, and ultimately allow one to make early conclusions regarding the potential success of this therapy in the clinical realm.

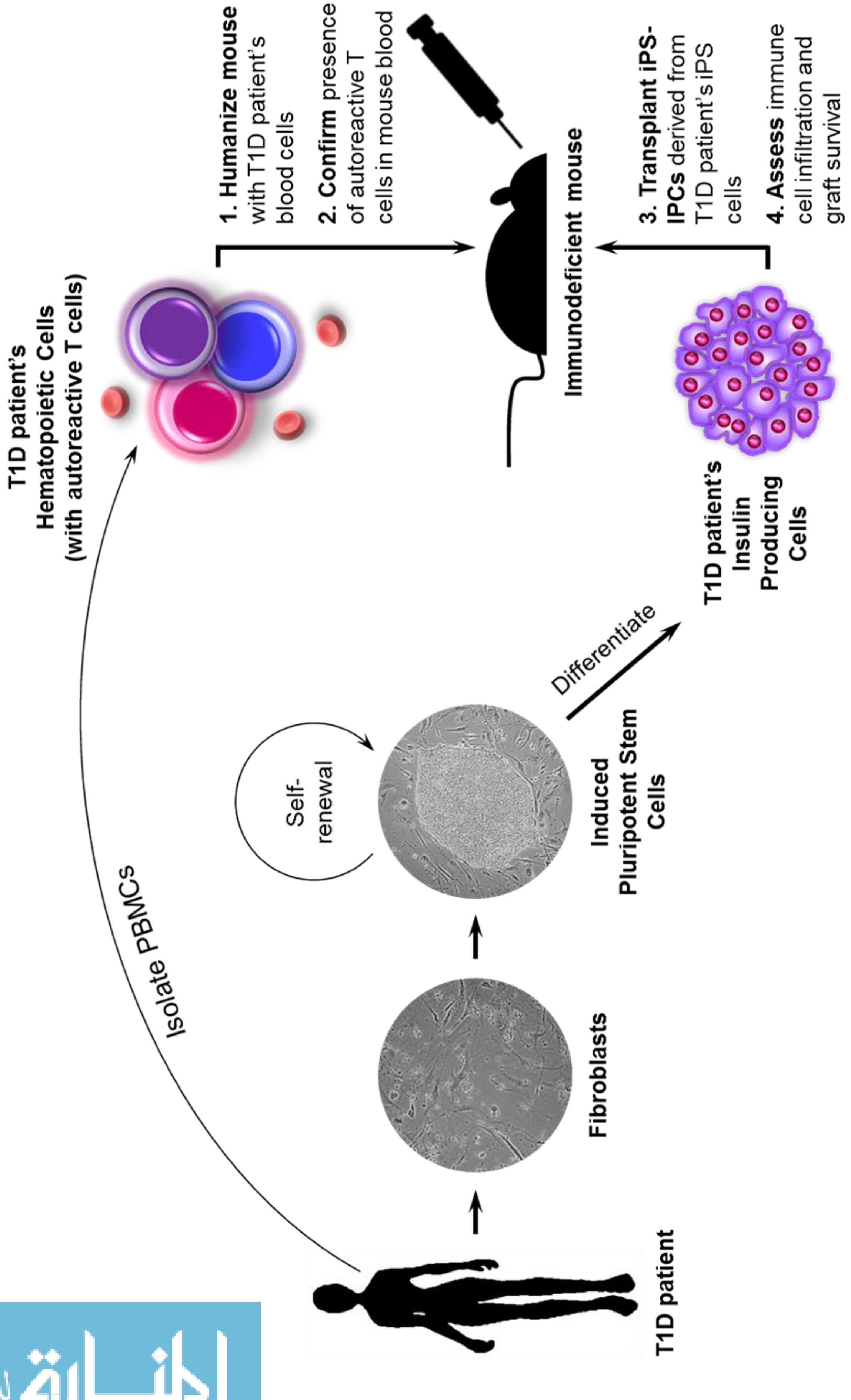
T1D patient
Isolate PBMCs
Fibroblasts
Self-renewal
Induced Pluripotent Stem Cells
Differentiate
T1D patient's Insulin Producing Cells
T1D patient's Hematopoietic Cells (with autoreactive T cells)
1. Humanize mouse with T1D patient's blood cells
2. Confirm presence of autoreactive T cells in mouse blood
3. Transplant iPS-IPCs derived from T1D patient's iPS cells
4. Assess immune cell infiltration and graft survival
Immunodeficient mouse

REFERENCES

1. Brissova, M. *et al.* Assessment of human pancreatic islet architecture and composition by laser scanning confocal microscopy. *J Histochem Cytochem* **53**, 1087-1097, doi:10.1369/jhc.5C6684.2005 (2005).

2. Pandol, S. J. in *The Exocrine Pancreas Colloquium Series on Integrated Systems Physiology: From Molecule to Function to Disease* (2010).

3. Leroux, C. *et al.* Lifestyle and Cardiometabolic Risk in Adults with Type 1 Diabetes: A Review. *Can J Diabetes* **38**, 62-69, doi:10.1016/j.jcjd.2013.08.268 (2014).

4. van Belle, T. L., Coppieters, K. T. & von Herrath, M. G. Type 1 diabetes: etiology, immunology, and therapeutic strategies. *Physiological reviews* **91**, 79-118, doi:10.1152/physrev.00003.2010 (2011).

5. Vantyghem, M. C. *et al.* Treating diabetes with islet transplantation: Lessons from the past decade in Lille. *Diabetes Metab*, doi:10.1016/j.diabet.2013.10.003 (2014).

6. Manzar, G. S., Kim, E. M., Rotti, P. & Zavazava, N. Skin deep: from dermal fibroblasts to pancreatic beta cells. *Immunol Res*, doi:10.1007/s12026-014-8546-8 (2014).

7. Raikwar, S. P. & Zavazava, N. Spontaneous in vivo differentiation of embryonic stem cell-derived pancreatic endoderm-like cells corrects hyperglycemia in diabetic mice. *Transplantation* **91**, 11-20 (2011).

8. Liberatore Rdel, R., Jr. & Damiani, D. Insulin pump therapy in type 1 diabetes mellitus. *J Pediatr (Rio J)* **82**, 249-254, doi:10.2223/JPED.1507 (2006).

9. Robinton, D. A. & Daley, G. Q. The promise of induced pluripotent stem cells in research and therapy. *Nature* **481**, 295-305, (2012).

10. Alvarez, C. V. *et al.* Defining stem cell types: understanding the therapeutic potential of ESCs, ASCs, and iPS cells. *Journal of molecular endocrinology* **49**, R89-111, doi:10.1530/JME-12-0072 (2012).

11. Goldthwaite Jr., C. A. Department of Health and Human Services: The Promise of Regenerative Medicine. *Regenerative Medicine*, 97-103 (2006).

12. D'Amour, K. A. *et al.* Production of pancreatic hormone-expressing endocrine cells from human embryonic stem cells. *Nature biotechnology* **24**, 1392-1401, doi:10.1038/nbt1259 (2006).

13. Kroon, E. *et al.* Pancreatic endoderm derived from human embryonic stem cells generates glucose-responsive insulin-secreting cells in vivo. *Nature biotechnology* **26**, 443-452, doi:10.1038/nbt1393 (2008).

14. Zhang, D. *et al.* Highly efficient differentiation of human ES cells and iPS cells into mature pancreatic insulin-producing cells. *Cell research* **19**, 429-438, doi:10.1038/cr.2009.28 (2009).

15. Xie, R. *et al.* Dynamic chromatin remodeling mediated by polycomb proteins orchestrates pancreatic differentiation of human embryonic stem cells. *Cell stem cell* **12**, 224-237, doi:10.1016/j.stem.2012.11.023 (2013).

16. Rezania, A. *et al.* Maturation of Human Embryonic Stem Cell–Derived Pancreatic Progenitors Into Functional Islets Capable of Treating Pre-existing Diabetes in Mice. *Diabetes* **61**, 2016-2029, doi:10.2337/db11-1711 (2012).

17. Takahashi, K. & Yamanaka, S. Induction of pluripotent stem cells from mouse embryonic and adult fibroblast cultures by defined factors. *Cell* **126**, 663-676, doi:10.1016/j.cell.2006.07.024 (2006).

18. Boland, M. J. *et al.* Adult mice generated from induced pluripotent stem cells. *Nature* **461**, 91-94, doi:10.1038/nature08310 (2009).

19. Takahashi, K. *et al.* Induction of pluripotent stem cells from adult human fibroblasts by defined factors. *Cell* **131**, 861-872, doi:10.1016/j.cell.2007.11.019 (2007).

20. Yu, J. *et al.* Induced pluripotent stem cell lines derived from human somatic cells. *Science* **318**, 1917-1920, doi:10.1126/science.1151526 (2007).

21. Yamanaka, S. A fresh look at iPS cells. *Cell* **137**, 13-17, doi:10.1016/j.cell.2009.03.034 (2009).

22. Anokye-Danso, F. *et al.* Highly efficient miRNA-mediated reprogramming of mouse and human somatic cells to pluripotency. *Cell stem cell* **8**, 376-388, doi:10.1016/j.stem.2011.03.001 (2011).

23. Gonzalez, F., Boue, S. & Izpisua Belmonte, J. C. Methods for making induced pluripotent stem cells: reprogramming a la carte. *Nature reviews. Genetics* **12**, 231-242, doi:10.1038/nrg2937 (2011).

24. Huangfu, D. *et al.* Induction of pluripotent stem cells from primary human fibroblasts with only Oct4 and Sox2. *Nature biotechnology* **26**, 1269-1275, doi:10.1038/nbt.1502 (2008).

25. Li, Z., Yang, C. S., Nakashima, K. & Rana, T. M. Small RNA-mediated regulation of iPS cell generation. *Embo J* **30**, 823-834, doi:10.1038/emboj.2011.2 (2011).

26. Stadtfeld, M., Nagaya, M., Utikal, J., Weir, G. & Hochedlinger, K. Induced pluripotent stem cells generated without viral integration. *Science* **322**, 945-949, doi:10.1126/science.1162494 (2008).

27. Loh, Y. H. *et al.* Generation of induced pluripotent stem cells from human blood. *Blood* **113**, 5476-5479, doi:10.1182/blood-2009-02-204800 (2009).

28. Aoi, T. *et al.* Generation of pluripotent stem cells from adult mouse liver and stomach cells. *Science* **321**, 699-702, doi:10.1126/science.1154884 (2008).

29. Aasen, T. *et al.* Efficient and rapid generation of induced pluripotent stem cells from human keratinocytes. *Nature biotechnology* **26**, 1276-1284, doi:10.1038/nbt.1503 (2008).

30. Zhou, T. *et al.* Generation of human induced pluripotent stem cells from urine samples. *Nature protocols* **7**, 2080-2089, doi:10.1038/nprot.2012.115 (2012).

31. Zhou, T. *et al.* Generation of induced pluripotent stem cells from urine. *Journal of the American Society of Nephrology : JASN* **22**, 1221-1228, doi:10.1681/ASN.2011010106 (2011).

32. Takebe, T. *et al.* Vascularized and functional human liver from an iPSC-derived organ bud transplant. *Nature* **499**, 481-484, doi:10.1038/nature12271 (2013).

33. Takebe, T. *et al.* Generation of a vascularized and functional human liver from an iPSC-derived organ bud transplant. *Nat. Protocols* **9**, 396-409, doi:10.1038/nprot.2014.020 (2014).

34. Christoforou, N. *et al.* Induced pluripotent stem cell-derived cardiac progenitors differentiate to cardiomyocytes and form biosynthetic tissues. *PLoS One* **8**, e65963, doi:10.1371/journal.pone.0065963 (2013).

35. Chambers, S. M. & Studer, L. Cell fate plug and play: direct reprogramming and induced pluripotency. *Cell* **145**, 827-830, doi:10.1016/j.cell.2011.05.036 (2011).

36. Burridge, P. W. *et al.* Chemically defined generation of human cardiomyocytes. *Nature methods* **11**, 855-860, doi:10.1038/nmeth.2999 (2014).

37. Chambers, S. M. *et al.* Highly efficient neural conversion of human ES and iPS cells by dual inhibition of SMAD signaling. *Nature biotechnology* **27**, 275-280, doi:10.1038/nbt.1529 (2009).

38. Lancaster, M. A. *et al.* Cerebral organoids model human brain development and microcephaly. *Nature* **501**, 373-379, doi:10.1038/nature12517 (2013).

39. Lam, A. Q. *et al.* Rapid and efficient differentiation of human pluripotent stem cells into intermediate mesoderm that forms tubules expressing kidney proximal tubular markers. *Journal of the American Society of Nephrology : JASN* **25**, 1211-1225, doi:10.1681/ASN.2013080831 (2014).

40. Song, B. *et al.* The directed differentiation of human iPS cells into kidney podocytes. *PLoS One* **7**, e46453, doi:10.1371/journal.pone.0046453 (2012).

41. Firth, A. L. *et al.* Generation of multiciliated cells in functional airway epithelia from human induced pluripotent stem cells. *Proceedings of the National Academy of Sciences of the United States of America* **111**, E1723-1730, doi:10.1073/pnas.1403470111 (2014).

42. Kim, E. M., Manzar, G. & Zavazava, N. Human iPS cell-derived hematopoietic progenitor cells induce T-cell anergy in in vitro-generated alloreactive CD8(+) T cells. *Blood* **121**, 5167-5175, doi:10.1182/blood-2012-11-467753 (2013).

43. Cyranoski, D. Japanese woman is first recipient of next-generation stem cells. *Nature News* (2014).

44. Shahjalal, H. M. *et al.* Generation of insulin-producing beta-like cells from human iPS cells in a defined and completely xeno-free culture system. *J Mol Cell Biol*, doi:10.1093/jmcb/mju029 (2014).

45. Yechoor, V. & Chan, L. Minireview: beta-cell replacement therapy for diabetes in the 21st century: manipulation of cell fate by directed differentiation. *Molecular endocrinology* **24**, 1501-1511, doi:10.1210/me.2009-0311 (2010).

46. Murtaugh, L. C. Pancreas and beta-cell development: from the actual to the possible. *Development (Cambridge, England)* **134**, 427-438, doi:10.1242/dev.02770 (2007).

47. Spence, J. R. & Wells, J. M. Translational embryology: using embryonic principles to generate pancreatic endocrine cells from embryonic stem cells. *Developmental dynamics : an official publication of the American Association of Anatomists* **236**, 3218-3227, doi:10.1002/dvdy.21366 (2007).

48. Raikwar, S. P. & Zavazava, N. Insulin producing cells derived from embryonic stem cells: are we there yet? *J Cell Physiol* **218**, 256-263, doi:10.1002/jcp.21615 (2009).

49. Wells, J. M. & Melton, D. A. Vertebrate endoderm development. *Annu Rev Cell Dev Biol* **15**, 393-410, doi:10.1146/annurev.cellbio.15.1.393 (1999).

50. Stoffers, D. A., Zinkin, N. T., Stanojevic, V., Clarke, W. L. & Habener, J. F. Pancreatic agenesis attributable to a single nucleotide deletion in the human IPF1 gene coding sequence. *Nature genetics* **15**, 106-110, doi:10.1038/ng0197-106 (1997).

51. Burlison, J. S., Long, Q., Fujitani, Y., Wright, C. V. & Magnuson, M. A. Pdx-1 and Ptf1a concurrently determine fate specification of pancreatic multipotent progenitor cells. *Dev Biol* **316**, 74-86, doi:10.1016/j.ydbio.2008.01.011 (2008).

52. Hart, A., Papadopoulou, S. & Edlund, H. Fgf10 maintains notch activation, stimulates proliferation, and blocks differentiation of pancreatic epithelial cells. *Developmental dynamics : an official publication of the American Association of Anatomists* **228**, 185-193, doi:10.1002/dvdy.10368 (2003).

53. Norgaard, G. A., Jensen, J. N. & Jensen, J. FGF10 signaling maintains the pancreatic progenitor cell state revealing a novel role of Notch in organ development. *Dev Biol* **264**, 323-338 (2003).

54. Chen, A. E., Borowiak, M., Sherwood, R. I., Kweudjeu, A. & Melton, D. A. Functional evaluation of ES cell-derived endodermal populations reveals differences between Nodal and Activin A-guided differentiation. *Development (Cambridge, England)* **140**, 675-686, doi:10.1242/dev.085431 (2013).

55. Sui, L., Bouwens, L. & Mfopou, J. K. Signaling pathways during maintenance and definitive endoderm differentiation of embryonic stem cells. *The International journal of developmental biology* **57**, 1-12, doi:10.1387/ijdb.120115ls (2013).

56. McLin, V. A., Rankin, S. A. & Zorn, A. M. Repression of Wnt/beta-catenin signaling in the anterior endoderm is essential for liver and pancreas development. *Development (Cambridge, England)* **134**, 2207-2217, doi:10.1242/dev.001230 (2007).

57. Tada, S. *et al*. Characterization of mesendoderm: a diverging point of the definitive endoderm and mesoderm in embryonic stem cell differentiation culture. *Development (Cambridge, England)* **132**, 4363-4374, doi:10.1242/dev.02005 (2005).

58. Loh, K. M. *et al.* Efficient endoderm induction from human pluripotent stem cells by logically directing signals controlling lineage bifurcations. *Cell stem cell* **14**, 237-252, doi:10.1016/j.stem.2013.12.007 (2014).

59. Mfopou, J. K., Chen, B., Sui, L., Sermon, K. & Bouwens, L. Recent advances and prospects in the differentiation of pancreatic cells from human embryonic stem cells. *Diabetes* **59**, 2094-2101, doi:10.2337/db10-0439 (2010).

60. Groppe, J. *et al.* Structural basis of BMP signalling inhibition by the cystine knot protein Noggin. *Nature* **420**, 636-642, doi:10.1038/nature01245 (2002).

61. Shih, H. P., Wang, A. & Sander, M. Pancreas organogenesis: from lineage determination to morphogenesis. *Annu Rev Cell Dev Biol* **29**, 81-105, doi:10.1146/annurev-cellbio-101512-122405 (2013).

62. Gradwohl, G., Dierich, A., LeMeur, M. & Guillemot, F. neurogenin3 is required for the development of the four endocrine cell lineages of the pancreas. *Proceedings of the National Academy of Sciences of the United States of America* **97**, 1607-1611 (2000).

63. Schaffer, A. E. *et al.* Nkx6.1 controls a gene regulatory network required for establishing and maintaining pancreatic Beta cell identity. *PLoS genetics* **9**, e1003274, doi:10.1371/journal.pgen.1003274 (2013).

64. Taylor, B. L., Liu, F. F. & Sander, M. Nkx6.1 is essential for maintaining the functional state of pancreatic beta cells. *Cell reports* **4**, 1262-1275, doi:10.1016/j.celrep.2013.08.010 (2013).

65. Afelik, S. & Jensen, J. Notch signaling in the pancreas: patterning and cell fate specification. *Wiley interdisciplinary reviews. Developmental biology* **2**, 531-544, doi:10.1002/wdev.99 (2013).

66. Murtaugh, L. C., Stanger, B. Z., Kwan, K. M. & Melton, D. A. Notch signaling controls multiple steps of pancreatic differentiation. *Proceedings of the National Academy of Sciences of the United States of America* **100**, 14920-14925, doi:10.1073/pnas.2436557100 (2003).

67. de Back, W., Zhou, J. X. & Brusch, L. On the role of lateral stabilization during early patterning in the pancreas. *Journal of the Royal Society, Interface / the Royal Society* **10**, 20120766, doi:10.1098/rsif.2012.0766 (2013).

68. Greenwood, A. L., Li, S., Jones, K. & Melton, D. A. Notch signaling reveals developmental plasticity of Pax4+ pancreatic endocrine progenitors and shunts them to a duct fate. *Mechanisms of Development* **124**, 97-107, (2007).

69. Qu, X. *et al.* Notch-mediated post-translational control of Ngn3 protein stability regulates pancreatic patterning and cell fate commitment. *Dev Biol* **376**, 1-12, doi:10.1016/j.ydbio.2013.01.021 (2013).

70. Massague, J. TGFbeta signalling in context. *Nat Rev Mol Cell Biol* **13**, 616-630, doi:10.1038/nrm3434 (2012).

71. Harmon, E. B. *et al.* GDF11 modulates NGN3+ islet progenitor cell number and promotes beta-cell differentiation in pancreas development. *Development (Cambridge, England)* **131**, 6163-6174, doi:10.1242/dev.01535 (2004).

72. Gellibert, F. *et al.* Identification of 1,5-naphthyridine derivatives as a novel series of potent and selective TGF-beta type I receptor inhibitors. *Journal of medicinal chemistry* **47**, 4494-4506, doi:10.1021/jm0400247 (2004).

73. Thatava, T. *et al.* Indolactam V/GLP-1-mediated differentiation of human iPS cells into glucose-responsive insulin-secreting progeny. *Gene therapy* **18**, 283-293, doi:10.1038/gt.2010.145 (2011).

74. Otonkoski, T., Beattie, G. M., Mally, M. I., Ricordi, C. & Hayek, A. Nicotinamide is a potent inducer of endocrine differentiation in cultured human fetal pancreatic cells. *The Journal of clinical investigation* **92**, 1459-1466, doi:10.1172/JCI116723 (1993).

75. Ye, D. Z., Tai, M. H., Linning, K. D., Szabo, C. & Olson, L. K. MafA expression and insulin promoter activity are induced by nicotinamide and related compounds in INS-1 pancreatic beta-cells. *Diabetes* **55**, 742-750 (2006).

76. Aguayo-Mazzucato, C. *et al.* Thyroid hormone promotes postnatal rat pancreatic beta-cell development and glucose-responsive insulin secretion through MAFA. *Diabetes* **62**, 1569-1580, doi:10.2337/db12-0849 (2013).

77. Rezania, A. *et al.* Reversal of diabetes with insulin-producing cells derived in vitro from human pluripotent stem cells. *Nature biotechnology* **32**, 1121-1133, doi:10.1038/nbt.3033 (2014).

78. Holz, G. G. Epac: A new cAMP-binding protein in support of glucagon-like peptide-1 receptor-mediated signal transduction in the pancreatic beta-cell. *Diabetes* **53**, 5-13 (2004).

79. Wang, X., Zhou, J., Doyle, M. E. & Egan, J. M. Glucagon-like peptide-1 causes pancreatic duodenal homeobox-1 protein translocation from the cytoplasm to the nucleus of pancreatic beta-cells by a cyclic adenosine monophosphate/protein kinase A-dependent mechanism. *Endocrinology* **142**, 1820-1827, doi:10.1210/endo.142.5.8128 (2001).

80. MacDonald, P. E. *et al.* The multiple actions of GLP-1 on the process of glucose-stimulated insulin secretion. *Diabetes* **51 Suppl 3**, S434-442 (2002).

81. Galvan, V., Logvinova, A., Sperandio, S., Ichijo, H. & Bredesen, D. E. Type 1 insulin-like growth factor receptor (IGF-IR) signaling inhibits apoptosis signal-regulating kinase 1 (ASK1). *J Biol Chem* **278**, 13325-13332, doi:10.1074/jbc.M211398200 (2003).

82. Vincent, A. M. & Feldman, E. L. Control of cell survival by IGF signaling pathways. *Growth hormone & IGF research : official journal of the Growth Hormone Research Society and the International IGF Research Society* **12**, 193-197 (2002).

83. Withers, D. J. *et al.* Irs-2 coordinates Igf-1 receptor-mediated beta-cell development and peripheral insulin signalling. *Nature genetics* **23**, 32-40, doi:10.1038/12631 (1999).

84. Hughes, C. S., Postovit, L. M. & Lajoie, G. A. Matrigel: a complex protein mixture required for optimal growth of cell culture. *Proteomics* **10**, 1886-1890, doi:10.1002/pmic.200900758 (2010).

85. Kleinman, H. K. & Martin, G. R. Matrigel: basement membrane matrix with biological activity. *Semin Cancer Biol* **15**, 378-386, doi:10.1016/j.semcancer.2005.05.004 (2005).

86. Takeuchi, H., Nakatsuji, N. & Suemori, H. Endodermal differentiation of human pluripotent stem cells to insulin-producing cells in 3D culture. *Sci. Rep.* **4**, doi:10.1038/srep04488 (2014).

87. Li, W. *et al.* Long-term persistence and development of induced pancreatic beta cells generated by lineage conversion of acinar cells. *Nature biotechnology* **32**, 1223-1230, doi:10.1038/nbt.3082 (2014).

88. Dahl, U., Sjodin, A. & Semb, H. Cadherins regulate aggregation of pancreatic beta-cells in vivo. *Development (Cambridge, England)* **122**, 2895-2902 (1996).

89. Hopcroft, D. W., Mason, D. R. & Scott, R. S. Structure-function relationships in pancreatic islets: support for intraislet modulation of insulin secretion. *Endocrinology* **117**, 2073-2080, doi:10.1210/endo-117-5-2073 (1985).

90. Meda, P. *et al.* Rapid and reversible secretion changes during uncoupling of rat insulin-producing cells. *The Journal of clinical investigation* **86**, 759-768, doi:10.1172/JCI114772 (1990).

91. Ravier, M. A. *et al.* Loss of connexin36 channels alters beta-cell coupling, islet synchronization of glucose-induced Ca2+ and insulin oscillations, and basal insulin release. *Diabetes* **54**, 1798-1807 (2005).

92. Konstantinova, I. *et al.* EphA-Ephrin-A-mediated beta cell communication regulates insulin secretion from pancreatic islets. *Cell* **129**, 359-370, doi:10.1016/j.cell.2007.02.044 (2007).

93. Bishop, J. R., Schuksz, M. & Esko, J. D. Heparan sulphate proteoglycans fine-tune mammalian physiology. *Nature* **446**, 1030-1037, doi:10.1038/nature05817 (2007).

94. Lin, X. Functions of heparan sulfate proteoglycans in cell signaling during development. *Development (Cambridge, England)* **131**, 6009-6021, doi:10.1242/dev.01522 (2004).

95. Hacker, U., Nybakken, K. & Perrimon, N. Heparan sulphate proteoglycans: the sweet side of development. *Nat Rev Mol Cell Biol* **6**, 530-541, doi:10.1038/nrm1681 (2005).

96. Schultz, G. S. & Wysocki, A. Interactions between extracellular matrix and growth factors in wound healing. *Wound Repair Regen* **17**, 153-162, doi:10.1111/j.1524-475X.2009.00466.x (2009).

97. Parnaud, G. *et al.* Blockade of beta1 integrin-laminin-5 interaction affects spreading and insulin secretion of rat beta-cells attached on extracellular matrix. *Diabetes* **55**, 1413-1420 (2006).

98. Peiris, H., Bonder, C. S., Coates, P. T., Keating, D. J. & Jessup, C. F. The beta-cell/EC axis: how do islet cells talk to each other? *Diabetes* **63**, 3-11, doi:10.2337/db13-0617 (2014).

99. Johansson, A. *et al.* Endothelial cell signalling supports pancreatic beta cell function in the rat. *Diabetologia* **52**, 2385-2394, doi:10.1007/s00125-009-1485-6 (2009).

100. Givant-Horwitz, V., Davidson, B. & Reich, R. Laminin-induced signaling in tumor cells. *Cancer letters* **223**, 1-10, doi:10.1016/j.canlet.2004.08.030 (2005).

101. Biden, T. J. *et al.* The diverse roles of protein kinase C in pancreatic beta-cell function. *Biochemical Society transactions* **36**, 916-919, doi:10.1042/BST0360916 (2008).

102. Pagliuca, F. W. *et al.* Generation of functional human pancreatic beta cells in vitro. *Cell* **159**, 428-439, doi:10.1016/j.cell.2014.09.040 (2014).

103. Bram, E. E., Stark, M., Raz, S. & Assaraf, Y. G. Chemotherapeutic drug-induced ABCG2 promoter demethylation as a novel mechanism of acquired multidrug resistance. *Neoplasia* **11**, 1359-1370 (2009).

104. Chaudhry, Z. Z. *et al.* Streptozotocin is equally diabetogenic whether administered to fed or fasted mice. *Laboratory animals* **47**, 257-265, doi:10.1177/0023677213489548 (2013).

105. Childs, R. W. & Berg, M. Bringing natural killer cells to the clinic: ex vivo manipulation. *Hematology / the Education Program of the American Society of Hematology. American Society of Hematology. Education Program* **2013**, 234-246, doi:10.1182/asheducation-2013.1.234 (2013).

106. Chetty, S. *et al.* A simple tool to improve pluripotent stem cell differentiation. *Nature methods* **10**, 553-556, doi:10.1038/nmeth.2442 (2013).

107. Bose, B., Shenoy, S. P., Konda, S. & Wangikar, P. Human embryonic stem cell differentiation into insulin secreting beta-cells for diabetes. *Cell biology international* **36**, 1013-1020, doi:10.1042/cbi20120210 (2012).

108. Greggio, C. *et al.* Artificial three-dimensional niches deconstruct pancreas development in vitro. *Development (Cambridge, England)* **140**, 4452-4462, doi:10.1242/dev.096628 (2013).

109. Wutz, A. Epigenetic regulation of stem cells : the role of chromatin in cell differentiation. *Advances in experimental medicine and biology* **786**, 307-328, doi:10.1007/978-94-007-6621-1_17 (2013).

110. Pennarossa, G. *et al.* Brief demethylation step allows the conversion of adult human skin fibroblasts into insulin-secreting cells. *Proceedings of the National Academy of Sciences of the United States of America* **110**, 8948-8953, doi:10.1073/pnas.1220637110 (2013).

111. Christman, J. K. 5-Azacytidine and 5-aza-2'-deoxycytidine as inhibitors of DNA methylation: mechanistic studies and their implications for cancer therapy. *Oncogene* **21**, 5483-5495, doi:10.1038/sj.onc.1205699 (2002).

112. Leontovyc, I. *et al.* The effect of epigenetic factors on differentiation of pancreatic progenitor cells into insulin-producing cells. *Transplantation proceedings* **43**, 3212-3216, doi:10.1016/j.transproceed.2011.10.025 (2011).

113. Liu, J. *et al.* Direct differentiation of hepatic stem-like WB cells into insulin-producing cells using small molecules. *Sci. Rep.* **3**, (2013).

114. Ohi, Y. *et al.* Incomplete DNA methylation underlies a transcriptional memory of somatic cells in human iPS cells. *Nature cell biology* **13**, 541-549, doi:10.1038/ncb2239 (2011).

115. Kim, K. *et al.* Epigenetic memory in induced pluripotent stem cells. *Nature* **467**, 285-290, doi:10.1038/nature09342 (2010).

116. Juttermann, R., Li, E. & Jaenisch, R. Toxicity of 5-aza-2'-deoxycytidine to mammalian cells is mediated primarily by covalent trapping of DNA methyltransferase rather than DNA demethylation. *Proceedings of the National Academy of Sciences of the United States of America* **91**, 11797-11801 (1994).

117. Shiroi, A. *et al.* Identification of insulin-producing cells derived from embryonic stem cells by zinc-chelating dithizone. *Stem cells* **20**, 284-292, doi:10.1634/stemcells.20-4-284 (2002).

118. Cozar-Castellano, I. *et al.* Lessons from the first comprehensive molecular characterization of cell cycle control in rodent insulinoma cell lines. *Diabetes* **57**, 3056-3068, doi:10.2337/db08-0393 (2008).

119. Jiang, G. & Zhang, B. B. Glucagon and regulation of glucose metabolism. *Am J Physiol Endocrinol Metab* **284**, E671-678, doi:10.1152/ajpendo.00492.2002 (2003).

120. Lumelsky, N. *et al.* Differentiation of embryonic stem cells to insulin-secreting structures similar to pancreatic islets. *Science* **292**, 1389-1394, doi:10.1126/science.1058866 (2001).

121. Hansson, M. *et al.* Artifactual insulin release from differentiated embryonic stem cells. *Diabetes* **53**, 2603-2609 (2004).

122. Norris, D. O. & Carr, J. A. in *Vertebrate Endocrinology (Fifth Edition)* (ed David O. NorrisJames A. Carr) 443-481 (Academic Press, 2013).

123. Pisania, A. *et al.* Quantitative analysis of cell composition and purity of human pancreatic islet preparations. *Laboratory investigation; a journal of technical methods and pathology* **90**, 1661-1675, doi:10.1038/labinvest.2010.124 (2010).

124. Ergun-Longmire, B. *et al.* Oral insulin therapy to prevent progression of immune-mediated (type 1) diabetes. *Annals of the New York Academy of Sciences* **1029**, 260-277, doi:10.1196/annals.1309.057 (2004).

125. Krishnamurthy, B. *et al.* Responses against islet antigens in NOD mice are prevented by tolerance to proinsulin but not IGRP. *The Journal of clinical investigation* **116**, 3258-3265, doi:10.1172/JCI29602 (2006).

126. Xu, D., Prasad, S. & Miller, S. D. Inducing immune tolerance: a focus on Type 1 diabetes mellitus. *Diabetes management* **3**, 415-426, doi:10.2217/dmt.13.36 (2013).

127. Li, X. C. & Raghavan, M. Structure and function of major histocompatibility complex class I antigens. *Current opinion in organ transplantation* **15**, 499-504, doi:10.1097/MOT.0b013e32833bfb33 (2010).

128. Holling, T. M., Schooten, E. & van Den Elsen, P. J. Function and regulation of MHC class II molecules in T-lymphocytes: of mice and men. *Human immunology* **65**, 282-290, doi:10.1016/j.humimm.2004.01.005 (2004).

129. Bonde, S. & Zavazava, N. Immunogenicity and engraftment of mouse embryonic stem cells in allogeneic recipients. *Stem cells* **24**, 2192-2201, doi:10.1634/stemcells.2006-0022 (2006).

130. Drukker, M. *et al.* Characterization of the expression of MHC proteins in human embryonic stem cells. *Proceedings of the National Academy of Sciences of the United States of America* **99**, 9864-9869, doi:10.1073/pnas.142298299 (2002).

131. Fandrich, F. *et al.* Preimplantation-stage stem cells induce long-term allogeneic graft acceptance without supplementary host conditioning. *Nat Med* **8**, 171-178, doi:10.1038/nm0202-171 (2002).

132. Li, L. *et al.* Human embryonic stem cells possess immune-privileged properties. *Stem cells* **22**, 448-456, doi:10.1634/stemcells.22-4-448 (2004).

133. Lammert, E., Cleaver, O. & Melton, D. Induction of pancreatic differentiation by signals from blood vessels. *Science* **294**, 564-567, doi:10.1126/science.1064344 (2001).

134. Pepper, A. R. *et al.* A prevascularized subcutaneous device-less site for islet and cellular transplantation. *Nature biotechnology* **33**, 518-523, doi:10.1038/nbt.3211 (2015).

135. Schulz, T. C. *et al.* A scalable system for production of functional pancreatic progenitors from human embryonic stem cells. *PLoS One* **7**, e37004, doi:10.1371/journal.pone.0037004 (2012).

136. Kehoe, D. E., Jing, D., Lock, L. T. & Tzanakakis, E. S. Scalable stirred-suspension bioreactor culture of human pluripotent stem cells. *Tissue engineering. Part A* **16**, 405-421, doi:10.1089/ten.TEA.2009.0454 (2010).

137. Prunieras, M., Regnier, M. & Woodley, D. Methods for cultivation of keratinocytes with an air-liquid interface. *The Journal of investigative dermatology* **81**, 28s-33s (1983).

138. Cortijo, C., Gouzi, M., Tissir, F. & Grapin-Botton, A. Planar cell polarity controls pancreatic beta cell differentiation and glucose homeostasis. *Cell reports* **2**, 1593-1606, doi:10.1016/j.celrep.2012.10.016 (2012).

139. Villasenor, A., Chong, D. C., Henkemeyer, M. & Cleaver, O. Epithelial dynamics of pancreatic branching morphogenesis. *Development (Cambridge, England)* **137**, 4295-4305, doi:10.1242/dev.052993 (2010).

140. Kesavan, G. *et al.* Cdc42-mediated tubulogenesis controls cell specification. *Cell* **139**, 791-801, doi:10.1016/j.cell.2009.08.049 (2009).

141. Strutt, H. & Strutt, D. Differential stability of flamingo protein complexes underlies the establishment of planar polarity. *Current biology : CB* **18**, 1555-1564, doi:10.1016/j.cub.2008.08.063 (2008).

142. Goh, S. K. *et al.* Perfusion-decellularized pancreas as a natural 3D scaffold for pancreatic tissue and whole organ engineering. *Biomaterials* **34**, 6760-6772, doi:10.1016/j.biomaterials.2013.05.066 (2013).

143. Baptista, P. M. *et al.* The use of whole organ decellularization for the generation of a vascularized liver organoid. *Hepatology* **53**, 604-617, doi:10.1002/hep.24067 (2011).

144. Bonvillain, R. W. *et al.* A nonhuman primate model of lung regeneration: detergent-mediated decellularization and initial in vitro recellularization with mesenchymal stem cells. *Tissue engineering. Part A* **18**, 2437-2452, doi:10.1089/ten.TEA.2011.0594 (2012).

145. Ott, H. C. *et al.* Perfusion-decellularized matrix: using nature's platform to engineer a bioartificial heart. *Nat Med* **14**, 213-221, doi:10.1038/nm1684 (2008).

146. Petersen, T. H. *et al.* Tissue-engineered lungs for in vivo implantation. *Science* **329**, 538-541, doi:10.1126/science.1189345 (2010).

147. Price, A. P., England, K. A., Matson, A. M., Blazar, B. R. & Panoskaltsis-Mortari, A. Development of a decellularized lung bioreactor system for bioengineering the lung: the matrix reloaded. *Tissue engineering. Part A* **16**, 2581-2591, doi:10.1089/ten.TEA.2009.0659 (2010).

148. Remlinger, N. T., Wearden, P. D. & Gilbert, T. W. Procedure for decellularization of porcine heart by retrograde coronary perfusion. *Journal of visualized experiments : JoVE*, e50059, doi:10.3791/50059 (2012).

149. Ross, E. A. *et al.* Embryonic stem cells proliferate and differentiate when seeded into kidney scaffolds. *Journal of the American Society of Nephrology : JASN* **20**, 2338-2347, doi:10.1681/ASN.2008111196 (2009).

150. Song, J. J. *et al.* Regeneration and experimental orthotopic transplantation of a bioengineered kidney. *Nat Med* **19**, 646-651, doi:10.1038/nm.3154 (2013).

151. Soto-Gutierrez, A. *et al.* A whole-organ regenerative medicine approach for liver replacement. *Tissue engineering. Part C, Methods* **17**, 677-686, doi:10.1089/ten.tec.2010.0698 (2011).

152. Uygun, B. E. *et al.* Organ reengineering through development of a transplantable recellularized liver graft using decellularized liver matrix. *Nat Med* **16**, 814-820, doi:10.1038/nm.2170 (2010).

153. Wainwright, J. M. *et al.* Preparation of cardiac extracellular matrix from an intact porcine heart. *Tissue engineering. Part C, Methods* **16**, 525-532, doi:10.1089/ten.TEC.2009.0392 (2010).

154. Thivolet, C. H., Chatelain, P., Nicoloso, H., Durand, A. & Bertrand, J. Morphological and functional effects of extracellular matrix on pancreatic islet cell cultures. *Experimental cell research* **159**, 313-322 (1985).

155. Lakey, J. R. *et al.* Improved islet survival and in vitro function using solubilized small intestinal submucosa. *Cell and tissue banking* **2**, 217-224, doi:10.1023/A:1021171200127 (2001).

156. Woods, E. J. *et al.* Improved in vitro function of islets using small intestinal submucosa. *Transplantation proceedings* **36**, 1175-1177, doi:10.1016/j.transproceed.2004.04.042 (2004).

157. De Carlo, E. *et al.* Pancreatic acellular matrix supports islet survival and function in a synthetic tubular device: in vitro and in vivo studies. *International journal of molecular medicine* **25**, 195-202 (2010).

158. Meissner, A. *et al.* Reduced representation bisulfite sequencing for comparative high-resolution DNA methylation analysis. *Nucleic acids research* **33**, 5868-5877, doi:10.1093/nar/gki901 (2005).

159. Smallwood, S. A. & Kelsey, G. Genome-wide analysis of DNA methylation in low cell numbers by reduced representation bisulfite sequencing. *Methods in molecular biology* **925**, 187-197, doi:10.1007/978-1-62703-011-3_12 (2012).

160. Blaschke, K. *et al.* Vitamin C induces Tet-dependent DNA demethylation and a blastocyst-like state in ES cells. *Nature* **500**, 222-226, doi:10.1038/nature12362 (2013).

161. Savickiene, J., Treigyte, G., Jazdauskaite, A., Borutinskaite, V. V. & Navakauskiene, R. DNA methyltransferase inhibitor RG108 and histone deacetylase inhibitors cooperate to enhance NB4 cell differentiation and E-cadherin re-expression by chromatin remodelling. *Cell biology international* **36**, 1067-1078, doi:10.1042/CBI20110649 (2012).

162. Ghoshal, K. *et al.* 5-Aza-deoxycytidine induces selective degradation of DNA methyltransferase 1 by a proteasomal pathway that requires the KEN box, bromo-adjacent homology domain, and nuclear localization signal. *Molecular and cellular biology* **25**, 4727-4741, doi:10.1128/MCB.25.11.4727-4741.2005 (2005).

163. Schneider-Stock, R. *et al.* 5-Aza-cytidine is a potent inhibitor of DNA methyltransferase 3a and induces apoptosis in HCT-116 colon cancer cells via Gadd45- and p53-dependent mechanisms. *The Journal of pharmacology and experimental therapeutics* **312**, 525-536, doi:10.1124/jpet.104.074195 (2005).

164. Ismail, I. H., McDonald, D., Strickfaden, H., Xu, Z. & Hendzel, M. J. A small molecule inhibitor of polycomb repressive complex 1 inhibits ubiquitin signaling at DNA double-strand breaks. *J Biol Chem* **288**, 26944-26954, doi:10.1074/jbc.M113.461699 (2013).

165. Davie, J. R. Inhibition of histone deacetylase activity by butyrate. *J Nutr* **133**, 2485S-2493S (2003).

166. Gottlicher, M. *et al.* Valproic acid defines a novel class of HDAC inhibitors inducing differentiation of transformed cells. *Embo J* **20**, 6969-6978, doi:10.1093/emboj/20.24.6969 (2001).

167. Mali, P. *et al.* Butyrate greatly enhances derivation of human induced pluripotent stem cells by promoting epigenetic remodeling and the expression of pluripotency-associated genes. *Stem cells* **28**, 713-720, doi:10.1002/stem.402 (2010).

168. Detich, N., Bovenzi, V. & Szyf, M. Valproate induces replication-independent active DNA demethylation. *J Biol Chem* **278**, 27586-27592, doi:10.1074/jbc.M303740200 (2003).

169. Thaler, R., Spitzer, S., Karlic, H., Klaushofer, K. & Varga, F. DMSO is a strong inducer of DNA hydroxymethylation in pre-osteoblastic MC3T3-E1 cells. *Epigenetics : official journal of the DNA Methylation Society* **7**, 635-651, doi:10.4161/epi.20163 (2012).

170. Gittes, G. K., Galante, P. E., Hanahan, D., Rutter, W. J. & Debase, H. T. Lineage-specific morphogenesis in the developing pancreas: role of mesenchymal factors. *Development (Cambridge, England)* **122**, 439-447 (1996).

171. Miralles, F., Czernichow, P., Ozaki, K., Itoh, N. & Scharfmann, R. Signaling through fibroblast growth factor receptor 2b plays a key role in the development of the exocrine pancreas. *Proceedings of the National Academy of Sciences of the United States of America* **96**, 6267-6272 (1999).

172. Sneddon, J. B., Borowiak, M. & Melton, D. A. Self-renewal of embryonic-stem-cell-derived progenitors by organ-matched mesenchyme. *Nature* **491**, 765-768, doi:10.1038/nature11463 (2012).

173. Dai, C., Huh, C. G., Thorgeirsson, S. S. & Liu, Y. Beta-cell-specific ablation of the hepatocyte growth factor receptor results in reduced islet size, impaired insulin secretion, and glucose intolerance. *The American journal of pathology* **167**, 429-436 (2005).

174. Johansson, M., Mattsson, G., Andersson, A., Jansson, L. & Carlsson, P. O. Islet endothelial cells and pancreatic beta-cell proliferation: studies in vitro and during pregnancy in adult rats. *Endocrinology* **147**, 2315-2324, doi:10.1210/en.2005-0997 (2006).

175. Brissova, M. *et al.* Pancreatic islet production of vascular endothelial growth factor--a is essential for islet vascularization, revascularization, and function. *Diabetes* **55**, 2974-2985, doi:10.2337/db06-0690 (2006).

176. Kota, S. K. *et al.* Aberrant angiogenesis: The gateway to diabetic complications. *Indian journal of endocrinology and metabolism* **16**, 918-930, doi:10.4103/2230-8210.102992 (2012).

177. Roccisana, J. *et al.* Targeted inactivation of hepatocyte growth factor receptor c-met in beta-cells leads to defective insulin secretion and GLUT-2 downregulation without alteration of beta-cell mass. *Diabetes* **54**, 2090-2102 (2005).

178. Garcia-Ocana, A. *et al.* Transgenic overexpression of hepatocyte growth factor in the beta-cell markedly improves islet function and islet transplant outcomes in mice. *Diabetes* **50**, 2752-2762 (2001).

179. Mellado-Gil, J. *et al.* Disruption of hepatocyte growth factor/c-Met signaling enhances pancreatic beta-cell death and accelerates the onset of diabetes. *Diabetes* **60**, 525-536, doi:10.2337/db09-1305 (2011).

180. Srijaya, T. C., Ramasamy, T. S. & Kasim, N. H. Advancing stem cell therapy from bench to bedside: lessons from drug therapies. *Journal of translational medicine* **12**, 243, doi:10.1186/s12967-014-0243-9 (2014).

181. Ausubel, L. J., Lopez, P. M. & Couture, L. A. GMP scale-up and banking of pluripotent stem cells for cellular therapy applications. *Methods in molecular biology* **767**, 147-159, doi:10.1007/978-1-61779-201-4_11 (2011).

182. Cyranoski, D. Stem cells: 5 things to know before jumping on the iPS bandwagon. *Nature* **452**, 406-408, doi:10.1038/452406a (2008).

183. Lee, A. S., Tang, C., Rao, M. S., Weissman, I. L. & Wu, J. C. Tumorigenicity as a clinical hurdle for pluripotent stem cell therapies. *Nat Med* **19**, 998-1004, doi:10.1038/nm.3267 (2013).

184. Pugliese, A., Reijonen, H. K., Nepom, J. & Burke, G. W., 3rd. Recurrence of autoimmunity in pancreas transplant patients: research update. *Diabetes management* **1**, 229-238, doi:10.2217/dmt.10.21 (2011).

185. Dolgin, E. Encapsulate this. *Nat Med* **20**, 9-11, doi:10.1038/nm0114-9 (2014).

186. Nakayama, M. *et al.* Prime role for an insulin epitope in the development of type 1 diabetes in NOD mice. *Nature* **435**, 220-223, doi:10.1038/nature03523 (2005).

187. von Herrath, M., Sanda, S. & Herold, K. Type 1 diabetes as a relapsing-remitting disease? *Nature reviews. Immunology* **7**, 988-994, doi:10.1038/nri2192 (2007).

188. Durinovic-Bello, I. Autoimmune diabetes: the role of T cells, MHC molecules and autoantigens. *Autoimmunity* **27**, 159-177 (1998).

189. Yu, L. *et al.* Antiislet autoantibodies usually develop sequentially rather than simultaneously. *The Journal of clinical endocrinology and metabolism* **81**, 4264-4267, doi:10.1210/jcem.81.12.8954025 (1996).

190. Chan, K. M., Bonde, S., Klump, H. & Zavazava, N. Hematopoiesis and immunity of HOXB4-transduced embryonic stem cell-derived hematopoietic progenitor cells. *Blood* **111**, 2953-2961, doi:10.1182/blood-2007-10-117366 (2008).

191. Kim, E. M. *et al.* ES Cell-Derived Hematopoietic Progenitor Cells (HPCs) Downregulate the CD3 xi Chain on T Cells, Abrogating Alloreactive T Cells. *Immunology*, doi:10.1111/imm.12268 (2014).